

CANCER STEM CELL ISOLATION FROM CHORDOMA CELL LINES:  
INTEGRATED MIRNA-MRNA ANALYSIS OF THE CANCER STEM CELLS



by  
Emre Can Tüysüz

Submitted to Graduate School of Natural and Applied Sciences  
in Partial Fulfillment of the Requirements  
for the Degree of Doctor of Philosophy in  
Biotechnology

Yeditepe University

2019

CANCER STEM CELL ISOLATION FROM CHORDOMA CELL LINES:  
INTEGRATED MIRNA-MRNA ANALYSIS OF THE CANCER STEM CELLS

APPROVED BY:

Prof. Dr. Ömer Faruk Bayrak  
(Thesis Supervisor)  
(Yeditepe University)

Prof. Dr. Dilek Telci Temeltaş  
(Yeditepe University)

Prof. Dr. Elif Damla Arısan  
(İstanbul Kültür University)

Assist. Prof. Dr. Ayşegül Kuşucu  
(Yeditepe University)

Assist. Prof. Dr. Elif Sibel Aslan  
(Biruni University)

DATE OF APPROVAL: ..../..../2019

## ACKNOWLEDGEMENTS

I would like to convey my thankfulness to Professor Ömer Faruk Bayrak for his huge patience and support during my PhD journey. Without his guidance and enthusiasm, I wouldn't have completed it. I'd like to thank Dr. Ayşegül Kuşkucu for her energy and always keeping me positive. I would like to special thank to Professor Uğur Türe and Dr. Cumhur KaanYaltırık who are part of this success. Finally, I have gratefulness for Professor Altay Burak Dalan whose support was prominent during my PhD.

This journey wouldn't be completed without wonderful lab mates. I am also so appreciated to work with Dr. Şükrü Güllüoğlu, Dr. Esra Aydemir Çoban, Mesut Şahin, Utku Özbey, Özlem Şilan Coşkun, Zeynel Demir, Nur Ekimci Gürcan, Melike Bayındır Bilgiç, Aysun Dilden Çağlayan, Dr. Özlem Türksoy, Engin Sümer, Uğur Aktaş, Dr. Öznur Suakar, Sezin Gürkan, Ebru Baktemur, Deniz Gül, Çiğdem Acar Yazıcıoğlu and Edanur Oranköylü.

Further thanks go to my dearest family; Kemal Tüysüz, Fatma Tüysüz and Ceren Tüysüz for their infinite support. They always motivate me throughout my life.

This thesis is dedicated to my uncle Faruk Baştürk, my grandfathers Ferhat Baştürk and Ahmet Tüysüz, and my grandmother Saniye Baştürk.

This study was supported by TÜBİTAK as a 3501-Career Project (Grant number: 112S485) and Yeditepe University Hospital.

## ABSTRACT

### **CANCER STEM CELL ISOLATION FROM CHORDOMA CELL LINES: INTEGRATED MIRNA-MRNA ANALYSIS OF THE CANCER STEM CELLS**

Chordoma is a rare, slowly growing tumor which is thought to originate from remnants of embryonic notochord associated with an aggressive outcome. Cancer stem-like cells (CSCs) are thought to be related to tumorigenesis, recurrence, and resistance in cancers. CD133<sup>+</sup>CD15<sup>+</sup> cells exhibited CSC phenotype with increased CSC- and Epithelial-Mesenchymal Transition (EMT)-related gene expression, invasion, migration, tumorsphere- and colony-forming abilities. In this study, differentially expressed miRNAs and mRNAs were determined in CSCs and their role in chordoma development was identified. *WNT5A*, *TGF- $\alpha$* , *BTG2* and *MYCBP* genes involved in CSC-related pathways, were targets of miR-140-3p, miR-148a-3p, miR-210-5p and miR-574-5p, respectively. Transfection of CSC-related miRNAs elevated migration and invasion capability along with stem cell phenotype. To show the concordance between in-vitro tests and patient data, fresh frozen chordoma tissues were used. The results showed that miR-140-3p and miR-148a-3p expressions were found to be associated with Ki67 while miR-140-3p and *TGF- $\alpha$*  expressions associated with p53 expression. Moreover, *MYCBP* expression that is positively associated with tumor volume and metastasis was correlated with the expression of miR-210-5p and *TGF- $\alpha$*  in our patient cohort. In addition, mRNA microarray analysis revealed that 226 mRNAs were dysregulated in recurrent chordoma samples in comparison to primary chordoma samples. High expression of both LGR5 and IGFBP2 was associated with poor prognosis in chordoma. In addition to these results, herein, a recurrent-clivus chordoma cell line firstly established and named as YU-Chor1.

Based on the findings, chordoma CD133<sup>+</sup>CD15<sup>+</sup> cells had unique miRNA profile, which can regulate stem-like properties of chordoma CSCs.

This study was supported by TÜBİTAK as a 3501-Career Project (Grant number: 112S485) and Yeditepe University Hospital.

## ÖZET

### **KORDOMA HÜCRE HATLARINDAN KANSER KÖK HÜCRE İZOLASYONU: KANSER KÖK HÜCRELERİN ENTEGRE MİRNA-MRNA ANALİZİ**

Kordoma embriyonik notokord kalıntılarından kökenlendiği düşünülen yavaş-ilerleyen ve agresif özellik gösteren nadir bir tümördür. Kanser Kök Hücreler (KKH) kanserde tümörigenez, nüks ve direnç ile ilişkilidir. CD133+CD15+ kordoma hücreleri, yüksek KKH- ve Epitelyal-Mezenkimal Geçiş (EMG) ile ilişkili gen ekspresyonu, invazyon, migrasyon, tümörküre ve koloni oluşturma yeteneği göstererek KKH fenotipi sergiledi. Bu çalışmada, farklı seviyede eksprese edilen miRNA ve mRNA'lar kordoma KKH'lerde belirlenerek kordomadaki rolleri belirlendi. KKH ile ilişkili olan WNT5A, TGF- $\alpha$ , BTG2 and MYCBP genlerinin sırasıyla miR-140-3p, miR-148a-3p, miR-210-5p ve miR-574-5p'nin hedefi olduğu tespit edildi. KKH ile ilişkili miRNA'ların transfeksiyonu kordoma hücrelerinin kök hücre özelliği ile birlikte invazyon ve migrasyon yeteneğini arttırdı bulundu. In vitro testler ve hasta verileri arasındaki uyumu göstermek için kordoma dokuları kullanılarak yapılan klinikopatolojik analizler, miR-140-3p ve miR-148a-3p ekspresyonunun Ki67 ile, miR-140-3p ve TGF- $\alpha$  ekspresyonunun ise P53 ile korele olduğu gösterdi. Son olarak, MYCBP ifadesinin tumor hacmi ile, miR-210-5p ve TGF- $\alpha$  ifadesinin ise metastaz ile ilişkili olduğu saptandı. Ayrıca, mRNA mikrodizin analizlerine göre, nüks kordoma örneklerinde 226 adet genin farklı seviyede eksprese edildiği saptandı. LGR5 ve IGF2BP2'nin yüksek ekspresyonunun, kötü prognoz ile ilişkisi olduğu belirlendi.

Bu sonuçlara ek olarak, bu çalışmamızda YU-Chorl isimli ilk nüks-klival kordoma hücre hattı geliştirilerek karakterize edilmiştir.

Bu bulgular, CD133+CD15+ kordoma KKH'lerinin kendine özgü miRNA düzeni ile kordoma KKH'lerinin devamlılığında rol aldığını göstermiştir.

Bu çalışma TÜBİTAK tarafından 3501-Kariyer Projesi (Proje no:112S485) olarak ve Yeditepe Üniversitesi Hastanesi tarafından desteklenmiştir.

## TABLE OF CONTENTS

ACKNOWLEDGEMENTS .....	iii
ABSTRACT.....	iv
ÖZET .....	v
LIST OF FIGURES .....	viii
LIST OF TABLES .....	xiii
LIST OF SYMBOLS/ABBREVIATIONS.....	xiv
1. INTRODUCTION .....	1
1.1. CANCER .....	1
1.1.1. Genetic Factors in Cancer.....	2
1.1.1.1. Tumor Suppressor Genes.....	3
1.1.1.2. Oncogenes.....	5
1.1.2. Environmental Factors.....	8
1.1.3. Epigenetics.....	9
1.1.4. Other Factors and Signaling Pathways During Tumor Initiation and Progression.....	10
1.2. BONE TUMORS .....	14
1.2.1. Chordoma.....	17
1.2.1.1. History .....	18
1.2.1.2. Cytogenetics of Chordoma .....	18
1.2.1.3. Signaling Pathways in Chordoma.....	18
1.2.1.4. Symptoms and Signs of Chordoma .....	20
1.2.1.5. Treatment of Chordoma.....	21
1.2.1.6. Prognosis of Chordoma .....	21
1.2.1.7. Chordoma Cell Lines .....	22
1.3. CANCER STEM CELLS .....	22
1.3.1. Chordoma CSCs .....	24
1.4. MIRNAS .....	24
1.4.1. Role of miRNAs in Cancer.....	25
1.4.1.1. Dysregulated miRNAs in Chordoma.....	26
1.5. THE AIM OF THE STUDY.....	27

2.	MATERIALS AND METHODS.....	29
2.1.	CHORDOMA SAMPLES .....	29
2.2.	CELL CULTURE .....	29
2.3.	STR ANALYSIS .....	30
2.4.	ARRAY CGH.....	30
2.5.	FLOW CYTOMETRY .....	30
2.6.	MIRNA AND MRNA MICROARRAY .....	30
2.7.	MIRNA AND ANTI-MIRNA TRANSFECTION .....	31
2.8.	GENE EXPRESSION ANALYSIS.....	31
2.9.	VIABILITY AND APOPTOSIS ASSAY .....	32
2.10.	INVASION AND MIGRATION ASSAY .....	32
2.11.	COLONY FORMATION ASSAY.....	33
2.12.	TUMOROSPHERE FORMATION ASSAY .....	33
2.13.	WOUND HEALING ASSAY .....	33
2.14.	ALDEFLOUR ASSAY.....	33
2.15.	STATISTICAL ANALYSIS .....	34
3.	RESULTS .....	35
3.1.	DYSREGULATED MIRNAS AND MRNAS IN CHORDOMA CSCS.....	35
3.1.1.	Identification and Characterization of CD133 <sup>+</sup> CD15 <sup>+</sup> Chordoma Cells .....	35
3.1.2.	Dysregulated miRNAs and mRNAs in Chordoma Cancer Stem-like Cells .....	41
3.1.3.	Candidate Targets of Selected miRNAs Were Validated Using qPCR.....	52
3.1.4.	CSC-related miRNAs Affected Proliferation, Apoptosis, Migration, Invasion, and Stemness Properties.....	53
3.1.5.	CSC-related miRNAs and Their Targets are Related with Clinicopathological Features of Chordoma Samples.....	61
3.2.	IDENTIFICATION OF RECURRENCE MECHANISM IN CHORDOMA .....	70
3.2.1.	Characterization of YU-Chor1 Cell Line.....	70
3.2.2.	Identification of Dysregulated mRNAs in Recurrent Chordoma Samples .....	76
4.	DISCUSSION .....	84
5.	CONCLUSION.....	90
	REFERENCES .....	92

## LIST OF FIGURES

Figure 1.1. Hallmark of Cancer .....	2
Figure 1.2. CSC hypothesis .....	23
Figure 1.3. miRNA Biogenesis.....	25
Figure 3.1. Relative ratio of CD133 <sup>+</sup> CD15 <sup>+</sup> cells in U-CH1, U-CH2, MUG-Chor1, and JHC7 chordoma cell lines. Representative figures from 3 independent trials. Q2 gate represents CD133 <sup>+</sup> CD15 <sup>+</sup> chordoma cells, P2 (Green) gate represents CD133 <sup>-</sup> CD15 <sup>-</sup> chordoma cells. ....	35
Figure 3.2. CD90, CD24 and CD44 characterization of chordoma cells. ± represents the SEM. Gates were determined using unstained controls for each cell line.....	36
Figure 3.3. Quantification of both chordoma and CSC-related gene expression in CD133 <sup>+</sup> CD15 <sup>+</sup> versus CD133 <sup>-</sup> CD15 <sup>-</sup> chordoma cells. The dashed line (=1-fold) symbolize the negative control (CD133 <sup>-</sup> CD15 <sup>-</sup> ). *: p<0.05.....	37
Figure 3.4. Migration and invasion capacity of CD133 <sup>+</sup> CD15 <sup>+</sup> chordoma cells versus CD133 <sup>-</sup> CD15 <sup>-</sup> . Migration and invasion capacity of the cells were evaluated 2 days after seeding. For the invasion assay, transwell inserts were coated with basement membrane matrigel. *: p<0.05.....	38
Figure 3.5. Pictures of migrative and invasive cells from CD133 <sup>+</sup> CD15 <sup>+</sup> and CD133 <sup>-</sup> CD15 <sup>-</sup> chordoma cells. For the invasion assay, transwell inserts were coated with basement membrane matrigel. Scale bar represents 100 µm.....	38
Figure 3.6. Colony-forming and tumorsphere-forming ability of CD133 <sup>+</sup> CD15 <sup>+</sup> chordoma cells and CD133 <sup>-</sup> CD15 <sup>-</sup> chordoma cells. Results were obtained 4 weeks after seeding. *: p<0.05.....	39



- Figure 3.7. Pictures of colony formation and tumorsphere formation from CD133<sup>+</sup>CD15<sup>+</sup> and CD133<sup>-</sup>CD15<sup>-</sup> chordoma cells. Scale bar represents 100  $\mu$ m. ....40
- Figure 3.8. Relative quantification of EMT-related gene expression in CD133<sup>+</sup>CD15<sup>+</sup> versus CD133<sup>-</sup>CD15<sup>-</sup> chordoma cells. The dashed line (=1-fold) symbolize the negative control (CD133<sup>-</sup>CD133<sup>-</sup>). \*: p<0.05. ....41
- Figure 3.9. miRNA microarray results. Number of upregulated and downregulated miRNAs with scatter plot and volcano plot generated by TAC software. ....42
- Figure 3.10. Confirmation of miRNA microarray analysis through qPCR using primers specific for (A) miR-140-3p, (B) miR-148a-3p, (C) miR-152-3p, (D) miR-574-5p and (E) miR-210-5p in CD133<sup>+</sup>CD15<sup>+</sup> chordoma cells versus CD133<sup>-</sup>CD15<sup>-</sup>. The dashed line represents 1, which is the normalized value for the CD133<sup>-</sup>CD15<sup>-</sup> for each group. \*: p<0.05. \*\*:p<0.01 .....43
- Figure 3.11. mRNA microarray results. Number of upregulated and downregulated mRNAs with scatter plot and volcano plot generated by TAC software.....46
- Figure 3.12. miRNA mimic (green) and DAPI were introduced into chordoma cell lines. DAPI (blue) was used for nuclear staining. “NC” is a representative image from non-transfected control groups. Scale bar represents 20  $\mu$ m. ....52
- Figure 3.13. Expression level of target genes once transfection of pre- and anti-mimics of miRNAs into chordoma cells. Pre-mir-scr or anti-mir-scr transfected cells were used for normalization. The dashed line represents 1 fold, which is the value for the pre-mir-scr or anti-miR-scr transfected cells for each group. \*: p<0.05, \*\*:p<0.01. ....53
- Figure 3.14. Percentage viability of U-CH1 and MUG-Chor1 upon transfection of miRNA constructs. Percent viability was calculated by normalizing results from MTS assay using pre-scr or anti-scr transfected control group. Viability was measured 3 days after transfection of pre-mimic-miRNA or anti-mimic-miRNA. The dashed line (=100%) is the value for the pre-mir-scr or anti-miR-scr transfected cells for each group. \*: p<0.05. ....54

- Figure 3.15. Apoptosis results representing the percentage of Annexin V<sup>+</sup>7-AAD<sup>-</sup> chordoma cells following miRNA transfection. Ratio of apoptotic cells were assessed 48 hours after transfection of pre-mimic-miRNA or anti-mimic-miRNA. Statistically significant results were shown. \*: p<0.05.....55
- Figure 3.16. Effect of collective transfection of CSC-related miRNAs or non-CSC-related miRNAs on cell migration and invasion capacity of chordoma cell lines. Invasion and migration ability of chordoma cells were evaluated 2 days after transfection. For the invasion assay, transwell inserts were coated with basement membrane matrigel. Mixture of pre- and anti-miR-scramble was used as control. \*: p<0.05. ....56
- Figure 3.17. Pictures of migration and invasion from CSC-related miRNAs, non-CSC-related miRNAs and Neg. Ctrl. For the invasion assay, transwell inserts were coated with basement membrane matrigel. Scale bar represents 100  $\mu$ m.....57
- Figure 3.18. Representative images of wound healing assay from CSC-related miRNAs, non-CSC-related miRNAs and Neg. Ctrl at day 0 and day 2. Scale bar represents 100  $\mu$ m. ....58
- Figure 3.19. Effect of collective miRNA transfection on migration ability of chordoma cell lines. Migration ability of cells was evaluated 48 hours after transfection. Mixture of pre- and anti-miR-scramble was used as control. \*: p<0.05. ....58
- Figure 3.20. Effect of transfection of miRNA groups on stem cell phenotype in A) U-CH1 and B) MUG-Chor1. ALDH activity was measured 72 hours after transfection of miRNA groups.  $\pm$  represents the SEM. C) Graphical representative of flow results. \*: p<0.05. ....60
- Figure 3.21. Correlation of A) miR-140-3p, B) miR-148a-3p, C) miR-210-5p, D) miR-574-5p, E) WNT5A, F) TGFA, G) BTG2 and H) MYCBP with P53 expression of patients with chordoma. p=significance, r=correlation coefficient.....66

- Figure 3.22. Correlation of A) miR-140-3p, B) miR-148a-3p, C) miR-210-5p, D) miR-574-5p, E) WNT5A, F) TGFA, G) BTG2 and H) MYCBP with Ki67 of patients with chordoma. p=significance, r=correlation coefficient.....67
- Figure 3.23. Correlation of A) miR-140-3p, B) miR-148a-3p, C) miR-210-5p, D) miR-574-5p, E) WNT5A, F) TGFA, G) BTG2 and H) MYCBP with tumor volume of patients with chordoma. p=significance, r=correlation coefficient.....68
- Figure 3.24. Overall survival analysis of A) miR-140-3p, B) miR-148a-3p, C) miR-210-5p, D) miR-574-5p, E) WNT5A, F) TGFA, G) BTG2 and H) MYCBP in patients with chordoma. ....69
- Figure 3.25. Microscopy image of YU-Chor1 cell line at 100X magnification. Scale bar represents 50  $\mu$ m.....70
- Figure 3.26. Percentage of both chordoma- and CSC- related surface proteins including CD90, CD24, CD44, CD133 and CD15 in chordoma cell lines. ....71
- Figure 3.27 Expression of chordoma-associated genes. Cell line which had the lowest expression for each gene among the cell lines were used for normalization. \*:  $p < 0.05$ , \*\*:  $p < 0.01$ .....72
- Figure 3.28. Expression level of MET-related genes. Cell line which had the lowest expression for each gene among the cell lines were used for normalization. \*:  $p < 0.05$ . ....73
- Figure 3.29. Expression level of EMT-related genes. Cell line which had the lowest expression for each gene among the cell lines were used for normalization. \*:  $p < 0.05$ , \*\*:  $p < 0.01$ .....74
- Figure 3.30. Array CGH profile of YU-Chor1 cell line. Red represents losses and blue represents gains.....76

Figure 3.31. mRNA microarray results for two recurrent and two primary chordoma tumor tissues. Number of upregulated and downregulated mRNAs with hierarchical clustering generated by TAC software. Number 1 represents recurrent chordoma samples; number 2 represents primary chordoma samples.....77

Figure 3.32. Expression level of CREB1, IGFBP6, LGR5 and TBX18. Patient sample which had the lowest expression for each gene among the patient samples were used for normalization. Graph bars indicate average fold change of each group. \*:  $p < 0.05$ . .....79

Figure 3.33. Overall survival analysis of chordoma samples using selected genes A) *CREB1*, B) *IGFBP6*, C) *LGR5* and D) *TBX18*. .....80

## LIST OF TABLES

Table 1.1. DNA repair mechanisms in human.....	12
Table 1.2. Enneking staging system for bone tumors.....	15
Table 3.1. Selected miRNAs from miRNA microarray analysis and their predicted targets .....	43
Table 3.2. Pathways in relation to miRNAs in chordoma CSCs against non-CSCs. miRNA count indicates the number of differentially expressed miRNAs. Predicted activation or inhibition has been provided.....	44
Table 3.3. Notable pathways in chordoma CSCs against non-CSCs. Gene count indicates the number of differentially expressed mRNAs in each pathway. List of cancers pathways of which were found to be related is listed. ....	47
Table 3.4. Prediction of activated or inhibited upstream regulators and notable molecules of chordoma CSCs against non-CSCs. For the CSCs vs. non-CSCs comparison, name of predictively activated or inhibited upstream regulators, molecule type and z-score are listed.....	50
Table 3.5. Correlation of selected miRNAs' expression level and their targets with clinicopathological features. P-value of significant results was shown in bold. ....	61
Table 3.6. STR analysis of YU-Chor1 cell line and patient's blood. ....	75
Table 3.7. Bioinformatical analysis of mRNA microarray results using DAVID database. .....	78
Table 3.8. Correlation of selected genes with clinicopathological features. P-value of significant results was shown in bold. ....	80

## LIST OF SYMBOLS/ABBREVIATIONS

7-AAD	7-Aminoactinomycin D
AID	Activation-induced deaminase
Akt	Protein kinase B
ALDH	Aldehyde dehydrogenase
CSC	Cancer stem cell
CTAB	Cetyltrimethylammonium bromide
DEAB	Diethylaminobenzaldehyde
DNA	Deoxyribonucleic acid
DNMT	DNA methyl Transferase
DRG1	Differentiation related gene1
DTAB	Dodecyltrimethylammonium bromide
ECM	Extra cellular matrix
EMT	Epithelial-mesenchymal transition
ER	Estrogen receptor
ESA	Epithelial-specific antigen
ESC	Embryonic stem cell
FACS	Fluorescence activated cell sorting
FBS	Fetal bovine serum
FGF	Fibroblast growth factor
GBM	Glioblastoma multiforme
HC	Hepatocellular carcinoma
HPV	Human papilloma virus
HR	Homologous recombination
IMDM	Iscoe's modified dulbecco's media
JAK	Janus kinases
KBP	Kilobase pair
KRT19	Cytokeratine 19
LIF	Leukemia inhibitory factor
LOH	Loss of heterozygosity
miRNA	Micro RNA

mRNA	Messenger RNA
MSC	Mesenchymal stem cell
Nf-Kb	Nuclear factor kappa B
NSCLC	Non-small cell lung carcinoma
oncomiR	Oncogenic miRNAs
PBS	Phosphate buffered saline
PCR	Polymerase chain reaction
PLKs	Polo-like kinases
RA	Retinoic acid
Rb	Retinoblastoma
RNA	Ribonucleic acid
ROS	Reactive oxygen species
RTK	Receptor tyrosine kinases
siRNA	Small interfering RNA
ssDNA	Single stranded DNA
STR	Short tandem repeat
TAC	Transcriptome analysis console
TGF	Transforming growth factor
TIMP2	Metalloproteinase-2
UV	Ultraviolet
YU-Chor1	Yeditepe university chordoma cell line 1

# 1. INTRODUCTION

## 1.1. CANCER

Cancer is the abnormal cell growth caused by disruption of the division and proliferation balance in cells. It can be formed from any kind of cell found in an organism. Its origin dates back to 5, 000 years in Egypt. Cancer initiation and progression are complicated processes that include genetic and environmental factors. Studies have revealed that both genetic and environmental factors act together during carcinogenesis [1]. Cancer cells have migration ability by disseminating to distant tissues and/or organs known as the metastasis that causes death. Although a great number of studies by physicians, biologists, and/or chemists have spent intensive research along with extreme funding, cancer still causes the death of people.

Ten basic characteristics were put forward by Hanahan and Weinberg for cancer (Fig. 1.1) : 1) self-proliferative ability, 2) no-response to anti-growth signals, 3) resistance to apoptosis, 4) immortalization, 5) angiogenesis ability, 6) invasion and metastasize, 7) tumor-promoting inflammation, 8) reprogramming energy metabolism, 9) avoiding immune destruction and 10) genome instability and mutation [2].



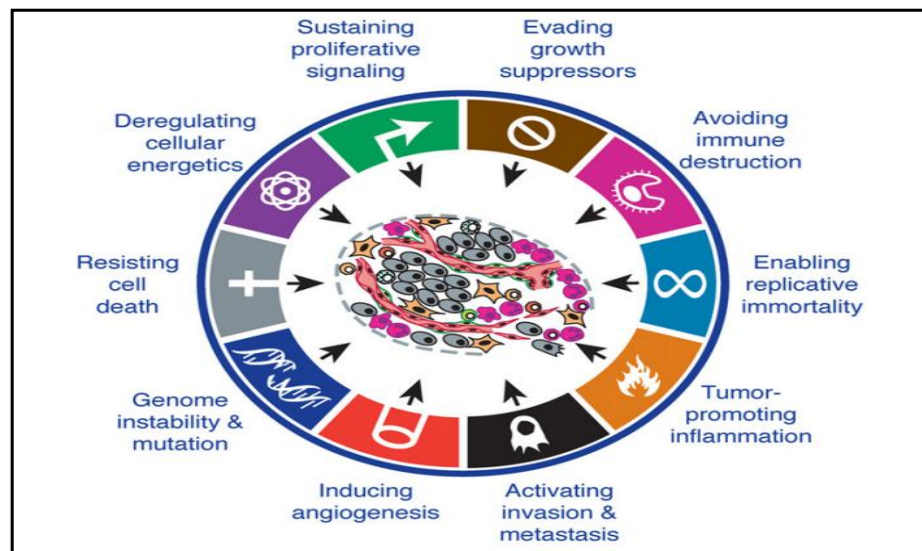


Figure 1.1. Hallmark of Cancer [2]

Stem cells (SCs) are found in a low rate in the body and have self-renewal ability and differentiation potential into much kind of cells. Differentiation of SCs into different cell types provides maintenance of tissues and organs [3]. Cancer stem cells (CSCs) are classified as a few number of subgroups in the heterogeneity cancer population and share many similar characteristics with normal stem cells such as self-renewal and differentiation. CSCs differentiate into different cancer cells that contribute phenotypic diversity to tumors. It is thought that non-CSCs have limited proliferation capacity. In other words, non-CSCs differentiate and die during tumorigenesis [4]. Targeting CSCs is a very important step to cure cancer completely.

### 1.1.1. Genetic Factors in Cancer

Cancer cells have several alterations in their DNA covering from a point mutation to gross chromosomal abnormalities like translocation, insertion and/or deletion. These alterations are irreversible and cause carcinogenesis. Activation of oncogenes and inactivation of tumor suppressor genes could cause cancer. Cancer-related genes are basically separated into two groups: 1) Tumor suppressor genes, 2) Oncogenes

### ***1.1.1.1. Tumor Suppressor Genes***

Tumor suppressor genes (anti-oncogene genes) hinder tumorigenesis and cell proliferation. They act as a break in the cell cycle. They are responsible in either blocking cell cycle and/or stimulating apoptosis. Inactivation of both copies of tumor suppressors through mutations is required for the tumorigenesis. It is known that inactivation of tumor suppressor genes provokes carcinogenesis in several cancers. Tumor suppressor genes can be classified into three groups: 1) Gatekeepers, 2) Caretakers and 3) Landscapers. Gatekeeper tumor suppressor genes regulate the cell cycle. They are specific for each cell type and interact with cyclin-Cdk complexes responsible in the cell cycle. Caretaker tumor suppressor genes sustain genome stability. They provide DNA repair and blocks accumulation of mutations in DNA through DNA base excision repair, nucleotide excision repair, prevention of oncogenic chromosomal rearrangement, non-homologous end joining, mismatch repair and telomere maintenance. Mutations in caretaker tumor suppressor genes cause genome instability, which is the main reason for cancer. Landscaper tumor suppressors regulate environments that control cell growth. Loss of function in landscaper tumor suppressor genes can cause transformation of normal cells through regulation of extracellular matrix protein, cellular adhesion molecules, surface markers, and growth factors.

Retinoblastoma (*Rb*) is firstly identified tumor suppressor gene in inherited Retinoblastoma. This protein acts as an inhibitor of cell proliferation by binding and suppressing transcription factors such as E2F and E1A etc. which are responsible during the cell division. Cyclin D and cyclin-dependent kinases (CDKs) can inactivate Rb. Inactivation of Rb in cells can activate E2F/DP transcription factor and it provides G1 to S phase transition [5]. It is mutated in several cancers [6–8]. Parisi *et al.* showed that inactivation of *Rb* caused metastatic colorectal cancer in mice [7]. Another study showed that loss of *Rb* caused increasing cell invasion through the aberrant expression of HIF1 $\alpha$ .

The P53 protein is a transcription factor that can be triggered during cell stress, DNA damage, aberrant growth signal, oncogene activation, etc. MDM2 protein can regulate it. Activation of P53 can cause cell cycle arrest, DNA repair, apoptosis and inhibition of angiogenesis. P53 contributes to expression of p21 and this expression induces cell cycle arrest and DNA repair. *NOXA*, *PUMA*, *P53AIP1*, *FOXO*, *FASR* and *IGF-BR3* which are pro-

apoptotic genes and *BCL-2* which is anti-apoptotic gene are regulated by P53. Activation of P53 stimulates apoptosis in cells. Furthermore, P53 activates Thrombospondin that inhibits angiogenesis. P53 is frequently inactivated during tumorigenesis [9]. Mutation in P53 can stimulate oncogenic properties of cancer and contribute to invasion, metastasis, proliferation and cell survival in several cancers [10]. P53 is mutated in several cancers [11]. A study indicated that wild-type (wt) P53 inhibits invasion capability of cancer cells through degradation of *SLUG*, whereas mutant P53 stabilizes it. In non-small cell lung carcinoma, mutant form of P53 caused low *MDM2* and *E-CAD* expression and high expression of *SLUG*. This expression pattern is poor prognostic marker and associated with decreased metastasis-free survival time [12]. Furthermore, mutation in P53 and overexpression of mutated P53 can cause drug resistant in breast cancer and lung cancer [13,14]. Studies also revealed that expression of P53 in patients with gastric and colorectal cancer correlated with tumor stage, early recurrence and death of patients from the disease [15].

*PTEN* is a tumor suppressor gene pinpointed on chromosome 10. It codes for a phosphatase with dual specificity: Protein phosphatase and lipid phosphatase. It dephosphorylates the membrane lipid PIP3 to form PIP2. De-phosphorylation of PIP3 provides blocking of AKT pathway (Lipid phosphatase activity). Protein phosphatase activity is weak in *PTEN* but this activity can regulate cell cycle and apoptosis [16]. *PTEN* mutation has been seen in several cancers [17–19]. Mutation or deletion in *PTEN* causes no or low *PTEN* activity in cancers [20]. Inactivation of *PTEN* which is deleted in most of prostate cancer (PC) provides resistant to chemotherapy and radiotherapy. Overexpression of *PTEN* in *PTEN* null PC cells make cancer cells more sensitive to chemotherapy [21]. Expression of *PTEN* regulates *DRG1* which is a metastasis suppressor gene and provides inhibition of tumor invasion in the breast and prostate cancer through blocking Akt pathway [22]. *PTEN* is a negative regulator of PI3K pathways and activation of PI3K causes metastasis and poor prognosis in cancer. Moreover, loss of *PTEN* is strongly associated with a poor prognosis in gastric cancer and endometrial cancer [23,24]. Therefore, it is clear that loss of *PTEN* is an indicator for poor prognosis in cancer.

*BRCA1* and *BRCA2* are the most recognized tumor suppressor genes that have crucial functions in initiation and progression of breast and ovarian cancer. They play a role during DNA repairing and provide preservation of genome stability. Damaged DNA

cannot be repaired upon loss of function and/or incorrect function in these genes, and it leads to cancer. Mutations in these genes are liable for 20-25 percent of inherited breast cancer and 5-10 percent of many breast cancer [25,26]. In addition, mutation in *BRCA1* and *BRCA2* genes represent 15 percent of ovarian cancer [27]. Both genes have a role in the same pathway, but their role in DNA repair is different. While *BRCA1* is responsible in both activation of the cell-cycle checkpoint and DNA repair, *BRCA2* act as regulator of homologous recombination [28]. Women harboring *BRCA1* mutation and/or *BRCA2* mutation have increased jeopardy for breast cancer approximately 4,5-5 times more compared with women not harboring *BRCA1* and/or *BRCA2* mutation. It's also riskier for ovarian cancer. In brief, women harboring *BRCA1* and *BRCA2* have increased risk approximately 30-times and 10-times for ovarian cancer, respectively [29,30].

#### ***1.1.1.2. Oncogenes***

Oncogenes are normally found in cells as proto-oncogene to regulate cell growth for development. Proto-oncogenes are highly active during embryogenesis because of the increased dividing activity of organs and tissues. Once completion of this process, most of the proto-oncogenes stop to produce a protein product. However, a mutation in proto-oncogene (gain of function) causes conversion of proto-oncogene to oncogene and overexpression of protein or mutated oncoprotein product. Overexpression and/or mutated oncoprotein led to cancer in organisms. It is known that oncogenes provide resistant to the apoptosis which is the characteristic of cancer cells [31]. *v-src* gene was firstly identified oncogene in cancer-causing retroviruses called Rous sarcoma virus in 1911. There are three mechanisms are found for proto-oncogene to oncogene conversion: 1) Mutation in proto-oncogene, 2) High expression of protein produced by several factors such as high activity of proto-oncogene, increased mRNA stability and duplication of proto-oncogene and 3) Translocation: translocation of proto-oncogene to a new chromosome region can increase activity of proto-oncogene. There is no common classifying the system for oncogenes.

*PDGF* is a growth factor (mitogen), which can act like oncogene and responsible for several process such as cell division, angiogenesis, metastasis and wound healing. *PDGFR* is a kind of Receptor Tyrosine Kinases (RTK) and classified into two groups: *PDGFR-a*

and PDGFR-B [32]. Overexpression of PDGF was shown in lots of cancer such as pancreas cancer, gastric cancer and glial tumors, etc. [33–35]. HIF1 $\alpha$  expression is involved in PDGFR-a expression and it is possible to regulate angiogenesis [36]. Another study revealed that TGF- $\beta$  induced PDGF pathway is elevated in hepatocyte cancer and provides tumorigenesis [37]. In addition, positive immunostaining of PDGF in advance breast cancer patients caused decreasing OS time and no response to chemotherapy. Overexpression of PDGF-BB also prognosticates for metastasis and poor prognosis in ovarium cancer [38].

*Ras* oncogene is a kind of GTPase and is separated into three groups: 1) H-Ras, 2) K-Ras, 3) N-Ras. Two major pathways are regulated by Ras: 1) MAPK and 2) PI3K. *K-Ras* mutation is found approximately 40 percent of colorectal cancer and cause high activation of MAPK continuously [39]. Treatment of EGFR-based therapy with Cetuximab and Panitimumab is unsuccessful in patients with colorectal cancer-bearing *K-Ras* mutation. *N-Ras* mutation is found widely in hematopoietic cancers and melanoma, whereas *K-Ras* mutation is found in colorectal and lung cancer. RAS/MAPK pathway is also over-expressed in pleomorphic sarcoma and predicts a poor prognosis [40]. Activation of Ras pathway associated with decreased overall survival time in Estrogen Receptor (ER)+ luminal breast carcinoma [41]. Ras also negatively regulates Pyruvate Dehydrogenase and contributes Glioblastoma Multiforme (GBM) tumorigenesis [42].

EGFR is a kind of tyrosine kinase found in the cell membrane as a cell surface receptor. Activation of EGFR through binding its ligands, such as EGF and TGF- $\alpha$  can stimulate several pathways including PI3K, STAT, RAF/MEK/ERK. Mutation in EGFR causes permanent activation of pathways and contributes the carcinogenesis process. Some cancer cell lines concurrent with high EGFR expression can be resistant to chemotherapy through PI3K activation. EGFR/STAT pathway can be activated by HIF1 $\alpha$  and activation of this pathway induce cell survival and EMT that switches cancer cells into more aggressive phenotype [43]. Overexpression of EGFR is poor prognostic marker for several cancers such as gastric, breast and colorectal cancers [44]. EGFR expression also presages for local recurrence in head and neck carcinoma [45].

VEGF is a kind of RTK that regulates angiogenesis. VEGF secreted from tumor cells binds receptors on endothelial cells and pericyte. Matrix metalloproteinase (MMP) degrade

extracellular matrix and endothelial cells secrete PDGF-BB that recruit pericyte. Finally, endothelial cells induce vessel stimulation. VEGF responsible for blood vessel formation during development of wound healing, muscle after sport. VEGFR2 induced AKT/mTOR pathway predicts decreased survival in patients with ovarian cancer [46]. In ovarian cancer, inactivation of PI3K/AKT pathway by apigenin inhibits VEGF production. Moreover, tube formation is blocked in endothelial cells through blocking same pathway. Therefore, inhibition of VEGF is crucial for the treatment of ovarian cancer to block tumor growth and angiogenesis [47]. Targeting to Stat3 pathway is also crucial to inhibit VEGF expression and angiogenesis [48]. VEGF expression also associated with a poor prognosis in patients with NSCLC [49].

*MYC* is a proto-oncogene whose product acts as a transcription factor and responsible in several cellular processes such as cell cycle, apoptosis, and transformation. Mutations in *MYC* gene are shown to be responsible for several cancers such as Burkitt Lymphoma and hematopoietic tumors. *MYC* can be activated through several pathways such as Wnt, Sonic Hedge Hog and MAPK pathways [50]. *MYC* family including *MYCN*, *L-Myc* and *c-myc* are found to dysregulated in hematopoietic cancer such as Multiple Myeloma, Acute Lymphocytic Leukemia and Diffuse Large Cell Lymphoma [51,52]. *MYC* rearrangements are also associated with poor prognosis in Diffuse Large Cell Lymphoma [53].

JAK/STAT signaling pathways is regulated by cytokines, interleukins and growth factors. Upon activation of JAK receptor cytoplasmic domain of receptor is phosphorylated and STATs bind to cytoplasmic domain of JAK. Once binding of STATs, dimerizations occur between STAT proteins. Upon phosphorylation of STATs on tyrosine residues by JAK or other RTKs, phosphorylated STATs are transported from cytoplasm to nucleus thereby binding promoter region to activate gene transcription responsible in tumor progression. JAK/STAT activity has been investigated in several cancers and researchers found several mutation signature in JAK [54]. Mutation in *JAK1* gene has been identified by Kan *et al.* in 9 percent of patients with Hepatitis-B-induced HC and this mutation was associated with phosphorylation of JAK1 and STAT3 that facilitate cytokine independent proliferation of cancer cells [55].

### 1.1.2. Environmental Factors

Several carcinogens can increase cancer risk. Carcinogens can be classified into three groups: 1) Biological Carcinogens, 2) Physical Carcinogens and 3) Chemical Carcinogens. The most well-known environmental factor causing cancer is smoking. Tobacco smoke contains approximately 7000 different chemical molecular and there are some well-known carcinogens such as nitrosamines, polonium, benzene, and toxins [56]. Lung cancer is first cancer linked to smoking. These carcinogens can be transported to any part of the body through circulation and can cause cancer. Ramakrishna *et al.* showed that smoking causes enrichment of CSC populations in pancreas cancer [57]. Studies suggested that CSCs can cause resistance to chemotherapy and radiotherapy, recurrence, metastasis and poor prognosis in several cancers.

Skin cancer is also associated with sunlight and ultraviolet (UV) light exposure [58]. This cancer commonly occurs in the head and neck because this location is exposed directly sun. The UV light in sunlight can cause damage in DNA, loss of tumor suppressor effect in immunity, and stimulate metastasis of melanoma. UV light exposure could control the expression of cytokines and chemokines that have anti-tumor effect of the immune system. In addition, UV light can induce ROS and cause oxidative stress. Expression of melanin and anti-oxidants is endogenous process increase to extinguish oxidative stress [59].

Aflatoxin is a kind of chemical produced by molds (especially *Aspergillus parasiticus* and *Aspergillus flavus*). It is known that high dose aflatoxin can provoke liver cancer in humans [60]. Liver cancer has a high incidence in Africa because of high aflatoxin level in food. Co-existence of hepatitis-B could have contributed to liver cancer formation in Africa [61]. Furthermore, aflatoxin can create a point mutation on P53 tumor suppressor gene at codon 249 and loss of P53 in HC can lead to activation of Nf-Kb signaling [62].

Viruses are a kind of agent that cannot live without a living organism. They replicate themselves using a cellular system of living organisms. Many studies have shown that a part of viruses are associated with cancer and cancer vaccines are developed to cure virus-induced cancer (also known as oncovirus). For example, Human Papilloma Virus (HPV) is a kind of DNA virus is known to liable in vagina, cervix, penis and anus cancer. E6 and E7 genes in HPV inhibit expression of P53 gene in host cell and can contribute to

tumorigenesis. Furthermore, integration of viral DNA to host DNA causes DNA alteration and contribute to the tumorigenic process [63].

### 1.1.3. Epigenetics

Epigenetic is a covalent modification of the genome, RNA or protein. It can change the regulation and activation of these molecules without changing their main sequence. DNA methylation, histone regulation, miRNAs, ubiquitination and phosphorylation are the most known epigenetic mechanisms.

Addition of methyl group to DNA sequence by DNA Methyl Transferase (DNMT) is referred to as DNA methylation. It is known that Cytosine base is converted to 5-methylcytosine through DNA methylation. DNA methylation in the promoter region of a gene can lead to gene silencing because transcription factor cannot bind to its sequence in a promoter. Furthermore, methylation of DNA provides acetylation of histone. Both mechanisms repress the transcription process. During tumorigenesis, lots of genes are hyper-methylated to inhibit transcription (especially tumor suppressor genes). Parella *et al.* showed that cell cycle regulator proteins *CCND2* is methylated in breast cancer [64]. Another study also showed that inhibition of metalloproteinase-2 (TIMP-2) through DNA methylation in prostate cancer caused increased invasion and migration ability in prostate cancer cells [65].

miRNAs are small RNA molecules (approximately 20-22 nucleotide) transcribed from non-coding regions of DNA but not translated and regulate gene expression. miRNAs were discovered in *C. elegans*. Nomenclature and function of miRNAs were fully understood in 2001. There are lots of studies on miRNAs because they have many roles in a cellular process. Calin *et al.* firstly described the relationship between cancer and miRNA [66]. They found that miR-15 and miR-16 were downregulated in chronic lymphocytic leukemia. Bottoni *et al.* also found that in pituitary adenoma miR-15a and miR-16-1 expression is less than that healthy hypophysis [67]. Cimmino *et al.* found that miR-15a and miR-16-1 regulate Bcl2 expression have a role in apoptosis [68].

Ubiquitination is a post-translational cellular-enzymatic process that involves the addition of ubiquitin molecule to a substrate protein. Ubiquitin added protein mostly degraded by



the proteasome. However, ubiquitin added protein can increase their activation. For instance, loss of PTEN which is a tumor suppressor gene is provided by ubiquitination [69]. In addition, ubiquitination of I $\kappa$ B in cytoplasm led to the transport of Nf-K $\beta$  protein from cytoplasm to nucleus. Nf-K $\beta$  is a transcription factor and can activate the expression of many genes that involves in a tumorigenesis such us inhibitor of apoptosis and anti-apoptotic proteins [70].

Phosphorylation is a post-translational modification could be explained as addition of phosphate group to an organic molecule. Phosphorylation has crucial roles in several cellular processes such as apoptosis, cell cycle, cell proliferation and activation of several pathways, etc. For example, phosphorylation increases activation of ERK1-2/MAPK pathway approximately 500-1000 folds [71]. Another study also showed that phosphorylation of ERK1-2 caused resistance to anti-hormonal therapy and decreased survival time in patients with breast cancer.

#### **1.1.4. Other Factors and Signaling Pathways During Tumor Initiation and Progression**

The genomic re-arrangements are the characteristics of all tumors. Inaccurate DNA repair might be the first step of cancer initiation causing new mutations and chromosomal abnormalities impressing oncogenes and tumor suppressor genes. These re-arrangements stimulate malignant transformation of cells. Both endogenous and exogenous factors can induce DNA damaging. ROS produced by mitochondria as by-products can contribute carcinogenesis with several processes such as deamination, depurination, depyrimidination, alkylation, and/or oxidation [72]. Deamination of cytosine (especially 5-meC in CpG island) is the most common mutation-causing process. Once deamination process converts the C into U or 5-meC to T, following replication in deaminated cells that results transition of C into T. This mechanism is also strongly associated with age [73]. APOBEC which commonly causes mutations in cancer and AID family of DNA cytosine deaminases, facilitates conversion of C into U in a ssDNA that could be turned into C-to-T during replication [74]. Depurination and depyrimidination are spontaneous hydrolysis processes, in which purine bases (Adenine and Guanine) or pyrimidine bases are cleaved from sugar construct that provide affranchising of Adenine and Guanine or Cytosine and

Thymine. Free nucleotides can be used for reinterceding for base excision repair. Depurination occurs in approximately 14000 of mammalian cells per day, whereas depyrimidination is found only 696 of mammalian cells per day [75]. Consequently, depurination has more tendency to initiate carcinogenesis than depyrimidination. As an example, by-product of estrogen named catechol estrogen-3,4-quinones can generate apurinic regions forming mutations in the genome and start and drive carcinogenesis processes [76]. Alkylation is an addition of alkyl group to DNA that can cause damages in DNA and lead to carcinogenesis. In human cells, alkylation of Guanine bases provide the formation of 6-O-Methylguanine that can be eliminated by *MGMT* gene whose decreased expression pattern is associated with tumor initiation and progression [77]. Oxidative stress is one of the exogenous cancer-causing processes due to high ROS amount in the cells. ROS can quickly diminish due to short half life time that's why it is hard to determine with conventional methods. Studies demonstrated that anti-oxidant enzymes are differentially expressed in cancers. ROS also could be responsible in whole stage of tumorigenesis. ROS accumulation in cells can damage DNA which cause mutagenesis and induce malignant transformation [78]. The well-characterized antioxidant agent is MnSOD also known as manganese superoxide dismutase and this antioxidant have a decreased expression pattern in several cancers including lung, prostate, and renal [79].

Both endogenous and exogenous factors can damage the DNA but stability of the genome could be maintained by the DNA Repair Mechanism. Genetic failure in the DNA repair mechanism has been linked with cancer initiation and progression for several years. DNA repair mechanisms in human cells were shown in Table 1.1 [80]. Recently, targeting DNA repair pathways is one of the most popular therapies to treat tumors.

Table 1.1. DNA repair mechanisms in human [80]

<b>Repair mechanism</b>	<b>Lesion feature</b>	<b>Genotoxic source</b>
Base excision repair (BER)	Oxidative lesions	ROS
Nucleotide excision repair (NER)	Helix-distorting lesions	UV radiation
Translesion synthesis	Various lesions	Various sources
Mismatch repair (MMR)	Replication errors	Replication
Single strand break repair (SSBR)	Single strand breaks	Ionizing radiation, ROS
Homologous recombination (HR)	Double-strand breaks	Ionizing radiation, ROS
Non-homologous end joining (NHEJ)	Double-strand breaks	Ionizing radiation, ROS
DNA interstrand crosslink repair pathway	Interstrand crosslinks	Chemotherapy

PARP has a distinctive function in both BER and SSBR. It is also responsible in DNA double strand breaks (DSB) repaired by Non-homologous end joining. BER can be classified into 4 steps: 1) Recognition, 2) incision/excision, 3) Re-synthesis and 4) Ligation. Several therapeutic approaches for cancer (especially platinum-based agents) induce DNA damage and the BER pathways could decide efficiency of the treatment. PARP inhibitors are the most used agents in order to cure cancer through targeting DNA repair mechanism in cancer. Targeting cancer cells specifically reduce toxicity in relationship with the cancer treatment. FDA has recently approved PARP inhibitors, which are effective in patients with ovarian cancer harboring mutations in BRCA1 and BRCA2. Moreover, cancer cells which have deficiency in Homologous Recombination (HR)-related genes were sensitive to PARP inhibitors [81]. DSB are repaired by two dissimilar reparation mechanisms in mammalian cells: 1) Homologous recombination (HR) and 2) NHEJ. HR is mediated during S and G2 phase because homologues DNA sequence and/or

sister chromatids are essential as a template. On the other hand, NHEJ can be activated in all phases of the cell cycle. Thus, NHEJ mechanism is largely activated in mammalian cells upon DSB (especially ionizing radiation-caused DSBs). The main steps of NHEJ consist of 4 different steps: 1) Recognition, 2) Formation of synaptic complex, 3) DNA end processing and 4) Ligation. NHEJ can also stimulate genomic re-arrangements such as translocations. Several studies suggested that elevated activation of NHEJ pathway were indicator for poor survival, radio-resistant, and metastasis [82]. KU70/80 and DNA-PK which are recruited upon DSB in genome are the well-characterized molecules involved in NHEJ. To date, there are no small molecules to target KU70/80. Thus, targeting DNA-PK molecules with several inhibitors such as Wortmannin and LY294002 make cancer cells sensitive to radiotherapy. Wortmannin is inhibitor of PI3-kinases. Moreover, it is also exhibited that Wortmannin also can inhibit DNA-PK and polo-like kinases (PLKs). However, required concentration of Wortmannin for DNA-PK inhibition is very high to overcome *in vivo* tumor radioresistance [83]. LY294002 is another inhibitor for DNA-PK and it also inhibits CK-II kinase. Both Wortmannin and LY294002 are not beneficial in radiosensitization due to quick cleaning, toxicity, low half-life time, and off-targets effects [84]. Therefore, different molecules were characterized to target DNA-PK such as NU7026 and NU7441. Both of them were improved from LY294002 and highly specific for DNA-PK (55-fold for NU7026, and 355-fold for NU7441). In addition, targeting other steps of NHEJ is also considerable for DSBs. As an example, ligation is the last step of NHEJ and SCR7, a specific DNA Ligase IV inhibitor. However, it was not therapeutically useful for cancer treatment. HR is also responsible in cancer initiation and development. Studies exhibited that inhibition of HR and/or HR-defective cancer cells are highly sensitive to anti-cancer drugs that cause DSBs in cancer genome. Activation of HR signaling pathway are associated with gross genomic re-arrangements in cancer [85]. Rad51 is one of the important staff in HR and studies suggested that high expression of this protein in cancer is related with chemo- and/or radio-resistance [86].

Disruption in cell cycle along with the increased proliferation is the characteristics of cancer cells. For this reason, targeting cell cycle-related proteins is potential treatment option for cancer. Studies indicated that while some of the cell cycle-related proteins aren't requisite for proliferation of non-malignant cells, numerous cancer cells required these proteins. Hence, it is very beneficial to target cyclin-dependent kinases (CDKs). Cell cycle

consists of 4 different steps; namely G0/G1, S, G2, and M. In healthy cells, cell cycle is arrested at G0 until mitogenic factors stimulate them. CDK4 and CDK6 are responsible in driving of cells into S-phase of the cell cycle, in which replication starts from G0/G1 phase. Both CDK4 and CDK6 are controlled by cyclin D1, cyclin D2, and/or cyclin D3. Additionally, members of the INK4 family including p16<sup>INK4A</sup>, p15<sup>INKB</sup>, p18<sup>INK4C</sup>, and p19<sup>INK4D</sup> can inhibit CDK4/6 [87]. Several drugs that inhibit CDK4 and CDK6 were discovered to inhibit proliferation of the cancer cells [88]. Cyclin D-CDK4 and Cyclin D-CDK6 stimulate cell cycle through two different mechanisms. First, this complex separate two CDK inhibitors (P21 and P27) thereby resulting in an activation of cyclin E-CDK2 kinase. Second, they phosphorylate their targets (particularly Rb) and E2F, a transcription factor, stimulated expression of the cell cycle-related genes. *CCND1*, *CDK4*, and *CDK6* genes are frequently activated among all cancers [89]. Moreover, *CDKN2A*, which is a negative regulator of CDK 4 and CDK6, is usually deleted in several cancers. Inactivation of Rb also stimulates CDK4 and CDK6 activation in cancers. CDK2, also known as p33 protein kinase, is an important regulator of G1-S transition and G2 modulation. Cyclin E-CDK2 and Cyclin A-CDK2 complexes are liable in an activate transition of G1-S and phosphorylation of various molecules for DNA replication along with an inactivation of E2F [90]. Inhibition of E2F activation is very important step for completion of S phase since E2F activation lacking Cyclin A-CDK2 could promote apoptosis. CDK1 activity is infrequently dysregulated in cancers. Cyclin A2 and Cyclin B bind to CDK1 and activate it in G2 phase. In the beginning of the M phase, Cyclin A2 is diminished and Cyclin B regulates activity of CDK1 for mitosis. PLKs have a crucial role during G2 phase. Briefly, they attend in maturation of centrosomes, activate Cyclin B-CDK1 protein and regulate cytokinesis. Aurora kinases are also responsible for maturation of centrosomes and regulate PLK1, which is the main stuff of PLKs in order to activate CDK1. Aurora B manages condensation of chromosomes and cytokinesis. Several molecules were contrived to target CDKs named pan-CDK inhibitors.

## 1.2. BONE TUMORS

Primary bone tumors are scarce tumors compared with other tumors. The most common types of bone tumors are osteosarcoma, chondrosarcoma and Ewing sarcoma, and the percentage of these tumors is just 0.2 percent in many tumors. Ratio of bone tumors in

children under 15 years old is approximately 5 percent of all tumors [91]. Bone tumors might come about because of inherited syndromes. However, histopathological characteristics do not differ from sporadic bone tumors [92,93]. Frequency of primary bone tumors is 35.1 percent for osteosarcoma, 25.8 percent for chondrosarcoma, 16 percent for Ewing's sarcoma, 8.4 percent for chordoma, 5.7 percent for malignant fibrous histiocytoma, 1.4 percent for angiosarcoma and 7.6 percent for others [94]. Bone tumors are not gender specific except some bone tumors such as Paget's sarcoma and chordoma which mainly occur in males. Although TNM staging system is utilized for tumors, it is not applicable for bone tumors because of sparseness. Thus, Enneking staging system is the most usable for patients with bone tumors. Table 1.2 shows the enneking staging system for bone tumors.

Table 1.2. Enneking staging system for bone tumors

Stage	Grade	Site	Metastasis
I-A	Low (G1)	Intracompartmental (T1)	No
I-B	Low (G1)	Extracompartmental (T2)	No
II-A	High (G2)	Intracompartmental (T1)	No
II-B	High (G2)	Extracompartmental (T2)	No
III	Any	Any	Yes

Osteosarcoma is an aggressive primary bone tumor producing osteoid. They frequently occur it in 1<sup>st</sup> and 2<sup>nd</sup> decades of life [95]. Surgical resection of the tumor provides increased overall survival time for patients with osteosarcoma. The best treatment option for a patient with osteosarcoma is combined chemotherapeutic agents concurrent with surgery [96]. 90 percent of osteosarcomas show aggressive phenotype along with different histological characteristic and chemotherapy is beneficial for this tumor, whereas, 10 percent of these tumors are assorted as low or intermediate grade and chemotherapeutic approach is not needful [97]. Several genomic re-arrangements were identified in osteosarcoma. For instance, inactivation of both P53 and Rb1 and activation of MDM are the most common genetic alterations in osteosarcoma [98]. Moreover, 70 percent of patients with osteosarcoma have genetic alterations in the Rb gene and loss of this gene is a poor prognostic marker for osteosarcoma [99]. Several genes and/or signaling pathways

including *FGF*, *C-MYC*, *PI3K*, *IGF* etc. were detected as activated in osteosarcomas [100]. Activation of *FGFR1* represents approximately 20 percent of osteosarcomas and it is the poor prognostic marker. Osteosarcoma concurrent with *FGFR1* activation is resistant to chemotherapy [101].

Chondrosarcoma is a chondroid-producing primary bone tumor and commonly occurs after the 4<sup>th</sup> decades. Chondrosarcoma is classified into two groups according to its originating cells: 1) Primary chondrosarcoma and 2) Secondary chondrosarcoma. Primary chondrosarcoma is originated from the bone. However, secondary chondrosarcoma arises from benign cartilage tumors. Chondrosarcoma is generally located in pelvis, shoulder and hip girdle. It shows a poor prognosis because of its anatomic location [102]. They are highly chemo- and/or radio-resistant cells as chordoma due to their ECM and slow-growing characteristics [103]. Studies suggested that chondrosarcomas could be chemoresistant owing to *MDR1* and P-glycoprotein [104,105]. While genetic alteration of *CDKN2A* is observed in high-grade chondrosarcomas, it isn't detected in low-grade chondrosarcomas [106]. At least one of *P53* and/or *Rb* LOH could be found in 96 percent of high-grade chondrosarcomas. Chondrosarcomas often are confused with chordomas due to location. However, the expression of several genes such as Brachyury, S100, and epithelial membrane antigene (EMA) can be used in order to set apart chordoma from chondrosarcoma. *COL2A1* gene is also hypermutability and type of mutations in *COL2A1* is unique for chondrosarcoma [107].

Ewing sarcoma is the third most common primary bone tumor and frequently detected in kids and teenagers. Most of this tumor has translocation of 11q24 and 22q12 that come out an fusion onco-protein named EWS/FL1. It is mainly located in long bones especially femur (26 percent) followed by tibia, fibula, pelvic girdle and the ribs [95]. It is histologically small-rounded, undifferentiated cells along with insufficient cytoplasm. Immunohistochemical (IHC) analysis demonstrated that vimentin, S100 and CD99 are highly expressed in Ewing sarcoma. Although EWS/FL1 is used as a marker for Ewing sarcoma diagnosis, origin of cell is still unclear [108]. However, researchers thought that Ewing sarcoma could be originated from either neural ectoderm or mesenchymal stem cell (MSC). Several chemotherapeutic agents such as ifosfamide, cyclophosphamide, vincristine, etoposide and doxorubicin could be used as a neoadjuvant therapy. Chemotherapeutic approaches can be combined radiotherapy and/or surgical resection of a

tumor. Ewing sarcoma is the most sensitive tumor of bone tumors to radiotherapy. Studies indicated that targeting CD99 in Ewing sarcoma stimulate the neuronal differentiation of Ewing sarcoma cells and decreased aggressiveness of tumor [109,110].

### **1.2.1. Chordoma**

Chordoma is a kind of rare bone tumor is thought to originate from remnants of embryonic notochord. It is a slow-growing but locally aggressive, capable to metastasize (particularly to bone, lung, and liver), the tendency to recurrence, non-epithelial tumor [111]. It prominently occurs between 5th and 6th decades of a lifetime. Chordoma is known to arise from the axial skeleton living on the sacrococcygeal region 50 percent of the incidents reported and 35 percent at the skull base and 15 percent along the vertebral region of the spine. Chordoma represents 1-4 percent of all bone tumors and one patient with chordoma is diagnosed per million people every year [112]. 10-40 percent of patients with chordoma show metastasis to distant tissue and organs [113,114]. Furthermore, chordomas are chemo-resistant and radio-resistant [115]. Consequently, surgical resection of the tumor is a main treatment followed by high-dose radiation therapy and/or proton beam [116].

Chordomas are classified as low-grade tumors because of their slow-growing characteristic and tendency to recur and metastasize locally which means they only grow into adjacent tissues [117]. Although chordoma occurs anywhere of the spine, it is frequently located in both ends of the spine namely sacrum and clivus. Three types of chordoma are classified histologically: 1) Classic chordoma, 2) Chondroid chordoma and 3) De-differentiated chordoma. The aggressiveness of chordoma decreases differentiated chordoma, classic chordoma, and chondroid chordoma, respectively.

Chordomas are often confused with chondrosarcomas. Brachyury, EMA, S-100 and cytokeratins (especially cytokeratin 19) are used to distinguish chordomas from chondrosarcomas [118]. Immunoperoxidase staining is also a useful tool to individuate chordomas from other types of tumors [112].



### **1.2.1.1. History**

Virchow firstly defined chordoma as cancer cells looked alike jelly-like located at clivus region of the spine and called it “*ecchondrosis physaliphora sphenoccipitalis*” in 1857. At first, Virchow classified these cells containing bubble-like vacuoles called physaliphorous cartilage-originated tumor. However, in 1858 Müller re-named this disease as “*ecchordosis physaliphora sphenoccipitalis*” [119]. After four decades, Ribbert investigated that nucleus pulposus cells transform into cells which look like chordoma.

### **1.2.1.2. Cytogenetics of Chordoma**

There are several studies about the deterioration of genetic stability in chordomas. Persons *et al.* firstly identified cytogenetic anomalies in chordomas [120]. Bayrakli *et al.* showed that 1p36, 1q25, 2p13, and 7q33 chromosomal regions are affected in both primary and recurrent chordomas [121]. Moreover, deletion of *CDKN2A* locus in 9p21 chromosomal region shows deletion in 70 percent of chordoma tumor samples [122]. Scheil *et al.* analyzed sixteen chordoma samples and revealed that 3p and 1p chromosomal arms were lost 50 percent and 44 percent, respectively [123].

### **1.2.1.3. Signaling Pathways in Chordoma**

Although chordoma referred to as a low-grade tumor, there is no approved chemotherapeutic agent and/or targeted therapy in order to cure chordoma. That's why pathways responsible in chordoma progression should be investigated in detail for better prognosis of patients with chordoma. Though lots of considerable investigations were carried out to elucidate the molecular mechanism of chordoma, several reasons including the rarity of chordoma, a small number of *in vivo* and *in vitro* studies about the pathogenesis of tumor and heterogeneity of tumor population make it difficult to cure chordoma. Thus, understanding the molecular mechanism of chordoma can contribute novel approaches to target the disease.

EGFR is a kind of RTK that responsible in metastasis, invasion, and migration of cancer cells [124–126]. EGFR status was evaluated in chordomas in various studies and was found EGFR amplification was not consistent in chordoma samples [127–129]. Weinberger *et al.* revealed that EGFR is highly expressed in chordomas compared with seventeen different malignancies and healthy control nucleus pulposus [130,131]. EGFR overexpression in spinal chordomas also cause poorer prognosis [132].

PDGFR is a RTK that execute growth, proliferation, tumorigenesis, and differentiation [133]. This receptor has two forms: PDGFR-alpha and PDGFR-beta. PDGFR is overexpressed in several cancers such as pancreas cancer, breast cancer etc. and responsible in tumor growth, metastasis, and angiogenesis [134,135]. Although both PDGFR-alpha and PDGFR-beta were highly expressed in chordoma, their expression is less than normal tissues. Furthermore, PDGFR-beta is more active in chordomas than PDGFR-alpha [136].

PI3K/Akt/mTOR pathway is a signaling pathway that regulates cell cycle, survival, tumorigenesis and motility in cancer. This signaling cascade was found to be activated in breast cancer and prostate cancer [137]. Several studies demonstrated that PI3K/Akt/mTOR signaling axis is highly active in chordoma [138,139]. Schwab *et al.* showed that inhibition of PI3K/Akt/mTOR pathway in U-CH1 inhibited proliferation and induced apoptosis [139]. Activation of Akt in chordomas also caused decreasing of overall survival [127].

Mitogen Activated Protein Kinase (MAPK) pathway begins with the activation of receptor RTK. Activation RTK contribute the phosphorylation of RAS protein, phosphorylated RAS protein activates MEK protein. MEK causes phosphorylation of ERK protein and it can activate many transcription factors responsible in cell proliferation, apoptosis resistance and resistance to chemotherapy and radiotherapy [140–143]. Expression of ERK1 and ERK2 proteins is highly active in chordoma [129,144]. There is a significant relationship between RAF1 and muscle invasion and recurrence. In addition, ERK1/2 expression is significantly related to tumor size [144].

Brachyury is a T-box transcription factor and manages the mesodermal formation of Embryonic Stem Cell (ESC) and tail formation in mice [145]. Their expression is also shown in teratomas and several cancers such as lung, prostate, colon and breast cancers.

Brachyury is highly active in chordoma. Although high brachyury expression indicator for poor prognosis in colon cancer, there is no association between brachyury expression and clinical outcome of chordoma [146,147].

c-met also known as Hepatocyte Growth Factor Receptor (HGFR) is also upregulated in chordoma [131,148,149] and age of a patient with chordoma is associated inversely with c-met expression [132,149].

Survivin (also known as BIRC5) expression in chordoma is firstly described from Chen *et al.* in 2013. 70 percent of 30 patients were positive for Survivin expression detected by immunohistochemistry. Moreover, *BIRC5* expression is positively correlated with recurrence [150]. A study suggested that silencing of Survivin in chordoma cells resulted G2/M arresting in cell cycle and decreased viability in a dose dependent manner [151].

#### ***1.2.1.4. Symptoms and Signs of Chordoma***

Therapeutic approaches are very limited for chordoma due to resistance to chemo- and radio-therapy. Patients with skull base chordoma who had undergone radical surgery had increased overall survival time but surgery still remains to be cautious as one may invade the dural barrier [152]. Sacral chordomas are also not applicable to operate due to tumor's anatomical location and infection risk. Pain in a location where found the tumor and several neurological signs such as headache, abnormality in vision, and disequilibrium are shown in patients with clival chordoma [153].

Local relapse of chordoma is associated with surgical margin. Briefly, while 10-20 percent of patients with chordoma who had operated with negative margins shows recurrence, recurrence ratio of patients with chordoma who had operated without negative margins is 70 percent [154,155]. In addition, 10-40 percent of patients with chordoma show metastasis to distant tissue and organs [113,114,156]. Nonetheless, metastasis ratio of patients with clivus chordoma is approximately 10 percent [114].

#### **1.2.1.5. Treatment of Chordoma**

Treatment options are very limited due to chordomas' nature. Surgical procedures for chordoma is separated into four groups: 1) Intralesional, 2) Marginal, 3) Wide and 4) Radical (is the most effective) [157,158]. *En bloc* resection of chordoma is the most useful method since it provides resection of tumors completely. *En bloc* resection is applicable for only 15-20 percent of the events [159]. Surgeons also need to be careful during the surgery since tumor might be close to parts of brain that affect patient's life. Radiotherapy and/or proton beam is the standard approach after the surgery.

Although chordoma is classified as radio-resistant, radiotherapy improves the prognosis of chordoma. Nowadays, proton beam used mostly for patients with skull-base chordoma is also operated to treat chordoma and it increases the life quality of patients with chordoma [160,161].

There is no approved chemotherapy approach for chordoma since it is highly resistant to chemotherapy. Several RTK-related signaling pathways including PDGF, Akt, mTOR etc. is activated in chordoma. Thus, RTK inhibitors might be useful for chordoma treatment. Imatinib, a kind of RTK inhibitor, can improve the prognosis of the disease. Phase-two studies are still going on for imatinib [162,163].

Lapatinib that targets both EGFR and HER2 is also beneficial for EGFR-positive chordomas [123]. Its phase-2 studies are also continuing. Cao *et al.* revealed that the mixture of PARP inhibitor and temozolomide had a great effect on tumorigenesis of chordoma [164]. Although lots of studies were carried out by researchers in order to overcome chordoma, effective treatment options still could not be emerged. Effective systemic therapy should be appeared for the treatment of patients with metastatic or relapsed chordoma.

#### **1.2.1.6. Prognosis of Chordoma**

Average survival time is approximately 7 years for patients with chordoma after the diagnosis. Percentage of 5-year and 10-year overall survival time after the surgery is 67.3 percent and 53.9 percent, respectively [165]. *En bloc* resection of chordoma is the best

method (if applicable) and increased a patient's lifetime. Radiotherapy and/or proton beam after surgery also increase disease-free survival time [166]. Patients with clival chordoma show worse prognosis than patients with sacral chordoma. Metastasis is also related with poor prognosis and reduced survival time.

#### ***1.2.1.7. Chordoma Cell Lines***

Over the years, lots of universally accepted chordoma cell lines were approved by chordoma foundation. Today, 17 different chordoma cell lines were available by chordoma foundation. Thirteen of them also can be provided by ATCC. Chordoma cell lines were classified according to tumor location, disease status, and age of a patient with chordoma. However, there is no universally accepted recurrent-clival chordoma cell line yet. As a result, *in vitro* modeling of recurrence mechanism in clival chordoma studies currently is not possible.

### **1.3. CANCER STEM CELLS**

CSCs share the similar characteristic with normal stem cells including self-renewal and differentiation potency. Several studies suggest that the initiation and progression of cancers are managed by small subpopulation called CSCs. This model is known as Cancer Stem Cell model [167,168]. CSCs are found in the low ratio in heterogenic tumor population and contribute to the maintenance of tumor growth for the long-term period [169]. CSCs are tumorigenic form of cancer cells and have the capability to give rise whole cancer population (Figure 2) [170]. CSCs have increased migration and migration ability along with EMT phenotype and cause metastasis. It is believed that tumor relapses following therapy due to the existence of CSCs in tumor population [171]. CSCs possess drug resistance, invasion and migration ability, metastatic ability, recurrence and tumorigenicity [172,173]. Thus, targeting CSCs could be more effective to cure cancer completely.

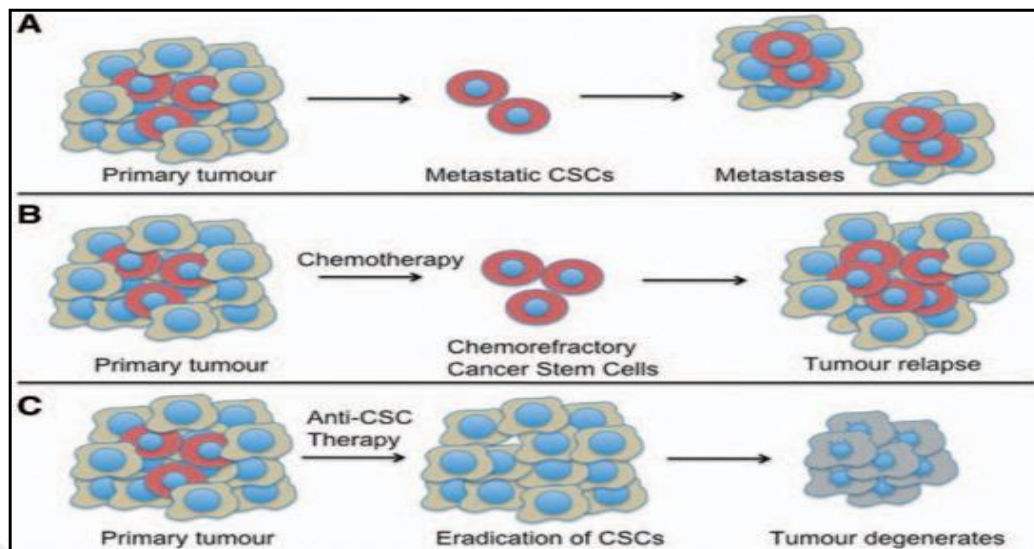


Figure 1.2. CSC hypothesis [170]

Presence of CSCs was firstly defined in acute myeloid leukemia[174]. CD133, also known as neural stem cell marker, was utilized to detect CSC population in pediatric brain tumors and it is found that CD133<sup>+</sup> pediatric brain tumors share similar characteristic with CSCs [175]. Several studies on brain tumors confirmed that CD133<sup>+</sup> tumor cells have CSC characteristic [176,177]. In addition, CSCs in brain tumors have an ability forming neurospheres, self-renewal capacity and share similar active genes which are also active in neural stem cell [178]. CD15<sup>+</sup> tumor cells are also defined as CSCs in brain tumors [179]. CD90<sup>+</sup>CD24<sup>-</sup>ESA<sup>+</sup> breast CSCs were firstly defined by researchers in 2002. They revealed that small number of CD90<sup>+</sup>CD24<sup>-</sup>ESA<sup>+</sup> breast cancer cells successfully form tumors in xenograft models [180]. Breast CSCs are also resistant to chemotherapeutic agents [181] and have increased migration, invasion and metastasis capacity [182,183]. CD90<sup>+</sup> population in high-grade gliomas showed CSCs characteristic [184]. In CSCs, expression of pluripotency-related genes such as *OCT4*, *KLF4*, *C-MYC*, *NANOG* and *SOX2* increased compared with non-CSCs [185]. Many studies suggested that surface markers indicating CSCs can be different and specific for each type of cancer [186].

CSCs can be isolated using one or more antibodies that target cell surface protein on the cancer cells. This technique is termed as fluorescence activated cell sorting (FACS). Briefly, one or more antibody tagged with fluorescence dye incubated with cancer cells and cells which have sparkle can be separated from the population. Separated cells were

then injected in mice in order to assess tumor initiation potential. Aside from antibodies, CSCs also could be detected ALDH activity and side population analysis.

### 1.3.1. Chordoma CSCs

CSC in chordoma was firstly demonstrated by Aydemir *et al.* Several markers including CD90, CD105, CD15, CD34, CD133, CD45, CD166 and CD73 in U-CH1 chordoma cell line were used to determine the ratio of these surface markers. U-CH1 chordoma cell line were then treated with Retinoic Acid (RA) and osteogenic differentiation medium and expression of CSC associated genes including *C-MYC*, *KLF4*, *OCT4*, *NESTIN*, *SOX2*, and *SMAD2* were checked. It is found that U-CH1 chordoma cell line and chordoma tissues express CSC-related genes and chordoma have a differentiation capacity. Moreover, CD133<sup>+</sup> U-CH1 cells showed approximately 10-fold more colony-forming ability when compared with CD133<sup>-</sup>. Taken together, presence of CSCs were firstly shown in chordoma [187]. The study showed that using chemotherapeutic agents with RA resulted in inhibition of U-CH1 chordoma cell line proliferation. Inhibition of chemo-resistance could result from presence of CSCs in chordoma [188]. ALDH activity, which is extensively used to identify CSCs, was measured in MUG-Chor1 chordoma cell line. It is found that MUG-Chor1 chordoma cell line exhibited ALDH activity in a low ratio [189]. Hu *et al.* also showed that tumorsphere-formation of chordoma cells had higher ALDH1 activity associated with CSC phenotype and injection of tumorspheres into mice initiated chordoma formation [190].

## 1.4. MIRNAS

miRNAs are small RNA molecules (approximately 20-22 nucleotide) transcribed from non-coding region of DNA but not translated and regulate gene expression [191]. miRNAs were firstly discovered in *C. elegans*. Nomenclature and function of miRNAs were fully understood in 2001 [192].

Pri-miRNA is transcribed from non-coding region of DNA. Drosha and Pasha cut pri-miRNA in nucleus and pre-miRNA (approximately 70 nucleotides) occurs. Pre-miRNA transported from nucleus to cytoplasm through Exportin-5 protein. DICER is an RNase III

enzyme cleaves pre-miRNA and mature miRNA formed in cytoplasm. miRNAs regulate gene expression through binding their complementary mRNA and cause degradation of mRNAs and/or inhibition of translation (Figure 3) [193].

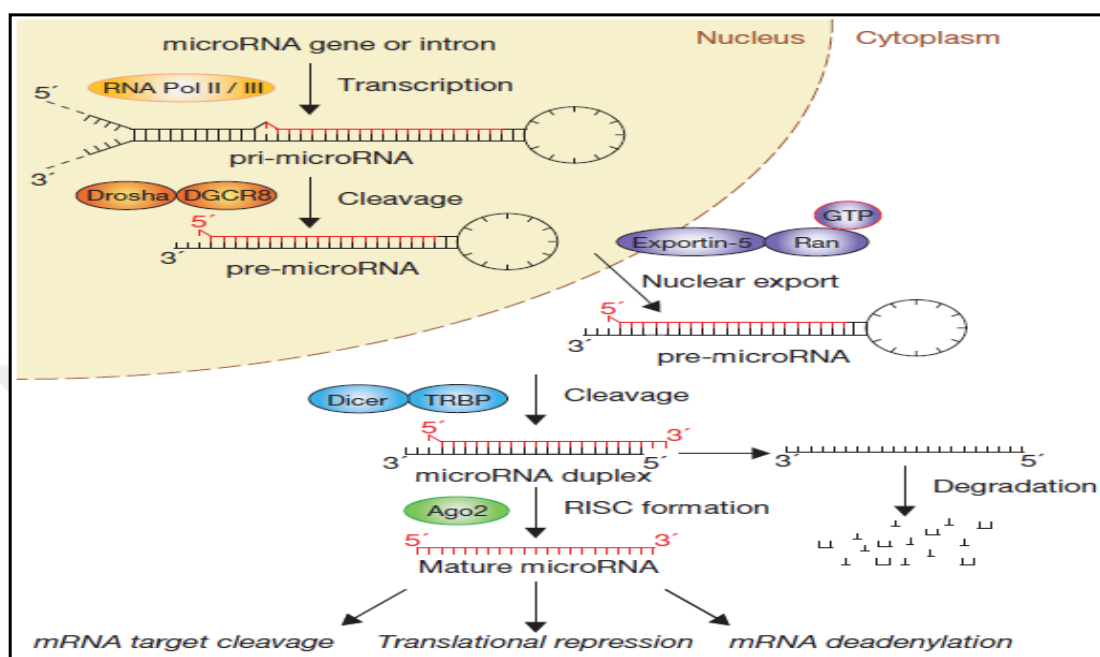


Figure 1.3. miRNA Biogenesis [193]

#### 1.4.1. Role of miRNAs in Cancer

miRNAs have very important roles in several cellular processes such as differentiation, cancer, growth, cell migration, metastasis etc. Their role in cancer has been found in almost all type of cancers. miRNAs responsible in cancer are classified into two groups: 1) Tumor suppressor miRNAs and 2) Oncogenic miRNAs.

Tumor suppressor miRNAs are usually diminished during initiation and progression of carcinogenesis. Overexpression of tumor suppressor miRNAs inhibits invasion and migration ability, metastasis, recurrence, chemo-resistance, proliferation etc. of cancer cells. For example, miR-15 and miR-16 targets BCL2 and stimulate apoptosis [68]. Calin et al. firstly described the relationship between cancer and miRNA. They found that miR-15 and miR-16 were downregulated in chronic lymphocytic leukemia [66]. Let-7 miRNA family which was identified firstly in *C. elegans* has 9 different members. They are downregulated in numerous types of cancers such as hepatocellular carcinoma, gastric



carcinoma, breast cancer etc. [194]. Studies revealed overexpression of let-7 can both activate apoptosis and cell cycle arrest and inhibit proliferation, chemoresistance, EMT and stem cell phenotype, and metastasis[195]. Expression of miR-34 family referred as tumor suppressor miRNAs also diminished in cancer. It is downregulated in breast cancer, epithelial ovarian cancer, hepatocellular carcinoma, osteosarcoma, and prostate cancer. miR-34 family have an important role in blocking tumorigenesis by involving several signaling pathways responsible in tumorigenesis such as TGF- $\beta$ , Smad, Wnt and Notch [196].

Oncogenic miRNAs (oncomiRs) are upregulated in cancer. Downregulation of oncomiRs stimulates apoptosis and cell cycle detention and inhibits tumor progression. As an example, miR-17-92 family is highly expressed in lymphoma and lung cancer compared with healthy tissue. Overexpression of this oncomiR increase growth of lung cancer and nascency of lymphoid tumors [197,198]. Furthermore, miR-17-92 directly regulates PTEN and RB also known as tumor suppressor genes [159]. miR-372 and miR-373 are also classified as oncomiRs. These oncomiRs target LATS2 and counteract P53-associated cyclin-dependent kinase (CDK) blocking [199].

#### ***1.4.1.1. Dysregulated miRNAs in Chordoma***

First miRNA study on chordoma was done by Duan *et al.* in 2009. miRNA profile of two primary chordoma tissue and two chordoma cell lines were compared with muscle cells. It is found that while miR-193a-5p was increased expression pattern in chordoma, miR-1 and miR-206 were diminished. Transfection of miR-1 to U-CH1 cell line caused silencing of Met and Slug expression and growth inhibition of U-CH1. Moreover, ectopic miR-1 expression decreased migration and invasion abilities of chordoma cells. In addition, decreased expression of miR-1 strongly related with overall survival time [200–202]. A study showed that expression of miR-155 was increased in chordoma and correlated with disease stage and metastasis. Overexpression of miR-155 also caused decreasing of overall survival time in chordoma patient and downregulation of miR-155 inhibited proliferation, migration, and invasion of chordoma cells in time- and dose-dependent manner [203]. When miRNA level of chordoma cell lines and primary chordoma cells checked against human fibroblast and astrocyte cells, it is found that miR-34a and miR-608 were

downregulated in chordoma. miR-34a directly regulated Met and miR-608 directly regulated EGFR. While proliferation and invasion were inhibited through ectopic expression of miR-34a and miR-608, apoptosis was promoted [204]. Transient transfection of mir-31 also inhibited proliferation of chordoma cells. Both mir-31 and anti-miR-148 transfection promoted apoptosis in chordoma cells. In addition, transfection of mir-31, anti-miR-140, anti-miR-148 and miR-222 arrested S phase in three chordoma cell lines. It is also found that miR-31 regulated *RDX* and *MET* expression, miR-148 regulated *DNMT1* and *DNMT3b* and miR-222 regulated *TRPS1*, *BIRC5* and *KIT* in chordoma cell lines [205,206]. Analyzing the both of miRNA and mRNA microarray profile of three chordoma samples and three embryonic notochords revealed that 33 miRNAs and 2791 mRNAs were expressed differentially. It is also revealed that 911 mRNAs paired with their candidate miRNA targets [207].

### **1.5. THE AIM OF THE STUDY**

Our group previously revealed that chordoma cell line U-CH1 and chordoma tissues express CSC related genes such as *NANOG*, *C-MYC*, *KLF4*, *OCT4*, *NESTIN*, *SOX2*, and *SMAD2* and CD133<sup>+</sup> U-CH1 cells have more colony forming ability than CD133<sup>-</sup> [187]. U-CH1 chordoma cell line was resistant to several chemotherapeutic agents and this resistance could be a result of CSC presence in a chordoma cell population. The aim of this study is to determine and characterize CSC population and identify miRNA and mRNA profile of CSCs in chordoma cell lines.

CSCs in chordoma were not fully characterized so this study will be first study about the detailed characterization of CSCs in chordoma. Several studies compared miRNA levels between chordoma and healthy tissues (Nucleus pulposus, muscle, embryonic notochord) but there is no study about miRNA and mRNA regulation in CSCs of chordoma. Characterization of CSCs in chordoma and identification of their miRNA and mRNA profile will help us to elucidate the roles of CSCs in chordoma which might provide more effective treatment of chordoma. Moreover, studies revealed that a small number of CSCs could cause recurrence of cancer and patients with chordoma die due to recurrence. Thus, identification of recurrence-related signaling pathways in chordomas

could also be prominent to treat chordoma which has high tendency to relapse after surgical resection of tumor.



## 2. MATERIALS AND METHODS

### 2.1. CHORDOMA SAMPLES

Human chordoma tissue samples were provided by the Department of Neurosurgery, Yeditepe University Hospital, in Istanbul, Turkey. None of the patients had treated with chemotherapeutic agents. Samples were stored immediately in  $-80^{\circ}\text{C}$  until RNA isolation. Clinicopathological data were collected retrospectively. The follow-up time was calculated as the time elapsed between the date of surgery and death or last contact time. While tumor samples pathologically defined as chordoma were included in the study, samples with insufficient patient information or follow-up time less than 6 months were excluded from the study. All samples were obtained in accordance with the approved ethical standards of the responsible committee of Yeditepe University Hospital and the study was approved by the institutional review board accordingly. Written informed consent was obtained from all participants.

### 2.2. CELL CULTURE

U-CH1, U-CH2, JHC7, and MUG-Chor1 were kindly gifted by Chordoma Foundation (Durham, NC). MUG-Chor1 was generated by Rinner *et al.* from a 58-years-old Caucasian female and characterized as recurrent morphologically ‘classic’ sacrococcygeal chordoma while U-CH1 and U-CH2 were generated by Bruderlein *et al.* and characterized as recurrent sacral chordoma. JHC7 was generated from a 61-years-old female primary sacral chordoma patient by Quinones-Hinojosa, Johns Hopkins University. Chordoma cell lines (except JHC7) were cultured in 0.1 percent gelatin (Sigma-Aldrich, USA) coated flask or plates and fed with IMDM/RPMI (4:1) medium supplemented with 10 percent Fetal Bovine Serum (FBS) and 1 percent antibiotics. JHC7 cell line was cultured in DMEM/F12 (1:1) medium supplemented with 10 percent FBS and 1 percent antibiotics. Routine checking was done for molecular markers, and Polymerase Chain Reaction (PCR)-based mycoplasma screening and sanger sequencing were used for Short Tandem Repeats (STR profile) to verify that characteristics of the original cell line were retained.

### **2.3. STR ANALYSIS**

DNA was extracted from the cell pellets using DTAB/CTAB method as previously described [208]. STR analysis was carried out AmpFISTR® Identifiler® PCR Amplification (Applied Biosystems, USA) according to manufacturer's instruction.

### **2.4. ARRAY CGH**

To detect genomic alterations in our samples, CytoScan™ Optima Training Kit (Thermo Fisher, USA) was used as manufacturer's instruction. Raw data was analyzed using Chas Analysis 4.0 software.

### **2.5. FLOW CYTOMETRY**

Chordoma cells were harvested with 0.05 percent trypsin when confluency reached to 80 percent and re-suspended in Phosphate Buffered Saline without Ca<sup>++</sup> and Mg<sup>++</sup>. FcR-blocking human reagent (Miltenyi Biotech, Germany) was added and incubated for 5 min on ice. Cells were then incubated with CD133 conjugated with APC (Cat no:130-090-826, Miltenyi Biotech, Germany) and CD15 conjugated with FITC (Cat no:133-113-484, Miltenyi Biotech, Germany) antibodies for 30 min and then washed with PBS without Ca<sup>++</sup> and Mg<sup>++</sup> to eliminate unbound antibodies. The unstained cells were used to determine gates and DAPI was used to eliminate dead cells. CD133<sup>+</sup>CD15<sup>+</sup> and CD133<sup>-</sup>CD15<sup>-</sup> chordoma cells were sorted through FACS Aria III (BD Biosciences, USA).

### **2.6. MIRNA AND MRNA MICROARRAY**

Total RNA was isolated by TRIzol (Cat no:15596018, Thermo Fisher Scientific, USA) from CD133<sup>+</sup>CD15<sup>+</sup> and CD133<sup>-</sup>CD15<sup>-</sup> chordoma cells and was used for whole transcriptome analysis using Human Gene 2.1 ST Array (Affymetrix, GeneAtlas System) and miRNA 4.1 Strip Array (Affymetrix, GeneAtlas System, USA) according to the manufacturer's protocol. Data were analyzed with Transcriptome Analysis Console 3

software (Affymetrix, USA) and Ingenuity Pathway Analysis (Qiagen) software [209]. miRNAs were selected according to fold-change in chordoma CSCs and their predictive targets' relationship with CSC-related signaling pathways.

## 2.7. MIRNA AND ANTI-MIRNA TRANSFECTION

Ambion FAM3 Dye-Labeled Pre-miR Negative Control #1 (Cat No: AM17121, Life Technologies, USA) was introduced into chordoma cell lines using X-tremeGENE siRNA Transfection Reagent (Sigma, USA) for 24 hours in order to evaluate transfection efficiency. Efficiency was evaluated with fluorescent microscopy. Transfection with pre-mir and anti-miR oligos including; pre-mir-140-3p (Cat no: PM12503, Thermo Fisher Scientific, USA), pre-mir-148a-3p (Cat no: PM10263, Thermo Fisher Scientific, USA), pre-mir-152-3p (Cat no: PM12269, Thermo Fisher Scientific, USA), pre-mir-210-5p (Cat no: PM27291, Thermo Fisher Scientific, USA), and pre-miR-574-5p (Cat no: PM13081, Thermo Fisher Scientific, USA) and anti-miR-140-3p (Cat no: AM12503, Thermo Fisher Scientific, USA), anti-miR-148a-3p (Cat no: AM10263, Thermo Fisher Scientific, USA), anti-miR-152-3p (Cat no: AM12269, Thermo Fisher Scientific, USA), anti-miR-210-5p (Cat no: AM27291, Thermo Fisher Scientific, USA), and anti-miR-574-5p (Cat no: AM13081, Thermo Fisher Scientific, USA) were set as 100 nM concentration into chordoma cell lines individually or collectively.

## 2.8. GENE EXPRESSION ANALYSIS

Total RNA was also isolated from both chordoma cell lines and chordoma tissues with Trizol Reagent. cDNA was synthesized from 1000 ng total RNA by High-Capacity cDNA Reverse Transcription Kit (Thermo Fisher Scientific, USA). Expression levels were detected by TaqMan™ Universal Master Mix II (Thermo Fisher, USA) and normalized using  $2^{-\Delta\Delta Ct}$  method. *GAPDH* was used as housekeeping gene. Control groups were used for normalization. For miRNA levels, cDNAs were synthesized from total RNAs and expression levels for selected miRNAs were

determined by miRCURY LNA RT Kit (Exiqon, Denmark). As an internal control 5S RNA was used.

## **2.9. VIABILITY AND APOPTOSIS ASSAY**

Chordoma cells were transfected individually to assess the function of pre- and anti-mimics of selected miRNAs on cell viability and apoptosis. MTS (Promega, Australia) was used in line with the producer's instruction in order to explore the role of selected miRNAs on viability after 72 hours of transfection. Briefly, MTS Solution was added to each well of 24-well plate contains transfected cells and incubated at 37 °C for 1 hour. The viability was measured by detecting absorbance at 490 nm with an ELx800 ELISA microplate reader (BioTek, USA). Scrambled miRNA groups were used as controls. PE Annexin V Apoptosis Detection Kit I (BD Pharmingen, USA) was used to detect apoptotic cells. Cells seeded as  $10^5$  cells/well in a 6-well plate were transfected with selected miRNAs and harvested after 48 hours, followed by staining with Annexin V conjugated with PE and 7-AAD. Results were evaluated using FACS Aria III (BD Biosciences). Unstained controls were used to determine gates.

## **2.10. INVASION AND MIGRATION ASSAY**

Transwell membrane inserts (Cat no: PIEP12R48, Millipore, USA) were used to detect invasion and migration ability of chordoma cells. For the invasion assay, chambers were coated with 100  $\mu$ l of 250  $\mu$ g/ml Basement Membrane Matrigel (Cat no: 354234, BD Biosciences, USA) and incubated overnight at 37 °C. Then, the upper chambers filled with 200  $\mu$ L culture media excluding FBS contained  $5 \times 10^4$  cells per chamber and the lower chambers filled with 1300  $\mu$ L culture media consisting of 10 percent FBS. After 48 hours of transfection at 37 °C cells were fixed with 3.7 percent paraformaldehyde, permeabilized with 100 percent methanol, and stained with 0.005 percent crystal violet. Cells were visualized and counted under an inverted microscope.

### **2.11. COLONY FORMATION ASSAY**

6-well plates were coated with 1 ml of chordoma complete medium mixed with 1 percent low melting agarose (Cat No: A9045, Sigma, USA) as a bottom layer and incubated at 37 °C. As a top layer, chordoma complete medium containing 0.7 percent low melting agarose mixed with  $1 \times 10^4$  chordoma CSCs and/or non-CSCs was prepared. Chordoma complete medium was added twice a week in order to avoid evaporation. After 4 weeks of incubation, plates were stained with 0.005 percent crystal violet in 40 percent methanol for 1 hour, washed with PBS, and colonies were counted under a light microscope.

### **2.12. TUMOROSPHERE FORMATION ASSAY**

Chordoma CSCs and non-CSCs were seeded onto an ultra-low attachment 24-well plate as  $2.5 \times 10^2$  per well in medium containing IMDM/RPMI (4:1) with 1 percent antibiotics, 100 ng/ml human FGF-2 (Cat No: 9952, Cell Signaling, USA), 100 ng/ml EGF (Cat. No: PHG0311, Thermo Fisher, USA), 1X N2 supplement (Cat No: 17502048, Thermo Fisher, USA), 1X B27 supplement (Cat No: 17504044, Thermo Fisher, USA). Sphere-forming medium was added onto the wells twice every week. The total number of the tumorspheres was counted under the light microscope after 4 weeks of incubation.

### **2.13. WOUND HEALING ASSAY**

Chordoma cell cells were seeded onto 24-well plate in medium containing IMDM/RPMI (4:1) with 10 percent FBS, and 1 percent antibiotics. Once cells transfected with miRNAs groups (CSC-related and non-CSC-related), a scratch was created using a 200 ul pipette tip. Images were taken 2 days after scratch was made. The closure was measured on day 2 using Image J.

### **2.14. ALDEFLOUR ASSAY**

Aldeflour Assay (Cat No: #01705, Stem Cell, USA) was carried out according to the producer's instruction. ALDH<sup>high</sup> cells were detected using FACS Aria III (BD



Biosciences, USA). Diethylaminobenzaldehyde (DEAB), an inhibitor of ALDH, treated cells were used to determine ALDH<sup>high</sup> cells.

## **2.15. STATISTICAL ANALYSIS**

Results of experiments are expressed as mean  $\pm$  SEM. The microarray data were analyzed with one-way repeated measures of ANOVA (paired). Spearman's two-tailed correlation test and the two-tailed chi-square test were used for clinicopathological features. Briefly, expression levels of relevant genes for each patient were correlated with the tumor volume before the surgery and positive percentage of P53 and Ki67 individually. For the chi-square test, patients' groups expressed low or high miRNA and mRNA groups were allocated according to the average expression level value and analysis was performed. Student's t-test was used for all other statistical analysis.  $P < 0.05$  was considered statistically significant. Significant outliers were excluded using Grubbs' test. All experiments were carried out triplicated.

### 3. RESULTS

#### 3.1. DYSREGULATED MIRNAS AND MRNAS IN CHORDOMA CSCS

This study has been published as “Distinctive role of dysregulated miRNAs in chordoma cancer stem-like cell maintenance.” *Experimental Cell Research* 2019;380(1):9-19, doi: <https://doi.org/10.1016/j.yexcr.2019.03.039> [210].

##### 3.1.1. Identification and Characterization of CD133<sup>+</sup>CD15<sup>+</sup> Chordoma Cells

Flow cytometry analysis revealed that CD133<sup>+</sup>CD15<sup>+</sup> chordoma cells represented 1-1.5 percent of the entire population in chordoma cell lines as expected (Fig. 3.1). CD133<sup>+</sup>CD15<sup>+</sup> chordoma cells are found approximately 1 percent ratio in 4 different chordoma cell lines. We also explored that CD90, CD24, and CD44 were positive more than 95 percent in all the chordoma cells (Fig. 3.2).

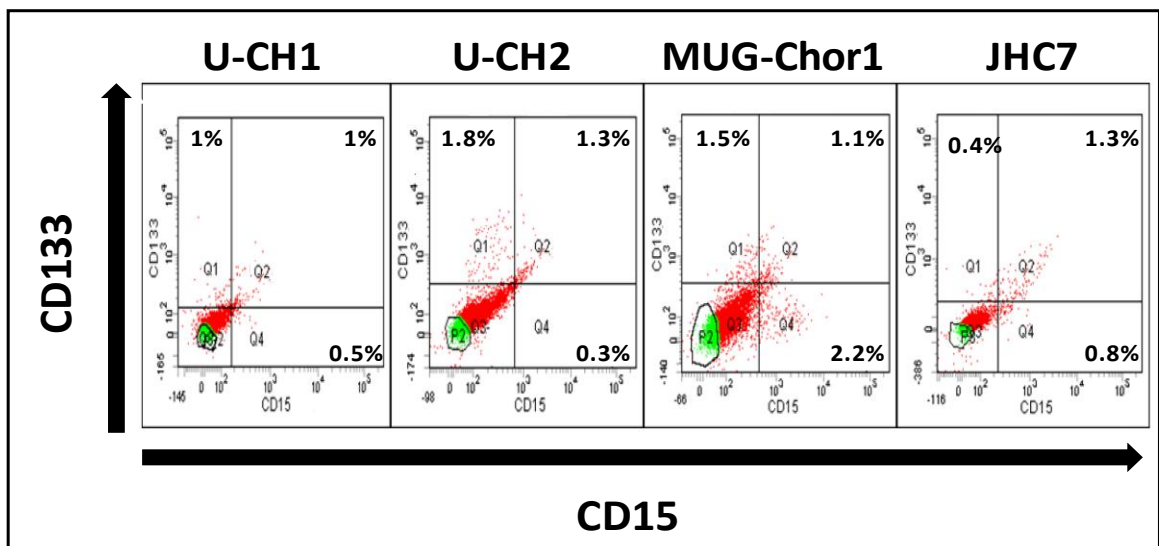


Figure 3.1. Relative ratio of CD133<sup>+</sup>CD15<sup>+</sup> cells in U-CH1, U-CH2, MUG-Chor1, and JHC7 chordoma cell lines. Representative figures from 3 independent trials. Q2 gate represents CD133<sup>+</sup>CD15<sup>+</sup> chordoma cells, P2 (Green) gate represents CD133<sup>-</sup>CD15<sup>-</sup> chordoma cells.

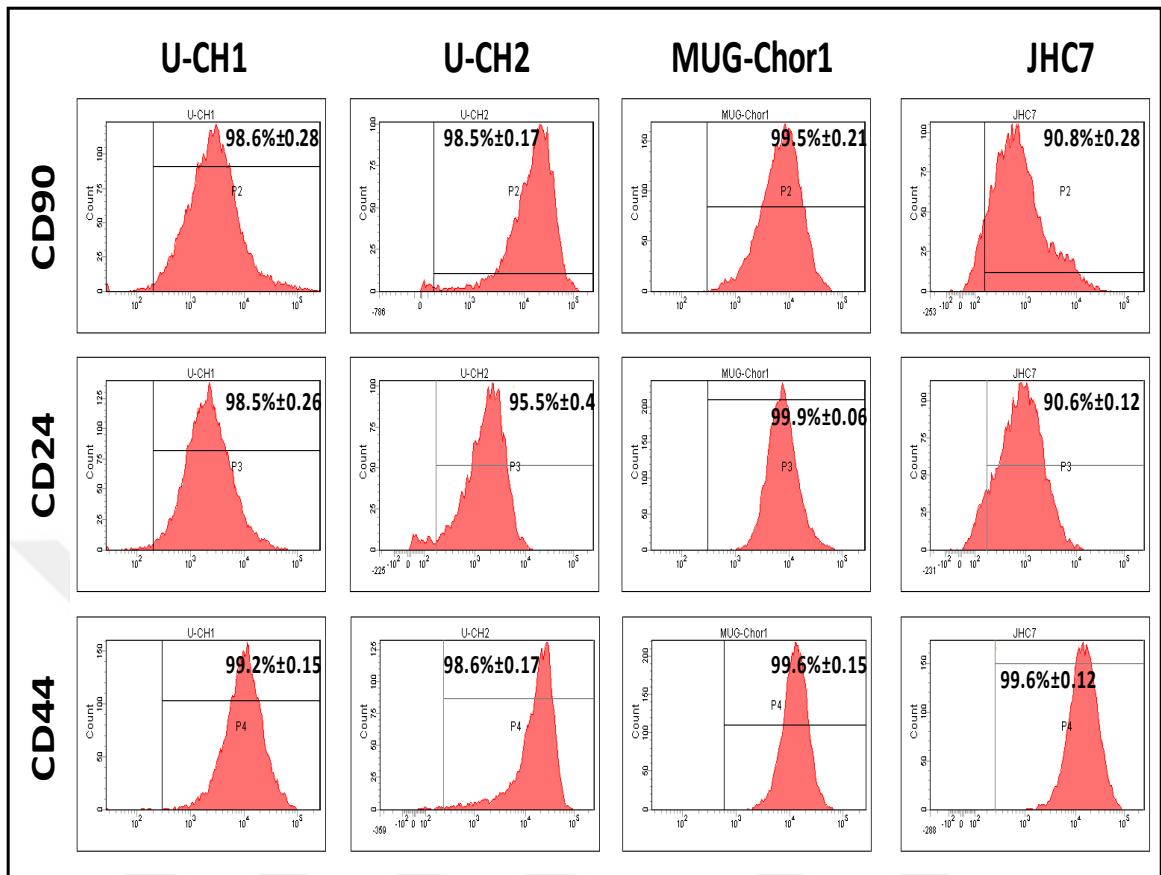


Figure 3.2. CD90, CD24 and CD44 characterization of chordoma cells.  $\pm$  represents the SEM. Gates were determined using unstained controls for each cell line.

CD133<sup>+</sup>CD15<sup>+</sup> and CD133<sup>-</sup>CD15<sup>-</sup> chordoma cells were sorted from the parental cell lines and analyzed for both CSCs and chordoma related gene expressions. According to qPCR analysis, the expression of CSC-related genes such as *C-MYC*, *OCT3/4*, *KLF4*, and *NANOG* was found to be increased in CD133<sup>+</sup>CD15<sup>+</sup> chordoma cells (Fig. 3.3). Expression of *C-MYC*, *OCT3/4*, *KLF4*, and *NANOG* was significantly upregulated in chordoma CSCs in comparison with chordoma non-CSCs (except *C-MYC* in U-CH2). Briefly, expression of *C-MYC* was higher approximately 1-fold in CD133<sup>+</sup>CD15<sup>+</sup> cells of U-CH1, MUG-Chor1 and JHC7. *OCT3/4* was found to be increased 1-fold, 0.8-fold, 2-fold and 0.5-fold in CD133<sup>+</sup>CD15<sup>+</sup> cells of U-CH1, U-CH2, MUG-Chor1 and JHC7, respectively. Expression of *KLF4* was increased up to 2.1-fold, 2-fold, 2-fold and 1.4-fold CD133<sup>+</sup>CD15<sup>+</sup> cells of U-CH1, U-CH2, MUG-Chor1 and JHC7, respectively. Lastly, *NANOG* was significantly upregulated 1.5-fold, 2-fold, 2.3-fold, and 2-fold in U-CH1, U-CH2, MUG-Chor1, and JHC7, respectively. *EMA*, *GAL3*, and *VIM* which are highly

expressed in chordoma showed different expression patterns among the cell lines. While *EMA* was significantly upregulated in just MUG-Chor1 CSCs, *VIM* was significantly upregulated in U-CH1 CSCs. Moreover, *GAL3* was found to be increased in both U-CH1 and MUG-Chor1 CSCs.

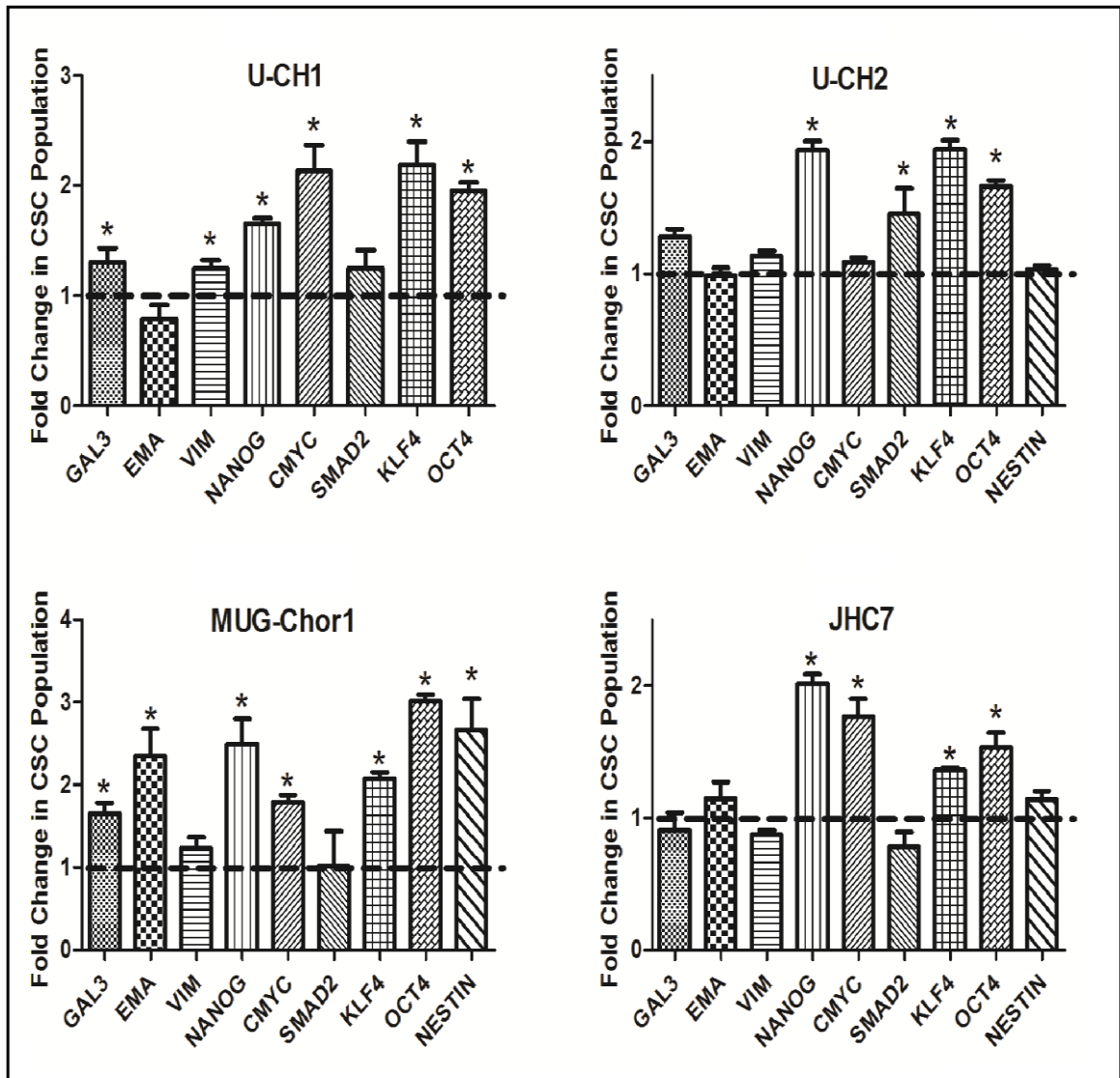


Figure 3.3. Quantification of both chordoma and CSC-related gene expression in CD133<sup>+</sup>CD15<sup>+</sup> versus CD133<sup>-</sup>CD15<sup>-</sup> chordoma cells. The dashed line (=1-fold) symbolize the negative control (CD133<sup>-</sup>CD15<sup>-</sup>). \*: p<0.05.

U-CH1 and MUG-Chor1, well-characterized chordoma cell lines, were used for the subsequent experiments. Invasion and migration capacity of CD133<sup>+</sup>CD15<sup>+</sup> chordoma

cells were checked. We found that CD133<sup>+</sup>CD15<sup>+</sup> chordoma cells had approximately 1.5 more migratory and invasive phenotype than CD133<sup>-</sup>CD15<sup>-</sup> chordoma cells approximately (Fig. 3.4) as indicated in representative images (Fig. 3.5).

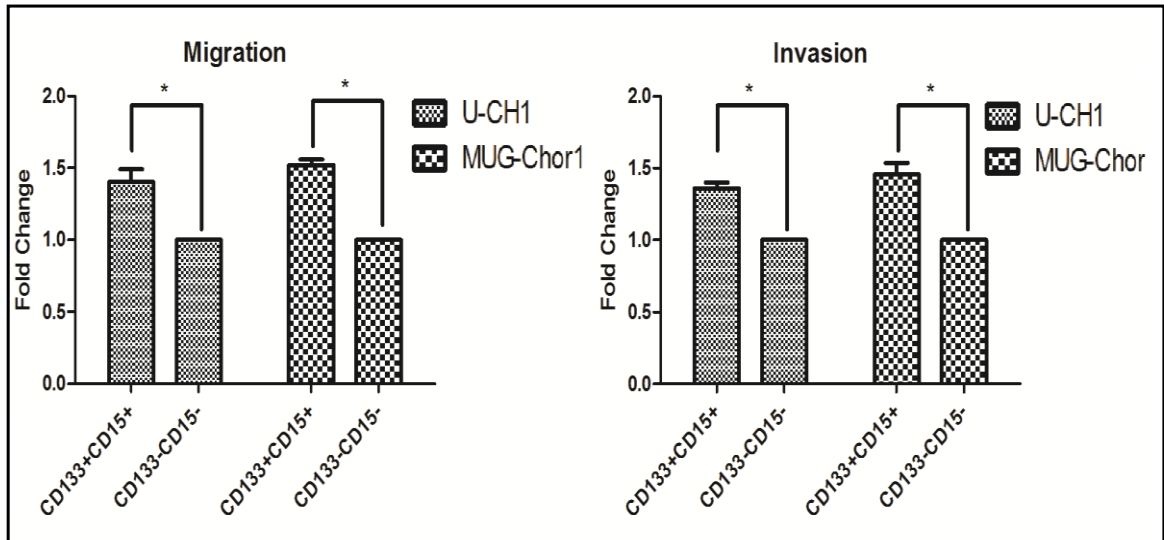


Figure 3.4. Migration and invasion capacity of CD133<sup>+</sup>CD15<sup>+</sup> chordoma cells versus CD133<sup>-</sup>CD15<sup>-</sup>. Migration and invasion capacity of the cells were evaluated 2 days after seeding. For the invasion assay, transwell inserts were coated with basement membrane matrigel. \*: p<0.05.

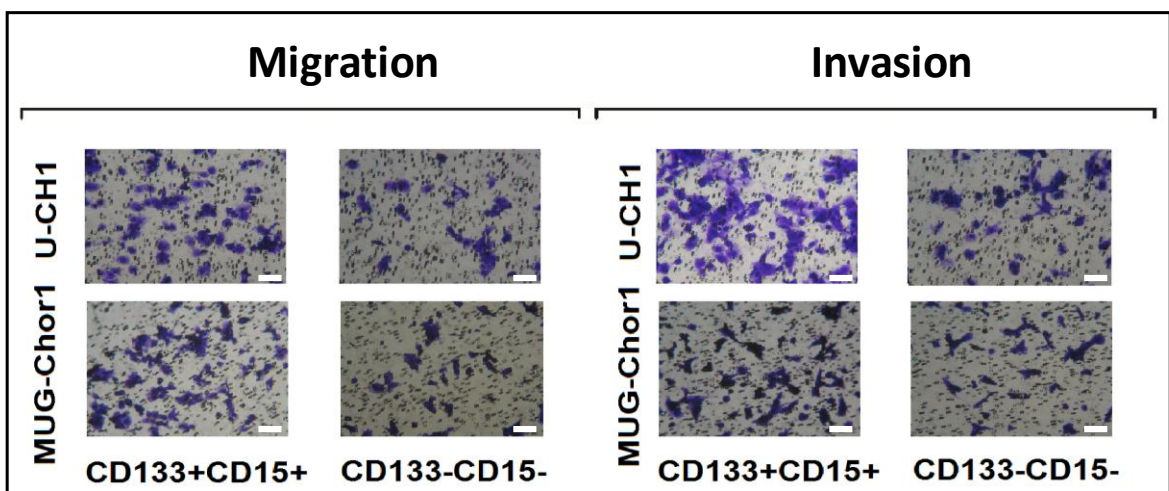


Figure 3.5. Pictures of migrative and invasive cells from CD133<sup>+</sup>CD15<sup>+</sup> and CD133<sup>-</sup>CD15<sup>-</sup> chordoma cells. For the invasion assay, transwell inserts were coated with basement membrane matrigel. Scale bar represents 100 μm.

Tumorsphere- and colony-forming abilities of CD133<sup>+</sup>CD15<sup>+</sup> chordoma cells were also increased compared with CD133<sup>-</sup>CD15<sup>-</sup> (Fig. 3.6) as indicated in representative images (Fig. 3.7). Briefly, colony-forming ability of chordoma CSCs was higher 5-fold and 1-fold in U-CH1 and MUG-Chor1, respectively. In addition, tumorsphere-forming ability of chordoma CSCs was higher 1.1-fold and 0.9-fold in U-CH1 and MUG-Chor1, respectively.

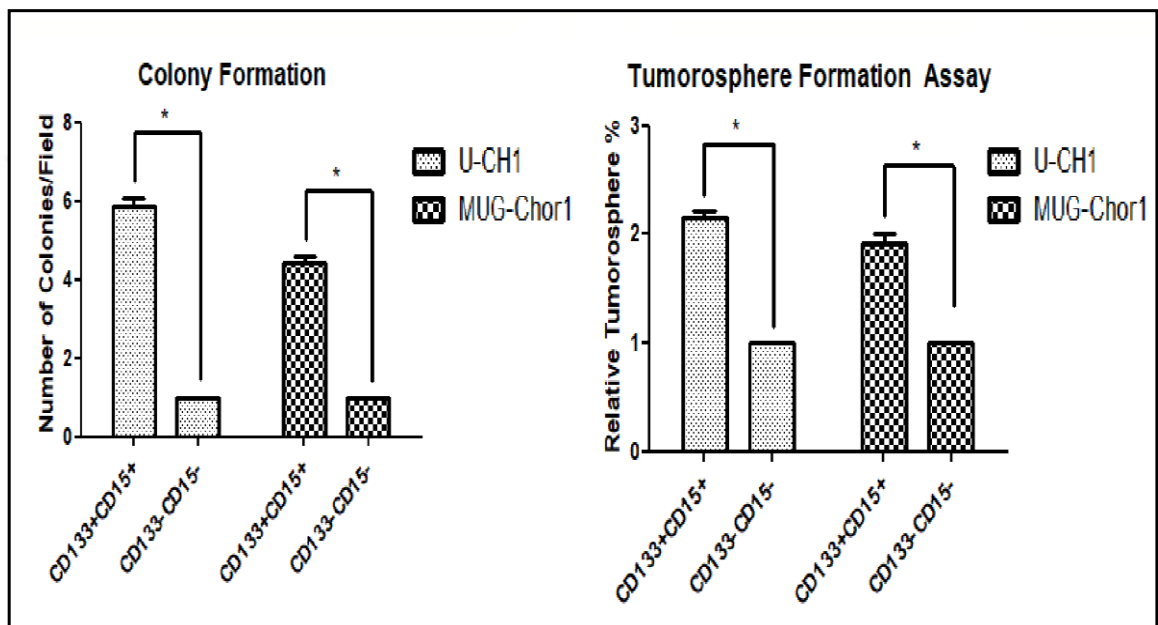


Figure 3.6. Colony-forming and tumorsphere-forming ability of CD133<sup>+</sup>CD15<sup>+</sup> chordoma cells and CD133<sup>-</sup>CD15<sup>-</sup> chordoma cells. Results were obtained 4 weeks after seeding. \*: p<0.05.

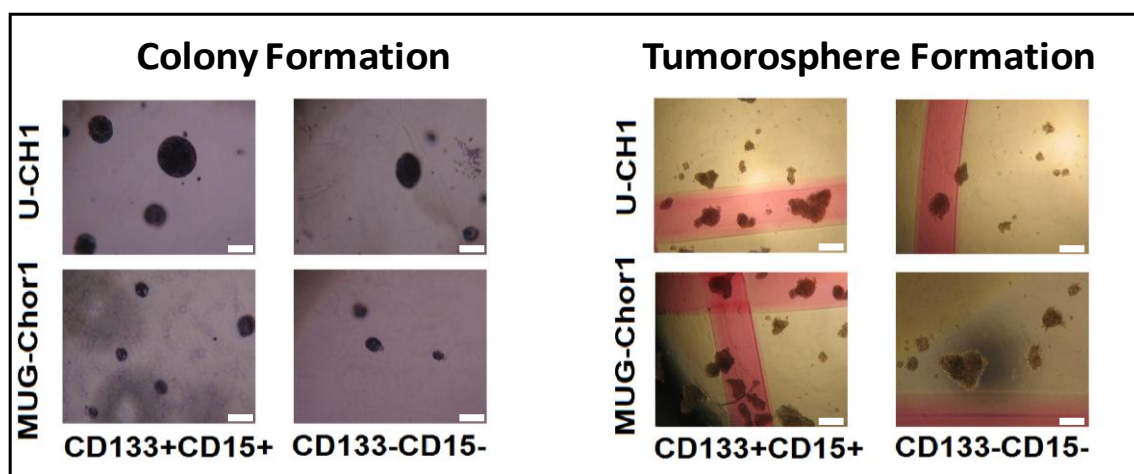


Figure 3.7. Pictures of colony formation and tumorsphere formation from  $CD133^+CD15^+$  and  $CD133^-CD15^-$  chordoma cells. Scale bar represents 100  $\mu\text{m}$ .

EMT profile was confirmed with increased expression of EMT markers including *SNAI*, *SLUG*, *N-CAD*, *ZEB2* and decreased of Mesenchymal-Epithelial Transition (MET) marker including *KRT19* in chordoma CSCs compared with chordoma non-CSCs (Fig. 3.8). While expression of *SLUG*, *SNAI*, *N-CAD*, and *ZEB2* was higher 0.9-fold, 0.4-fold, 2-fold, 0.8-fold in U-CH1 CSCs, their expression was higher 0.2-fold, 1.3-fold, 0.3-fold and 0.3-fold in MUG-Chor1 CSCs, respectively. Furthermore, Expression of *KRT19* was found to be decreased 0.4-fold and 0.8-fold in U-CH1 and MUG-Chor1 CSCs compared with non-CSCs, respectively.

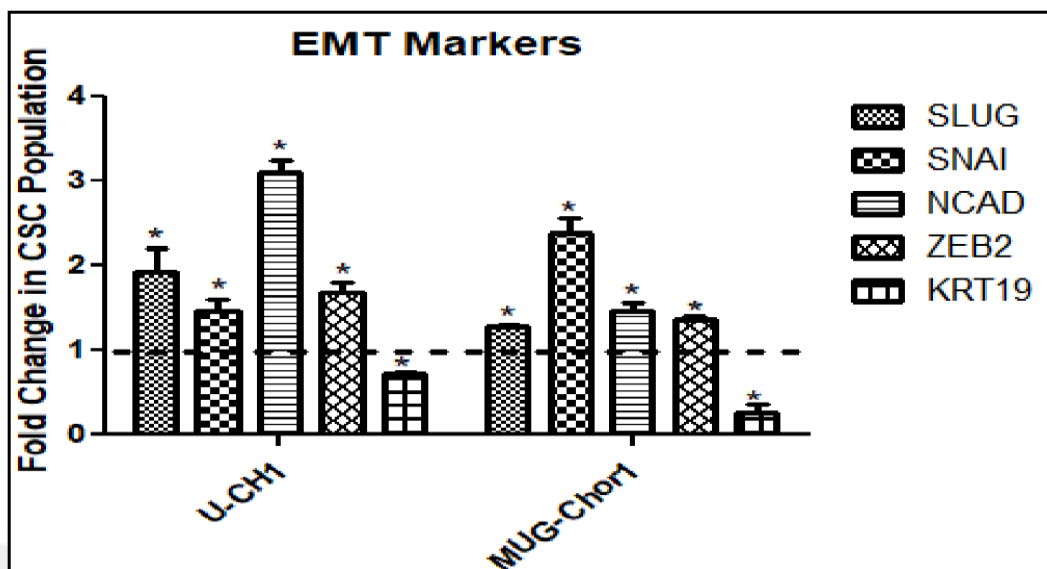


Figure 3.8. Relative quantification of EMT-related gene expression in CD133<sup>+</sup>CD15<sup>+</sup> versus CD133<sup>-</sup>CD15<sup>-</sup> chordoma cells. The dashed line (=1-fold) symbolize the negative control (CD133<sup>-</sup>CD133<sup>-</sup>). \*: p<0.05.

### 3.1.2. Dysregulated miRNAs and mRNAs in Chordoma Cancer Stem-like Cells

Chordoma cell lines were used to determine dysregulated miRNAs in chordoma CSCs. miRNA microarray analyses indicated that 238 miRNAs (15 upregulated, 223 downregulated) were differentially expressed in chordoma CSCs (Fig. 3.9).



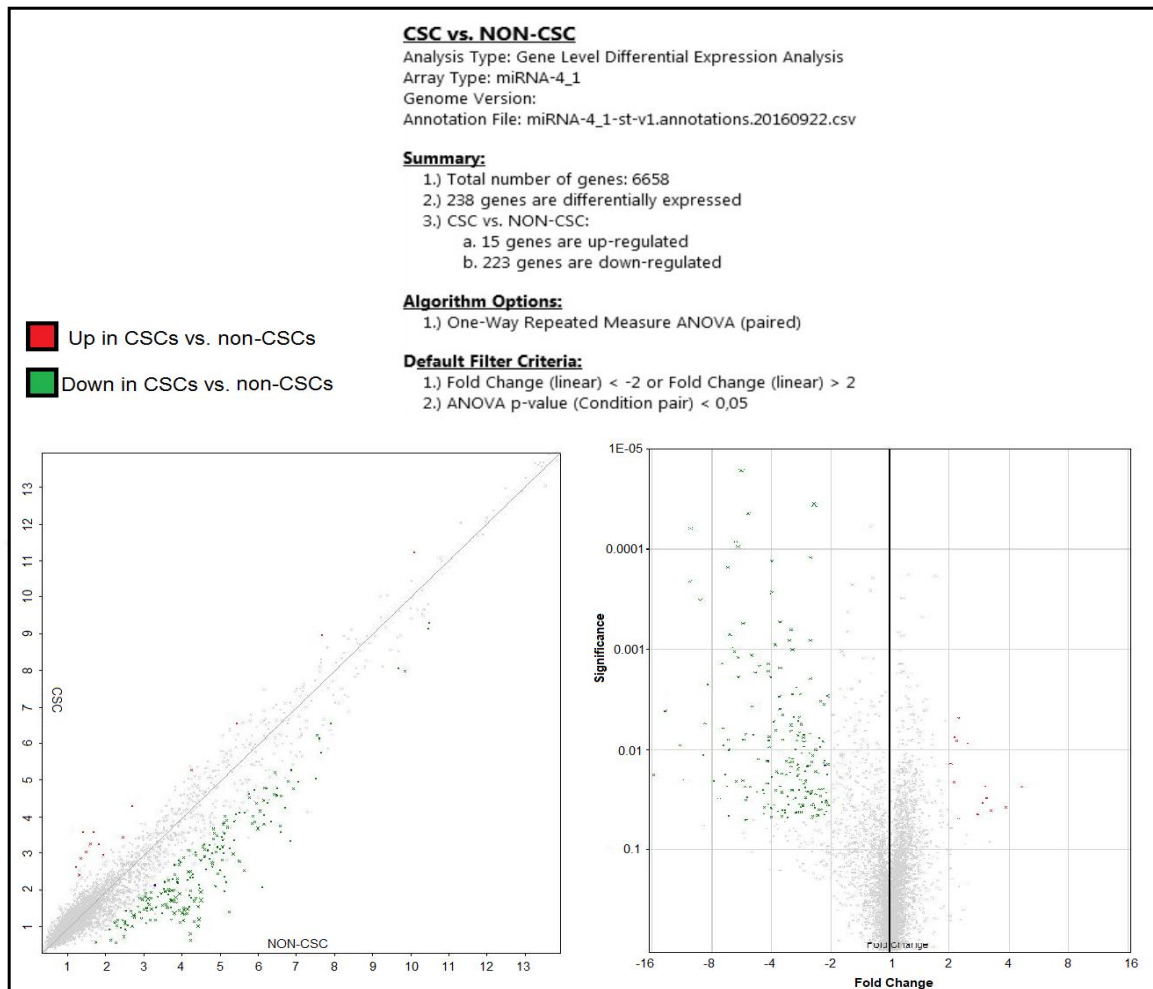


Figure 3.9. miRNA microarray results. Number of upregulated and downregulated miRNAs with scatter plot and volcano plot generated by TAC software.

Five different miRNAs were selected and their predictive targets were identified (Table 3.1) using bioinformatic tools based on their fold change in chordoma CSCs and their targets' association with CSC-related pathways using databases stated in references [211–215]. Based on the analysis, miR-140-3p, miR-148a-3p, miR-152-3p, and miR-574-5p were downregulated and miR-210-5p was upregulated in chordoma CSCs. miRNA microarray results were then confirmed through qPCR. Gene expression analyses verified that miR-140-3p, miR-148a-3p, miR-152-3p, and miR-574-5p were downregulated in range from 0.2-fold to 0.8-fold and miR-210-5p was upregulated in range from 1.2-fold to 2-fold in chordoma CSCs compared with non-CSCs (Fig. 3.10).

Table 3.1. Selected miRNAs from miRNA microarray analysis and their predicted targets

Targeting miRNA	miRNA Fold Change	Predicted Targets
hsa-miR-140-3p	-3.6	WNT5A
hsa-miR-148a-3p	-3.35	TGF-A
hsa-miR-152-3p	-6.57	MAPK1
hsa-miR-210-5p	4.64	TNFAIP2, BTG2
hsa-miR-574-5p	-10.31	MYCBP

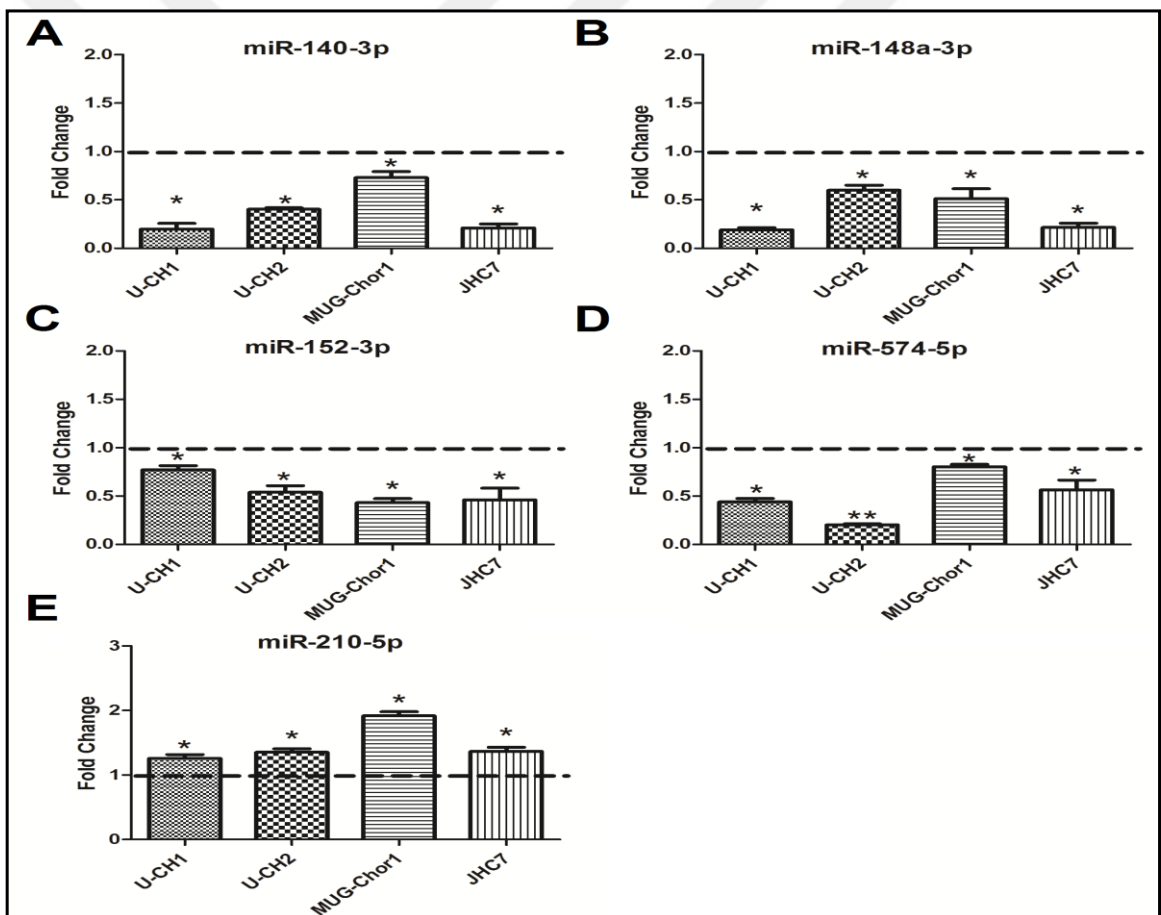


Figure 3.10. Confirmation of miRNA microarray analysis through qPCR using primers specific for (A) miR-140-3p, (B) miR-148a-3p, (C) miR-152-3p, (D) miR-574-5p and (E) miR-210-5p in CD133<sup>+</sup>CD15<sup>+</sup> chordoma cells versus CD133<sup>-</sup>CD15<sup>-</sup>. The dashed line represents 1, which is the normalized value for the CD133<sup>-</sup>CD15<sup>-</sup> for each group. \*: p<0.05. \*\*:p<0.01

p<0.05. \*\*:p<0.01

Dysregulated miRNAs (238 miRNAs) were analyzed in Ingenuity Pathway Analysis software. As a result, miRNAs which activate cell cycle arrest, self-renewal capacity, migration, invasion, and metastasis in cancer and miRNAs, which inhibited apoptosis and proliferation were found to be differentially expressed in chordoma CSCs (Table 3.2).

Table 3.2. Pathways in relation to miRNAs in chordoma CSCs against non-CSCs. miRNA count indicates the number of differentially expressed miRNAs. Predicted activation or inhibition has been provided.

Related Pathways	miRNA Count	Notable miRNAs/ Fold Change		Activated or Inhibited
Cell Cycle Arrest	3	miR-27a-3p/-7.82	miR-20a-5p/-15.63	Activated
		miR-26b-5p/-3.12		
Cell Proliferation	7	miR-23a-3p/-2.52	miR-130a-3p/-2.75	Inhibited
		miR-18a-5p/-3.02	miR-20a-5p/-15.63	
		miR-24-3p/-3.02	miR-27a-3p/-7.82	
		miR-19b-3p/-4.17	miR-193a-3p/-2.60	
Self-Renewal Capacity	1	miR-29a-3p/-4.18		Activated
Migration and Invasion	8	miR-193a-3p/-2.60	miR-181b-5p/-4.19	Activated
		Let-7i-5p/-13.71	miR-20a-5p/-15.63	
		miR-26b-5p/-3.12	miR-29a-3p/-4.18	

		miR-138-5p/-6.56	miR-15b-5p/-5.49	
Apoptosis	6	miR-4651/-2.87	miR-29a-3p/-4.18	Inhibited
		miR-181b-5p/-4.19	miR-15b-5p/-5.49	
		miR-138-5p/-6.56	Let-7i-5p/-13.71	
Metastasis	5	miR-23a-3p/-2.52	Let-7i-5p/-13.71	Activated
		miR-148a-3p/-3.35	miR-20a-5p/-15.63	
		miR-27a-3p/-7.82		

mRNA microarray results revealed that 1064 mRNAs (176 mRNAs were upregulated, 888 mRNAs were downregulated) were differentially expressed in chordoma CSCs (Fig. 3.11). According to the DAVID online software analysis, various pathways including Cell cycle, DNA replication, Spliceosome, Mismatch repair, FoxO signaling, P53 Signaling, Hippo signaling, and BRCA2 and ATR in Cancer Susceptibility were dysregulated in chordoma CSCs (Table 3.3).

mRNA microarray results were also analyzed by Ingenuity Pathway Analysis software to detect notable molecules and upstream regulators in chordoma CSCs. *In silico* analysis revealed that *NUPRI*, *CDKN2A*, *TCF3*, *BNIP3L*, and *KDM5B* genes were predictively activated, whereas, *HGF*, *VEGF*, *CSF2*, *ERBB2*, and *PTGER2* genes were inhibited in chordoma CSCs. In addition, *mir-154*, *FNI*, *LBP*, *IGH*, and *CYP2B6* genes were found to be as notable molecules that could be used as diagnostic, prognostic, efficacy and safety biomarkers (Table 3.4).

The microarray data have been submitted into GEO database (GEO numbers: GSE109943 and GSE109944).

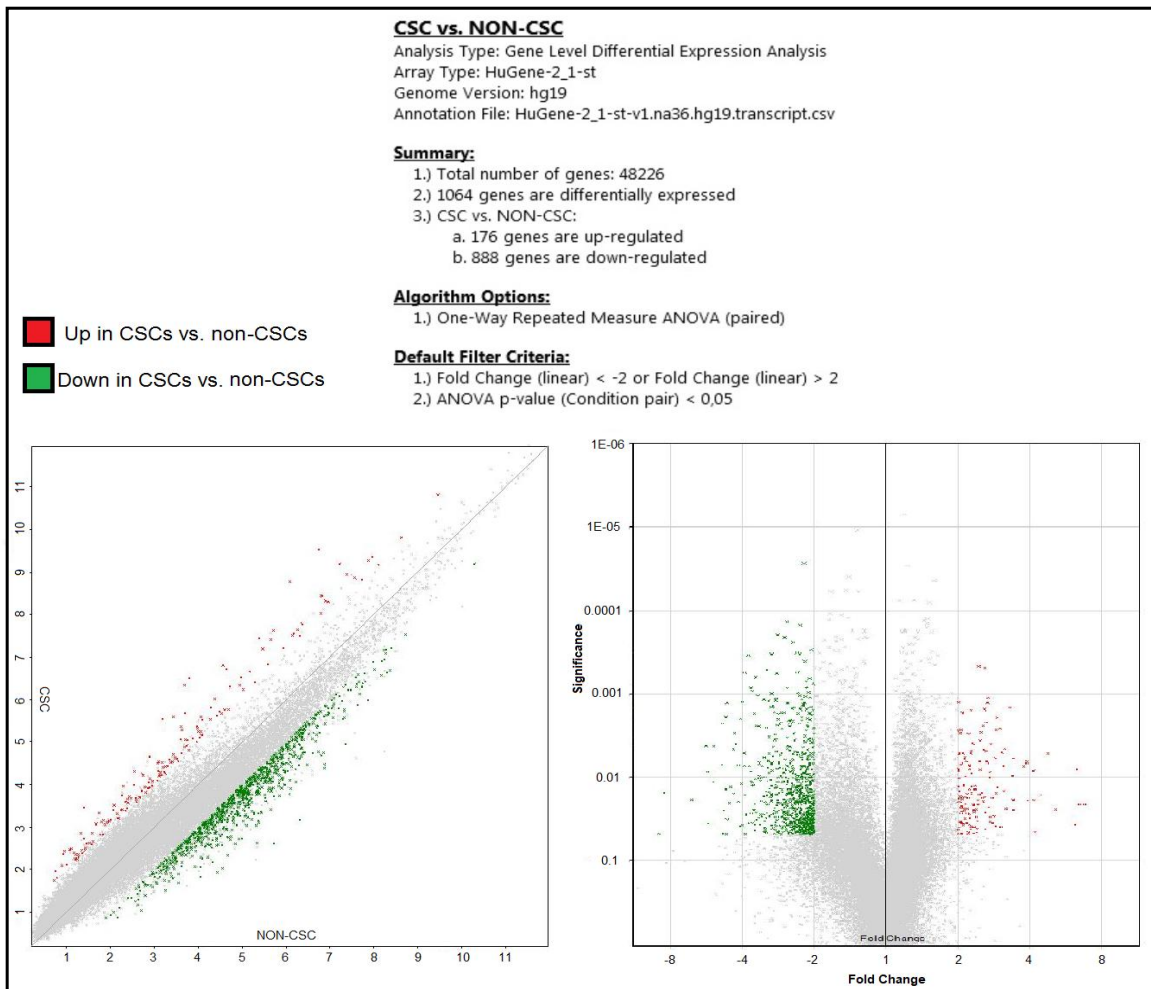


Figure 3.11. mRNA microarray results. Number of upregulated and downregulated mRNAs with scatter plot and volcano plot generated by TAC software.

Table 3.3. Notable pathways in chordoma CSCs against non-CSCs. Gene count indicates the number of differentially expressed mRNAs in each pathway. List of cancers pathways of which were found to be related is listed.

Notable Pathways	Gene Count	Notable Genes/ Fold Change		p-Value	Fold Enrichment
Cell Cycle	20	BUB1/-2.39	CDC23/-2.01	1.1E-7	4.3
		DBF4/-2.06	CCNA2/-2.91		
		RB1/-2.62	CCNB1/-3.03		
		RBL1/-2.68	CCNB2/-2.36		
		SKP2/-3.11	CCNE2/-2.21		
		SMAD2/-2.04	CDK4/-2.19		
		CDC20/-3.1	PLK1/-3.93		
		MCM3/-2.55	MCM5/-2.21		
		MCM7/-2.78	ORC6/-2.4		
		SMC3/-2.27	YWHAB/-2.02		
DNA Replication	10	POLA1/-2.53	PRIM1/-2.25	4.5E-6	7.5
		POLD3/-3.03	RFC1/-2.08		
		MCM3/-2.55	RFC5/-2.01		
		MCM5/-2.21	RPA1/-2.14		
		MCM7/-2.78	RNASEH2A/-2.53		
Spliceosome	17	DDX46/-2.34	SNRPD1/-2.84	2.9E-5	3.4
		XAB2/-2.27	SNRNP40/-2.3		
		HSPA6/2.53	SNRPA/-2.19		
		PPIL1/-2.49	SNRPB2/-2.17		
		PRPF3/-2.19	SF3B3/-2.47		
		PRPF38A/-3.19	SF3B4/-2.08		
		PRPF38B/-2.11	SMNDC1/-2.46		
		PRPF4/-2.24	TRA2B/-2.74		
		SRSF10/-2.89			
Mismatch Repair	6	POLD3/-3.03	RFC1/-2.08	1.3E-3	7.0
		EXO1/-2.19	RFC5/-2.01		
		MSH2/-2.02	RPA1/-2.14		
FoxO Signaling	11	RAF1/-2.06	MAPK9/-2.25	2.7E-2	2.2

Pathway		SKP2/-3.11	NRAS/-2.87		
		SMAD2/-2.04	PLK1/-3.93		
		CCNB1/-3.03	PLK4/-2.06		
		CCNB2/-2.36	STK4/-2.03		
		EGF/-2.89			
p53 Signaling Pathway	7	EI24/-2.23	CCNB2/-2.36	3.7E-2	2.8
		GTSE1/-2.31	CCNE2/-2.21		
		CASP3/-2.08	CDK4/-2.19		
		CCNB1/-3.03			
Hippo Signaling Pathway	11	SMAD2/-2.04	NF2/-2.53	5.3E-2	2.0
		TEAD1/-2.13	PRKCI/-2.22		
		BIRC5/-2.49	SAV1/-3.36		
		DLG1/-3.22	SNAI2/-3.18		
		FZD6/-2.4	YWHAB/-2.02		
		LATS1/-2.36			
Associated Cancers	26	Colorectal cancer (8)		7.6E-3	3.5
		Non-small cell lung cancer (7)		1.7E-2	3.4
		Bladder cancer (5)		6.4E-2	3.3
		Prostate Cancer (6)		9.2E-2	2.5
TNFR1 Signaling Pathway	8	DFFA/-2.01	CASP3/-2.08	4.0E-4	5.4
		JUN/-2.06	LMNB1/-3.78		
		RB1/-2.62	LMNB2/-2.21		
		CASP2/-2.31	PARP1/-2.24		
FAS signaling pathway ( CD95 )	8	DFFA/-2.01	CASP3/-2.08	6.2E-4	5.1
		FAF1/-2.16	LMNB1/-3.78		
		JUN/-2.06	LMNB2/-2.21		
		RB1/-2.62	PARP1/-2.24		
Caspase Cascade in Apoptosis	6	DFFA/-2.01	LMNB1/-3.78	4.9E-3	5.1
		CASP2/-2.31	LMNB2/-2.21		
		CASP3/-2.08	PARP1/-2.24		
CDK Regulation of DNA Replication	4	MCM3/-2.55	MCM7/-2.78	5.3E-2	4.5
		MCM5/-2.21	ORC6/-2.4		

Role of BRCA1. BRCA2 and ATR in Cancer Susceptibility	4	<table border="1"> <tbody> <tr> <td data-bbox="603 365 855 409">BRCA1/-2.26</td> <td data-bbox="855 365 1110 409">FANCF/-2.06</td> </tr> <tr> <td data-bbox="603 409 855 454">FANCD2/-2.93</td> <td data-bbox="855 409 1110 454">HUS1/-2.23</td> </tr> </tbody> </table>	BRCA1/-2.26	FANCF/-2.06	FANCD2/-2.93	HUS1/-2.23	8.8E-2	3.7
BRCA1/-2.26	FANCF/-2.06							
FANCD2/-2.93	HUS1/-2.23							
Apoptotic DNA fragmentation and tissue homeostasis	4	<table border="1"> <tbody> <tr> <td data-bbox="603 645 855 689">DFFA/-2.01</td> <td data-bbox="855 645 1110 689">TOP2A/-5.32</td> </tr> <tr> <td data-bbox="603 689 855 734">CASP3/-2.08</td> <td data-bbox="855 689 1110 734"></td> </tr> </tbody> </table>	DFFA/-2.01	TOP2A/-5.32	CASP3/-2.08		9.7E-2	5.5
DFFA/-2.01	TOP2A/-5.32							
CASP3/-2.08								



Table 3.4. Prediction of activated or inhibited upstream regulators and notable molecules of chordoma CSCs against non-CSCs. For the CSCs vs. non-CSCs comparison, name of predictively activated or inhibited upstream regulators, molecule type and z-score are listed.

<b>Prediction of Activated or Inhibited Upstream Regulators</b>					
<b>Activated Upstream Regulators</b>			<b>Inhibited Upstream Regulators</b>		
<b>Upstream Regulators</b>	<b>Molecule Type</b>	<b>z-score</b>	<b>Upstream Regulators</b>	<b>Molecule Type</b>	<b>z-score</b>
NUPR1	Transcription Regulator	7.410	HGF	Growth Factor	-6.229
CDKN2A	Transcription Regulator	4.380	Vegf	Group	-5.984
TCF3	Transcription Regulator	4.123	CSF2	Cytokine	-5.892
BNIP3L	Other	3.988	ERBB2	Kinase	-5.037
KDM5B	Transcription Regulator	3.288	PTGER2	G-Protein Coupled Receptor	-5.014
CDKN1A	Kinase	3.102	FOXM1	Transcription Regulator	-4.974
RBL2	Other	3.082	RABL6	Other	-4.796
SMARCB1	Transcription Regulator	3.040	MITF	Transcription Regulator	-4.742
Rb	Group	3.018	AREG	Growth Factor	-4.571
ZFP36	Transcription Regulator	2.804	TBX2	Transcription Regulator	-4.461
CST5	Other	2.524	CCND1	Transcription Regulator	-4.183
HCAR2	G-Protein Coupled Receptor	2.449	E2F1	Transcription Regulator	-4.092
E2F6	Transcription Regulator	2.449	FOXO1	Transcription Regulator	-4.041
PAX6	Transcription Regulator	2.433	AR	Ligand-Dependent Nuclear Receptor	-3.907
SPARC	Other	2.345	ESR1	Ligand-Dependent Nuclear Receptor	-3.873
<b>Notable Molecules</b>					

<b>Symbol</b>	<b>Expression Fold Change</b>	<b>Location</b>	<b>Molecule Type</b>	<b>Biomarker Application</b>	<b>Drug(s)</b>
mir-154	2.64	Cytoplasm	microRNA	Diagnosis	
FN1	2.59	Extracellular Space	Enzyme	Diagnosis, Efficacy, Prognosis,	Ocriplasmin, L19-IL2 Monoclonal Antibody-Cytokine Fusion Protein
LBP	2.48	Plasma Membrane	Transporter	Diagnosis, Efficacy	
IGH	2,4	Other	Other	Diagnosis, Prognosis	
CYP2B6	2.32	Cytoplasm	Enzyme	Efficacy, Prognosis	
HBA1/H BA2	2.07	Extracellular Space	Transporter	Diagnosis, Efficacy, response to therapy, safety	Iron Dextran, Mefloquine
SKP2	-3.11	Nucleus	Enzyme	Diagnosis	
CDH11	-3.38	Plasma Membrane	Other	Efficacy, Prognosis	
IL7	-3.78	Extracellular Space	Cytokine	Efficacy	
MKI67	-4.34	Nucleus	Other	Diagnosis, disease progression, Efficacy, Prognosis, Response to Therapy	
KIF14	-5.69	Cytoplasm	Enzyme	Diagnosis	

### 3.1.3. Candidate Targets of Selected miRNAs Were Validated Using qPCR

Before validation of target genes in chordoma cell lines, efficiency of our transfection protocol was confirmed. Briefly, 4 different chordoma cell lines were transfected with FAM3 dye-labeled miRNAs and visualized under fluorescent microscope following 24 hours and successful transfection was monitored (Fig. 3.12).

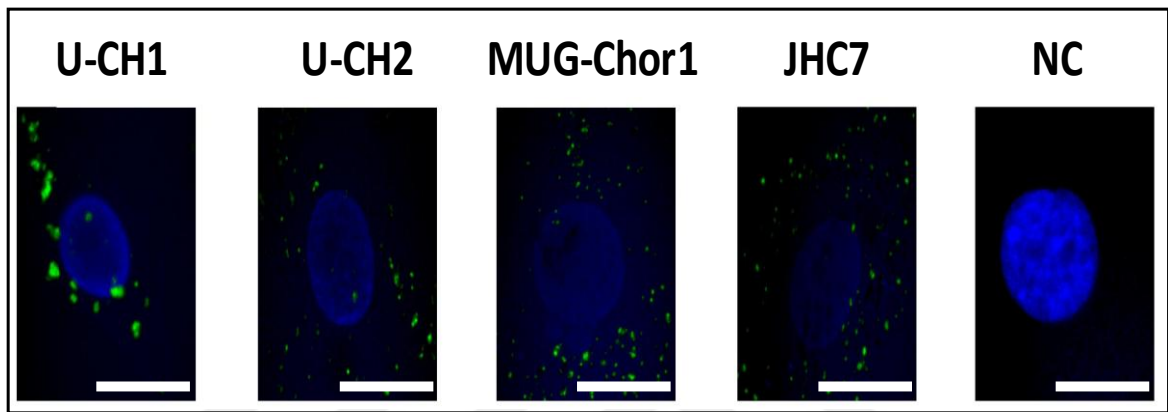


Figure 3.12. miRNA mimic (green) and DAPI were introduced into chordoma cell lines. DAPI (blue) was used for nuclear staining. “NC” is a representative image from non-transfected control groups. Scale bar represents 20  $\mu\text{m}$ .

Subsequently, pre- and anti- mimics of miRNAs were introduced into chordomas. Upon 72 hours of incubation, the candidate targets of miRNAs were measured and compared with pre-scrambled miRNA or anti-scrambled miRNA. qPCR results suggested that *WNT5A*, *TGF- $\alpha$* , *BTG2*, and *MYCBP* were regulated by miR-140-3p, miR-148a-3p, miR-210-5p and miR-574-5p, respectively. While the transfection of pre-mimic miRNAs caused downregulation in their target genes, transfection of anti-mimic miRNAs increased expression levels of target genes in all chordoma cell lines (Fig. 3.13). Transfection of pre-mir-140-3p reduced expression of *WNT5A* approximately down to 30 percent, 20 percent, 30 percent and 40 percent in U-CH1, U-CH2, MUG-Chor1 and JHC7 respectively, whereas transfection of anti-miR-140-3p increased expression of *WNT5A* 70 percent, 35 percent, 25 percent and 40 percent. Upon transfection of pre-mir-148a-3p, expression of *TGF- $\alpha$*  reduced 65 percent, 35 percent, 55 percent and 65 percent in U-CH1, U-CH2, MUG-Chor1 and JHC7, respectively. Transfection of anti-miR-148a-3p increased

expression of *TGF- $\alpha$*  up to 50 percent, 30 percent, 40 percent and 20 percent in the cell lines. While transfection of pre-mir-210-5p diminished its target gene expression in range from 30 percent to 45 percent, transfection of anti-miR-210-5p increased it up to 55 percent in cell lines. Expression of *MYCBP* was decreased by nearly 30 percent, 50 percent, 20 percent, and 60 upon transfection of pre-mir-574-5p in U-CH1, U-CH2, MUG-Chor1, and JHC7, respectively, whereas the expression of *MYCBP* was increased roundly 10 percent, 30 percent, 20 percent and 65 percent.

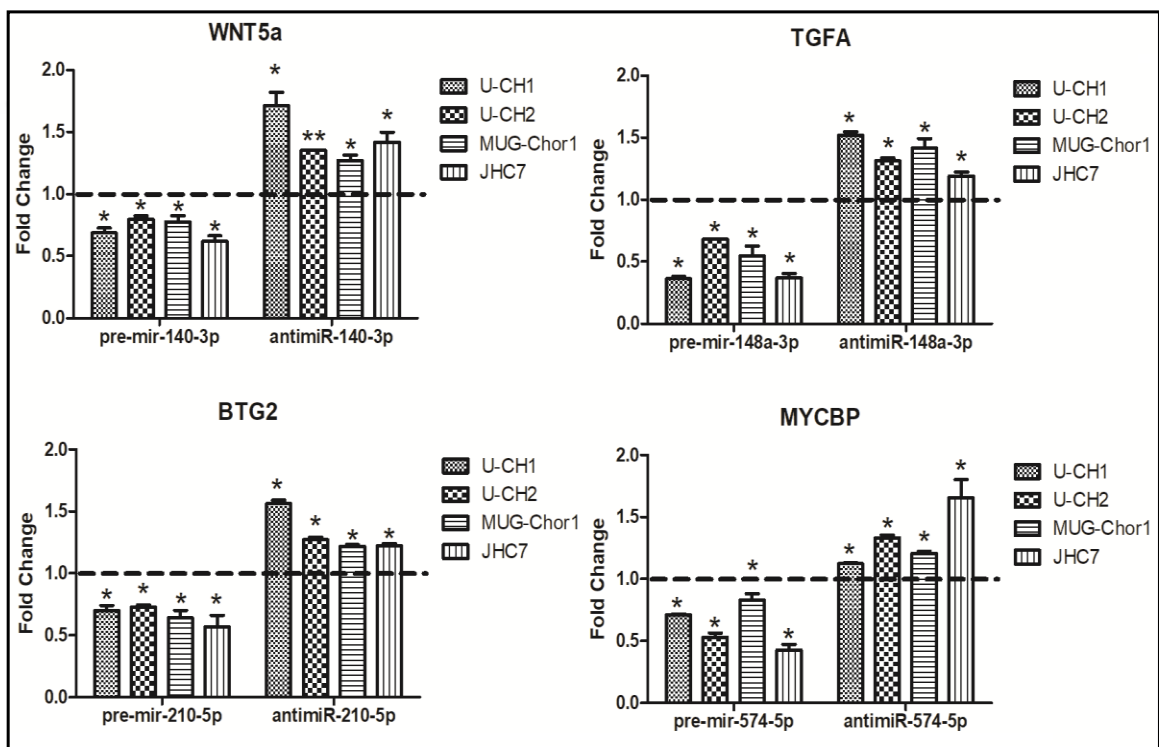


Figure 3.13. Expression level of target genes once transfection of pre- and anti-mimics of miRNAs into chondroma cells. Pre-mir-scr or anti-mir-scr transfected cells were used for normalization. The dashed line represents 1 fold, which is the value for the pre-mir-scr or anti-miR-scr transfected cells for each group. \*:  $p < 0.05$ , \*\*:  $p < 0.01$ .

### 3.1.4. CSC-related miRNAs Affected Proliferation, Apoptosis, Migration, Invasion, and Stemness Properties

miRNAs were transiently transfected into chondroma cell lines to assess their role in proliferation, apoptosis, migration and invasion. Pre- and anti- mimic of CSC related

miRNAs were transfected into chordoma cells individually. Viability was measured after 72 hours of transfection (Fig. 3.14). Pre-miR-140-3p significantly increased the viability approximately up to 20 percent in U-CH1, while anti-miR-140-3p decreased down to 15 percent. Interestingly, both pre-mir-140-3p and anti-miR-140-3p transfection did not change viability in MUG-Chor1. While pre-miR-148a-3p decreased viability in U-CH1, it behaved oppositely in MUG-Chor1. Anti-miR-148a-3p transfection caused reduction in viability in both chordoma cell lines. Viability was decreased by 20 percent and 10 percent upon transfection of pre-miR-210-5p in U-CH1 and MUG-Chor1 cell lines, respectively, whereas the viability was increased by approximately 5 percent upon transfection of anti-miR-210-5p. Pre-mir-574-5p transfection decreased viability in U-CH1, yet anti-miR-574-5p transfection did not change the viability. In addition, both pre-mir-574-5p and anti-miR-574-5p had not affected the viability in MUG-Chor1 cells as well as pre- and anti-mimic of miR-140-3p.

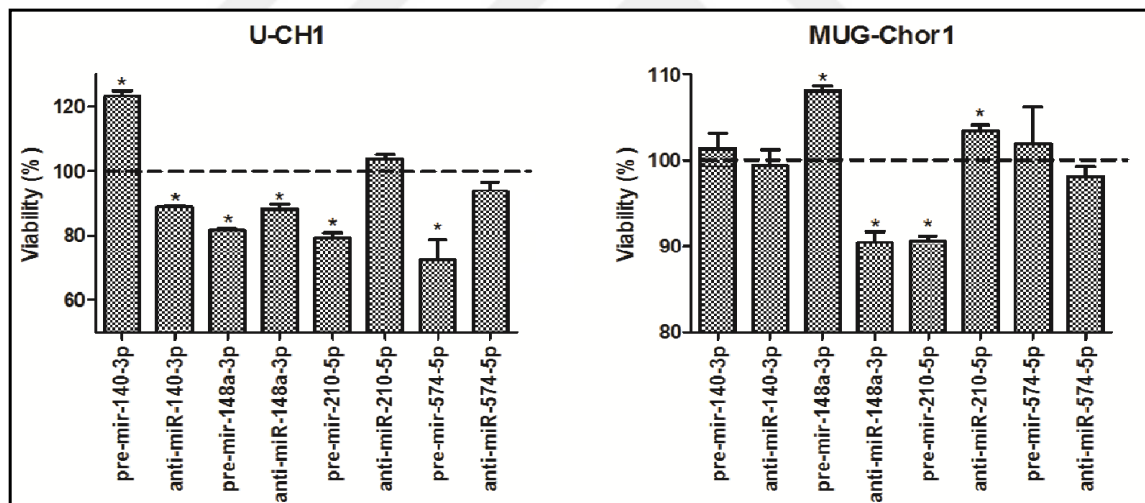


Figure 3.14. Percentage viability of U-CH1 and MUG-Chor1 upon transfection of miRNA constructs. Percent viability was calculated by normalizing results from MTS assay using pre-scr or anti-scr transfected control group. Viability was measured 3 days after transfection of pre-mimic-miRNA or anti-mimic-miRNA. The dashed line (=100%) is the value for the pre-mir-scr or anti-miR-scr transfected cells for each group. \*:  $p < 0.05$ .

Early apoptotic marker represented by the presence of phosphatidylserine on the outer leaflet of the plasma membrane of chordoma cells transfected with the pre-mir and anti-miR of interest were investigated upon staining with Annexin V. Annexin V<sup>+</sup> and 7-Amino

Actinomycin D (7-AAD)<sup>+</sup> cells were identified by FACS Aria III. Apoptosis assay revealed that transfection of anti-miR-140-3p, anti-miR-148a-3p, pre-mir-210-5p, and pre-mir-574-5p significantly increased apoptosis in U-CH1 by approximately 35 percent, 20 percent, 25 percent and 40 percent, respectively, whereas pre-mir-140-3p and anti-miR-210-5p decreased the number of apoptotic cells 20 percent and 40 percent. Furthermore, while anti-miR-140-3p, anti-miR-148a-3p, and anti-miR-574-5p induced apoptosis in MUG-Chor1 cells up to 10 percent, 55 percent and 65 percent, respectively; pre-mir-574-5p inhibited apoptosis down to 40 percent (Fig.3.15).

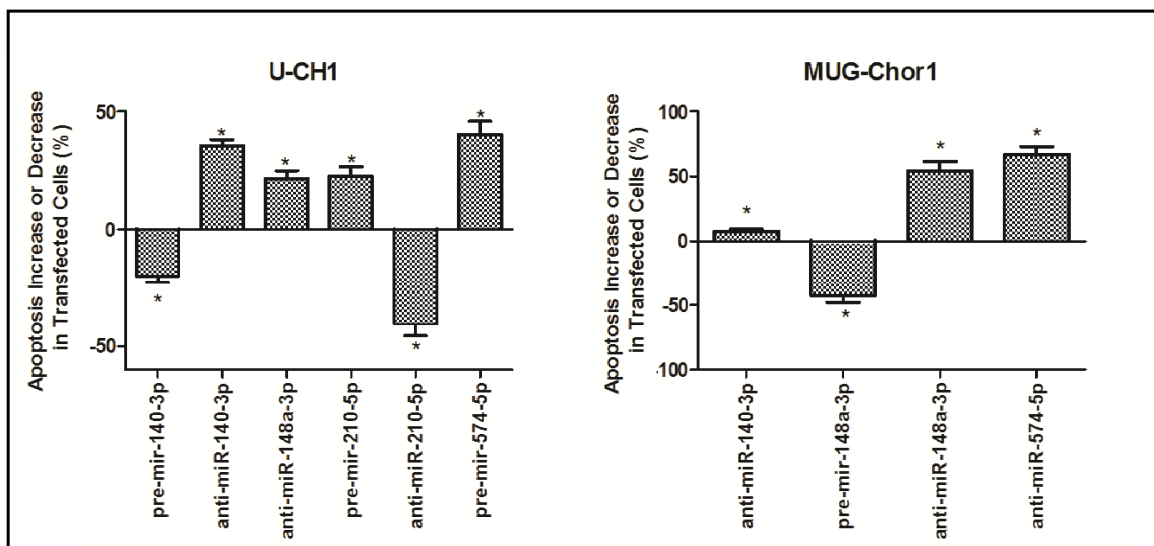


Figure 3.15. Apoptosis results representing the percentage of Annexin V<sup>+</sup>7-AAD<sup>-</sup> chordoma cells following miRNA transfection. Ratio of apoptotic cells were assessed 48 hours after transfection of pre-mimic-miRNA or anti-mimic-miRNA. Statistically significant results were shown. \*:  $p < 0.05$ .

Invasion and migration assays were then performed to find role of miRNAs. Microarray results elicited that miR-140-3p, miR-148a-3p, and miR-574-5p were downregulated and miR-210-5p was upregulated in chordoma CSCs. Dysregulated miRNAs were collectively introduced into chordoma cells. Migration and invasion capacity of cells were then assessed. Briefly, anti-miR-140-3p, anti-miR-148a-3p, pre-mir-210-5p and anti-miR-574-5p (referred CSC-related miRNAs) and pre-mir-140-3p, pre-mir-148a-3p, anti-miR-210-5p and pre-mir-574-5p (referred as non-CSC-related miRNAs) were transfected into chordoma cell lines. The mixture of pre-scrambled miRNA and anti-scrambled miRNA

transfected cells were used as negative controls. Transfection of CSC-related miRNAs increased invasion and migration capacity for both chordoma cell lines. Transfection of non-CSC-related miRNAs also decreased invasion and migration capacity (Fig. 3.16) as indicated in representative images (Fig. 3.17). In brief, while transfection of CSC-related miRNAs increased both migration (30 percent) and invasion (15 percent) ability of U-CH1, transfection of non-CSC-related miRNAs decreased migration (15 percent) and invasion (10 percent). Furthermore, upon transfection of CSC-related miRNAs to MUG-Chor1, migration and invasion ability were increased by 35 percent and 25 percent, respectively, whereas, transfection of non-CSC-related miRNAs decreased migration and invasion ability of the cells down to 30 percent and 12 percent.

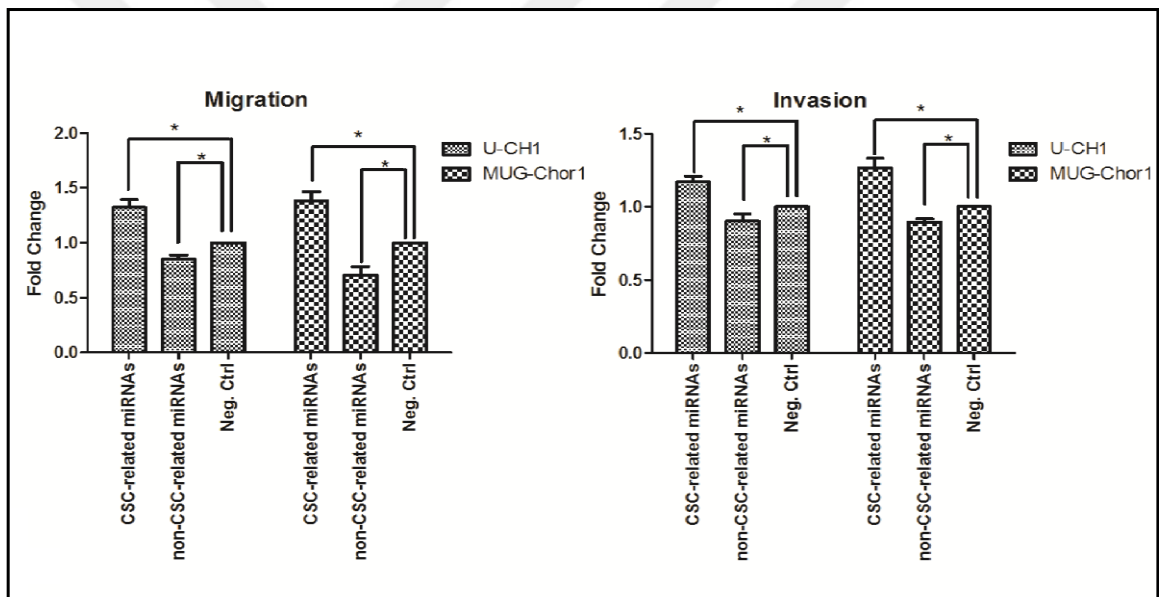


Figure 3.16. Effect of collective transfection of CSC-related miRNAs or non-CSC-related miRNAs on cell migration and invasion capacity of chordoma cell lines. Invasion and migration ability of chordoma cells were evaluated 2 days after transfection. For the invasion assay, transwell inserts were coated with basement membrane matrigel. Mixture of pre- and anti-miR-scramble was used as control. \*:  $p < 0.05$ .

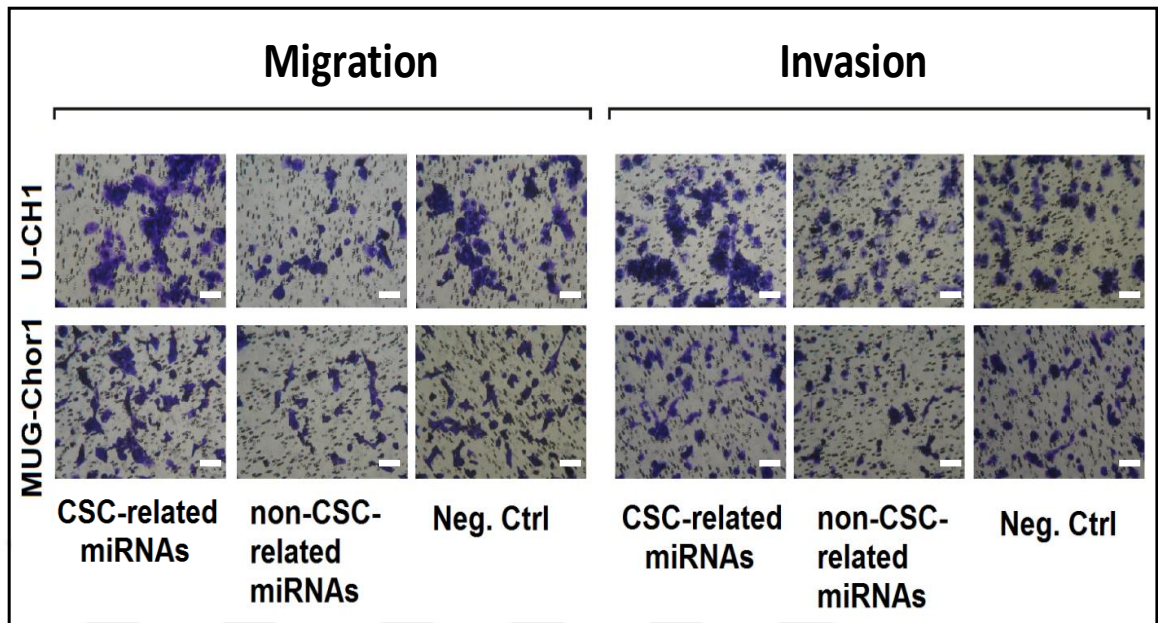


Figure 3.17. Pictures of migration and invasion from CSC-related miRNAs, non-CSC-related miRNAs and Neg. Ctrl. For the invasion assay, transwell inserts were coated with basement membrane matrigel. Scale bar represents 100  $\mu$ m.

Wound healing assay revealed that upon transfection with CSC-related miRNAs, migration ability were increased by 22 percent and 15 percent in U-CH1 and MUG-Chor1, respectively, while non-CSC-related miRNAs decreased it by 17 percent and 11 percent (Fig. 3.18 and 3.19).



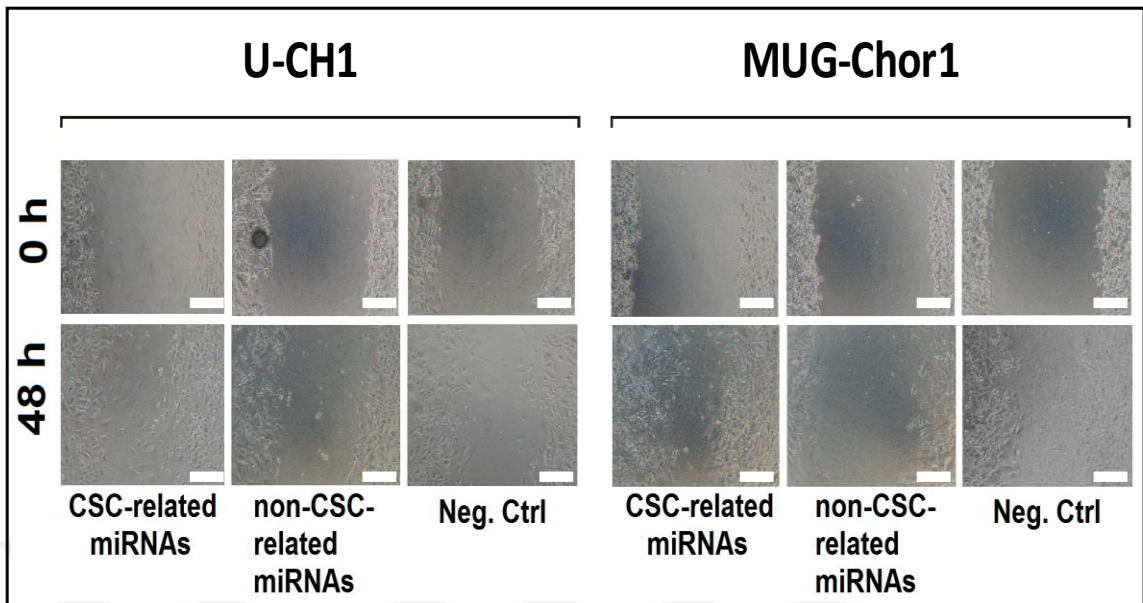


Figure 3.18. Representative images of wound healing assay from CSC-related miRNAs, non-CSC-related miRNAs and Neg. Ctrl at day 0 and day 2. Scale bar represents 100  $\mu$ m.

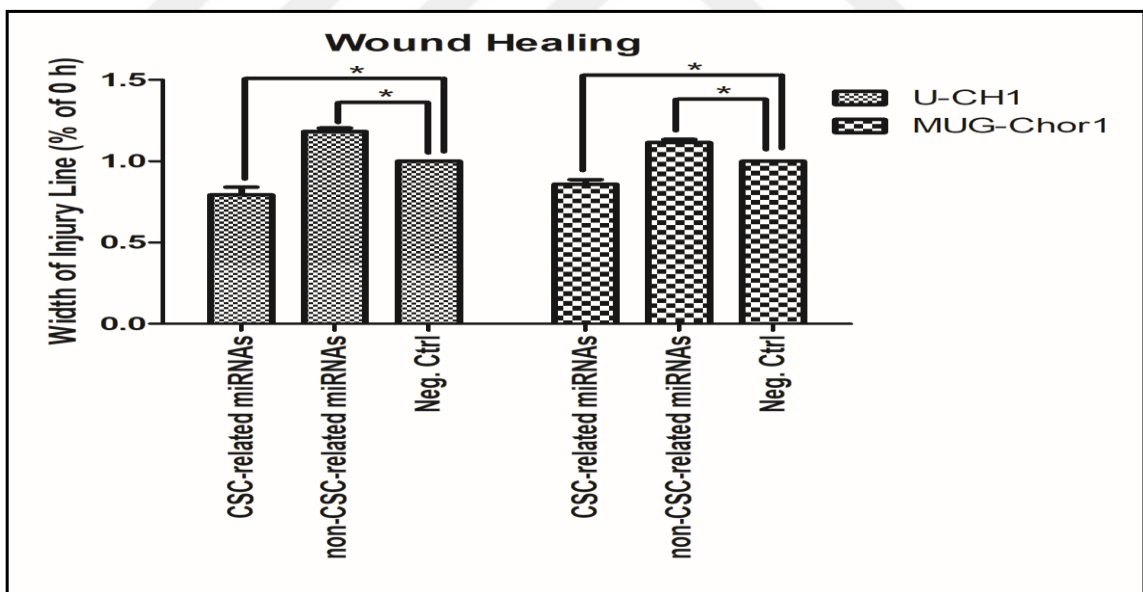


Figure 3.19. Effect of collective miRNA transfection on migration ability of chordoma cell lines. Migration ability of cells was evaluated 48 hours after transfection. Mixture of pre- and anti-miR-scramble was used as control. \*:  $p < 0.05$ .

As aldehyde dehydrogenase is known to be highly expressed by stem cells and stem-like cells. Aldeflour assay was used next to determine changes in stem cell properties upon transfection of miRNA groups. Thus, stem-like properties were assessed by Aldeflour Assay and according to that CSC-related miRNAs increased the number of ALDH<sup>high</sup> cells from 0.65 percent to 2.55 percent in U-CH1 and from 0.37 percent to 3.1 percent MUG-Chor1, whereas non-CSC-related miRNAs decreased the number of ALDH<sup>high</sup> cell down to 0.15 percent and 0.07 percent in U-CH1 and MUG-Chor1, respectively (Fig. 3.20).



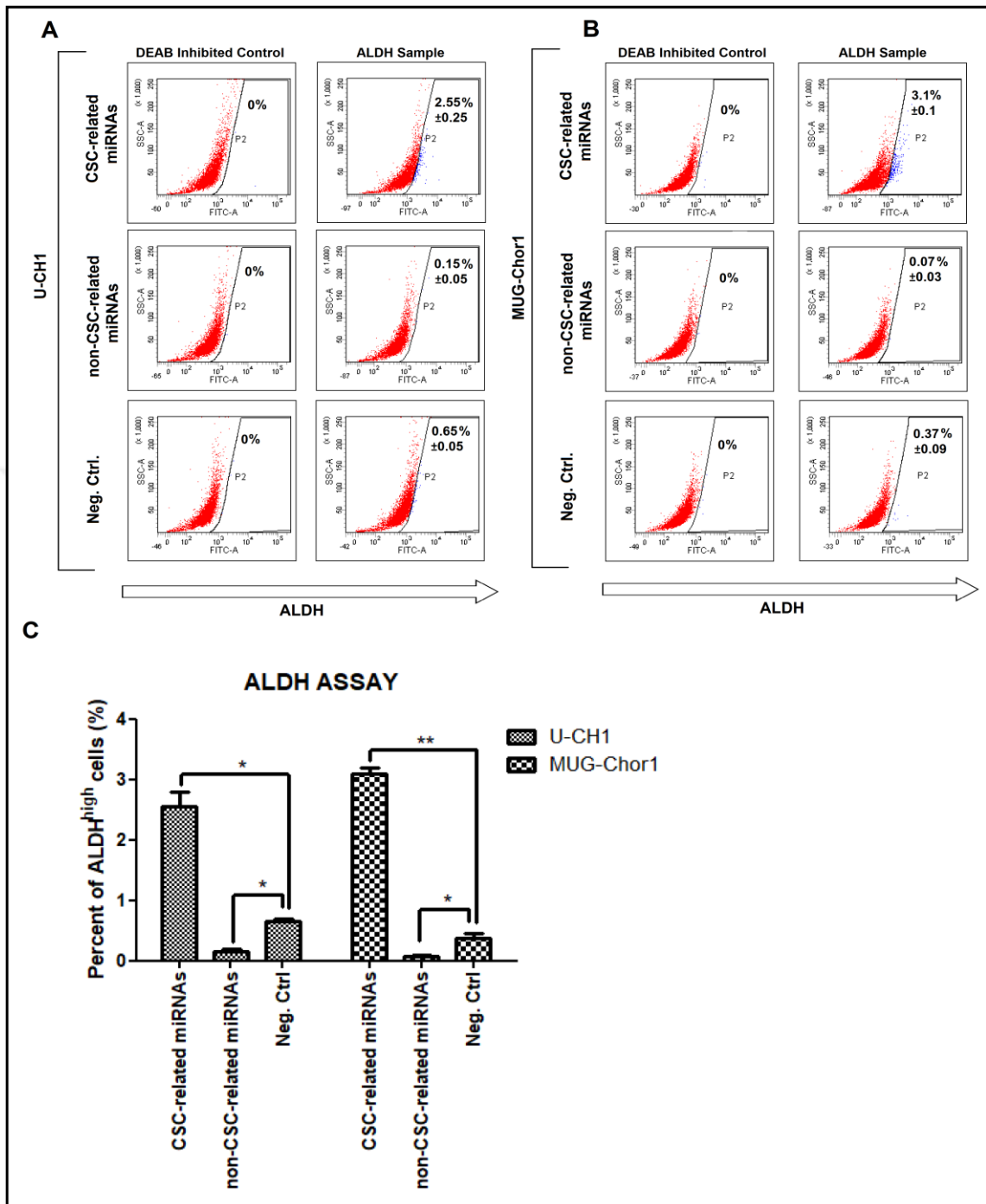


Figure 3.20. Effect of transfection of miRNA groups on stem cell phenotype in A) U-CH1 and B) MUG-Chor1. ALDH activity was measured 72 hours after transfection of miRNA groups.  $\pm$  represents the SEM. C) Graphical representative of flow results. \*:  $p < 0.05$ .

### 3.1.5. CSC-related miRNAs and Their Targets are Related with Clinicopathological Features of Chordoma Samples

The relationship between miR-140-3p, miR-148a-3p, miR-210-5p, miR-574-5p, *WNT5A*, *TGF- $\alpha$* , *BTG2*, and *MYCBP* levels and clinicopathological features of chordoma patients including gender, age, tumor volume, p53 and Ki67 levels, metastasis, recurrence and overall survival time were assessed using chi-square test and correlation coefficient test. miR-140-3p was associated with Ki67 and p53 level of chordoma tissue samples positively. In addition, miR-148a-3p level was associated with Ki67 level positively. Metastasis was also positively correlated with expression of *TGF- $\alpha$*  and miR-210-5p (Table 3.5).

Table 3.5. Correlation of selected miRNAs' expression level and their targets with clinicopathological features. P-value of significant results was shown in bold.

Clinicopathological Features	Molecule Name	Low	High	Total	p-Value
<b>P53</b>	<b>miR-140-3p</b>				
	< 3%	8	5	13	<b>0.0186</b>
	$\geq$ 3%	0	5	5	
	<b>miR-148a-3p</b>				
	< 3%	6	7	13	0.8139
	$\geq$ 3%	2	3	5	
	<b>miR-210-5p</b>				
	< 3%	7	6	13	0.5987
	$\geq$ 3%	2	3	5	
	<b>miR-574-5p</b>				
	< 3%	6	7	13	0.5987
	$\geq$ 3%	3	2	5	
	<b>WNT5A</b>				
	< 3%	8	5	13	0.1144
	$\geq$ 3%	1	4	5	
	<b>TGFA</b>				
	< 3%	8	5	13	0.1144

	≥ 3%	1	4	5	
	<b>BTG2</b>				
	< 3%	7	6	13	0.1955
	≥ 3%	1	4	5	
	<b>MYCBP</b>				
	< 3%	6	8	13	0.9116
	≥ 3%	2	3	5	
<b>Ki67</b>	<b>miR-140-3p</b>				
	< 8%	10	6	16	<b>0.0253</b>
	≥ 8%	0	4	4	
	<b>miR-148a-3p</b>				
	< 8%	10	6	16	<b>0.0253</b>
	≥ 8%	0	4	4	
	<b>miR-210-5p</b>				
	≥ 8%	8	8	16	1.0000
	≥ 8%	2	2	4	
	<b>miR-574-5p</b>				
	≥ 8%	9	7	16	0.2636
	≥ 8%	1	3	4	
	<b>WNT5A</b>				
	≥ 8%	8	8	16	1.0000
	≥ 8%	2	2	4	
	<b>TGFA</b>				
	≥ 8%	9	7	16	0.2636
	≥ 8%	1	3	4	
	<b>BTG2</b>				
	≥ 8%	8	8	16	1.0000
≥ 8%	2	2	4		
<b>MYCBP</b>					
≥ 8%	9	7	16	0.2636	
≥ 8%	1	3	4		
<b>Age</b>	<b>miR-140-3p</b>				
	< 50	5	5	10	

	≥ 50	5	6	11	0.8350
	<b>miR-148a-3p</b>				
	< 50	3	7	10	0.1232
	≥ 50	7	4	11	
	<b>miR-210-5p</b>				
	< 50	6	5	10	0.5051
	≥ 50	4	6	11	
	<b>miR-574-5p</b>				
	< 50	5	6	10	0.8350
	≥ 50	5	5	11	
	<b>WNT5A</b>				
	< 50	5	5	10	0.8350
	≥ 50	5	6	11	
	<b>TGFA</b>				
	< 50	6	3	10	0.1775
	≥ 50	4	7	11	
	<b>BTG2</b>				
	< 50	4	6	10	0.3711
	≥ 50	6	4	11	
	<b>MYCBP</b>				
	< 50	5	5	10	1.0000
	≥ 50	5	5	11	
<b>Recurrence</b>	<b>miR-140-3p</b>				
	Yes	4	5	9	1.0000
	No	6	6	12	
	<b>miR-148a-3p</b>				
	Yes	4	5	9	1.0000
	No	6	6	12	
	<b>miR-210-5p</b>				
	Yes	3	6	9	0.2563
	No	7	5	12	
	<b>miR-574-5p</b>				
	Yes	3	6	9	0.2563
	No	7	5	12	
	<b>WNT5A</b>				

	Yes	3	6	9	0.2563
	No	7	5	12	
	<b>TGFA</b>				
	Yes	2	7	9	0.0805
	No	8	4	12	
	<b>BTG2</b>				
	Yes	4	5	9	1.0000
	No	6	6	12	
	<b>MYCBP</b>				
	Yes	3	6	9	0.3870
	No	7	5	12	
	<b>Metastasis</b>	<b>miR-140-3p</b>			
Yes		1	2	3	0.5865
No		10	8	18	
<b>miR-148a-3p</b>					
Yes		2	1	3	1.0000
No		9	9	18	
<b>miR-210-5p</b>					
Yes		0	3	3	<b>0.0497</b>
No		11	7	18	
<b>miR-574-5p</b>					
Yes		2	1	3	1.0000
No		9	9	18	
<b>WNT5A</b>					
Yes		2	1	3	1.0000
No		9	9	18	
<b>TGFA</b>					
Yes		0	3	3	<b>0.0497</b>
No		11	7	18	
<b>BTG2</b>					
Yes		1	2	3	0.5865
No		10	8	18	
<b>MYCBP</b>					
Yes		1	2	3	0.5865
No		10	8	18	

<b>Gender</b>	<b>miR-140-3p</b>				
	Female	5	8	13	0.3870
	Male	5	3	8	
	<b>miR-148a-3p</b>				
	Female	5	8	13	0.3870
	Male	5	3	8	
	<b>miR-210-5p</b>				
	Female	5	8	13	0.3870
	Male	5	3	8	
	<b>miR-574-5p</b>				
	Female	6	7	13	1.0000
	Male	4	4	8	
	<b>WNT5A</b>				
	Female	6	7	13	1.0000
	Male	4	4	8	
	<b>TGFA</b>				
	Female	5	8	13	0.3870
	Male	5	3	8	
	<b>BTG2</b>				
	Female	6	7	13	1.0000
	Male	4	4	8	
	<b>MYCBP</b>				
	Female	5	8	13	0.3870
	Male	5	3	8	

In addition, correlation analysis suggested that miR-140-3p, *MYCBP*, and *TGF- $\alpha$*  were positively correlated with Ki67, tumor volume and p53, respectively (Fig. 3.21, Fig. 3.22 and Fig. 3.23). No association between miRNAs (and their targets) and overall survival was determined (Fig. 3.24).



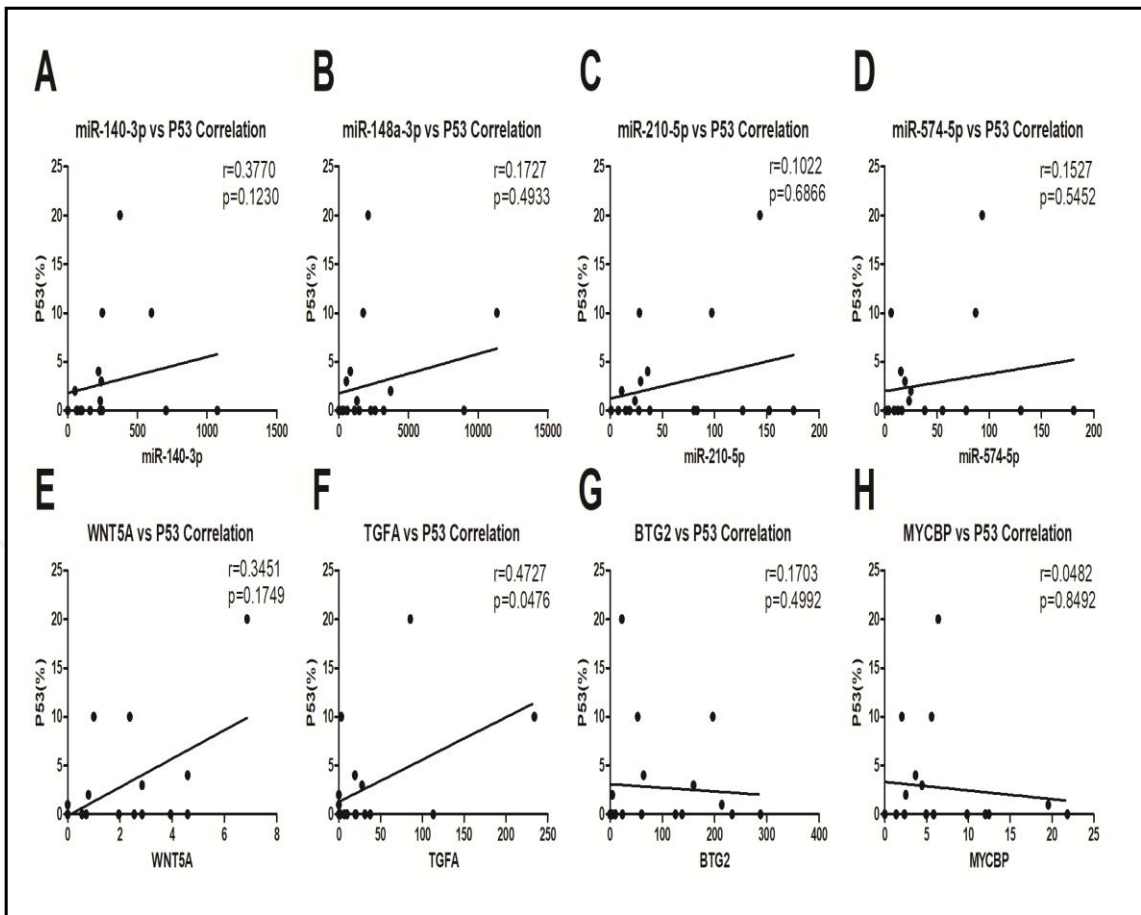


Figure 3.21. Correlation of A) miR-140-3p, B) miR-148a-3p, C) miR-210-5p, D) miR-574-5p, E) WNT5A, F) TGFA, G) BTG2 and H) MYCBP with P53 expression of patients with chordoma.  $p$ =significance,  $r$ =correlation coefficient.

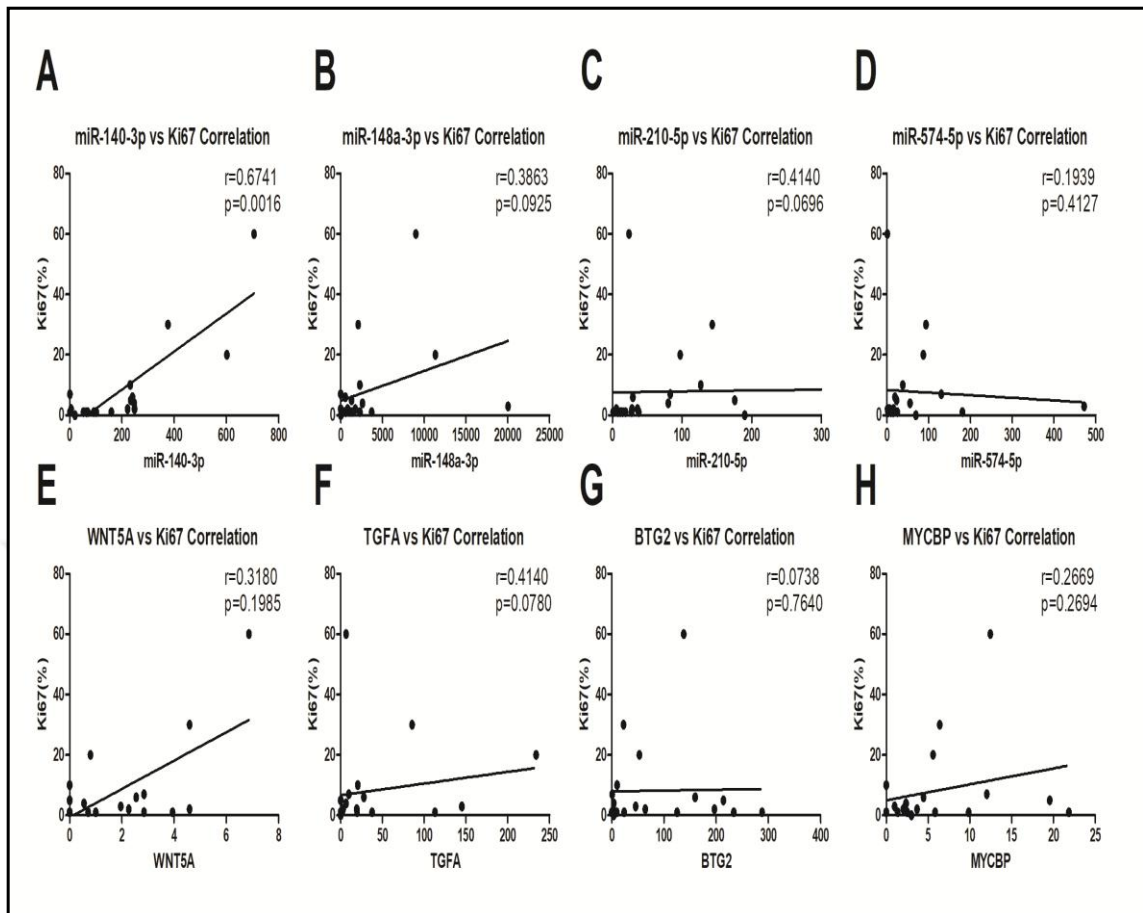


Figure 3.22. Correlation of A) miR-140-3p, B) miR-148a-3p, C) miR-210-5p, D) miR-574-5p, E) WNT5A, F) TGFA, G) BTG2 and H) MYCBP with Ki67 of patients with chordoma.  $p$ =significance,  $r$ =correlation coefficient.

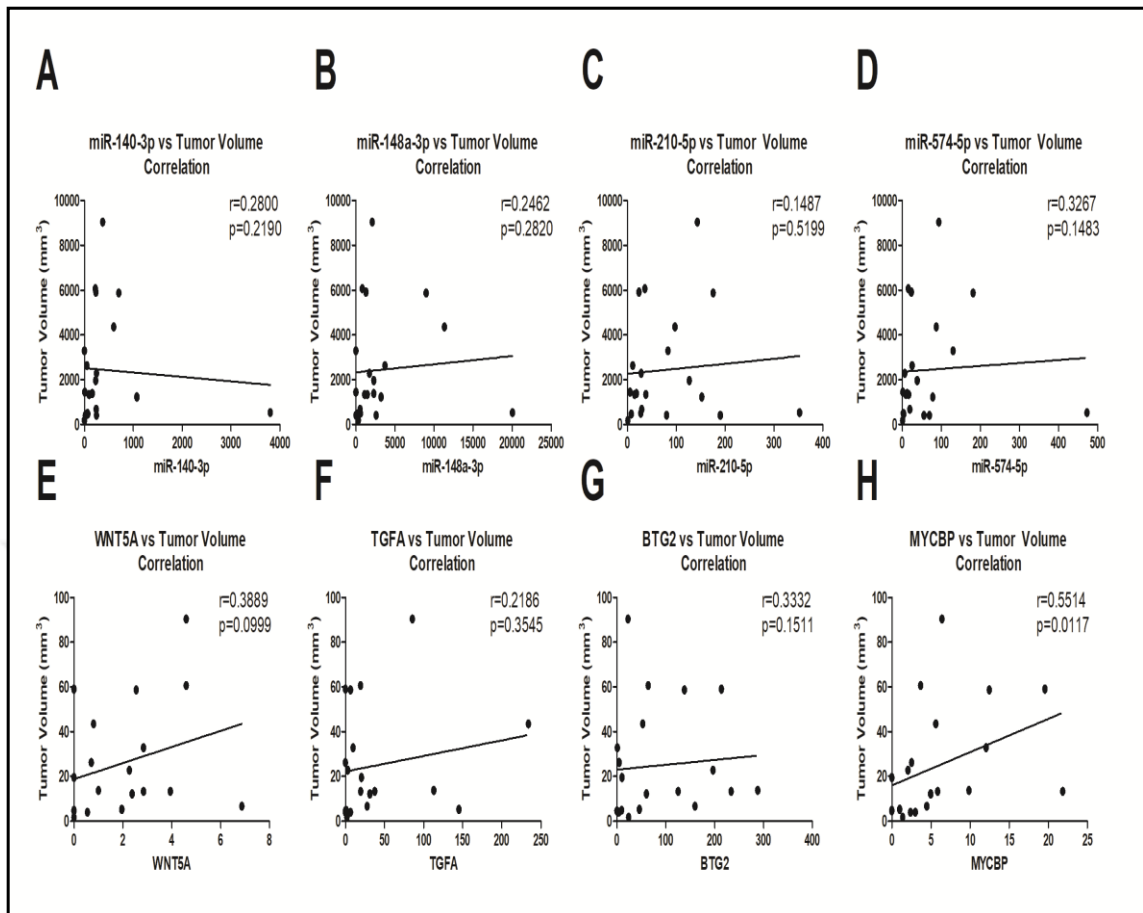


Figure 3.23. Correlation of A) miR-140-3p, B) miR-148a-3p, C) miR-210-5p, D) miR-574-5p, E) WNT5A, F) TGFA, G) BTG2 and H) MYCBP with tumor volume of patients with chordoma. p=significance, r=correlation coefficient.

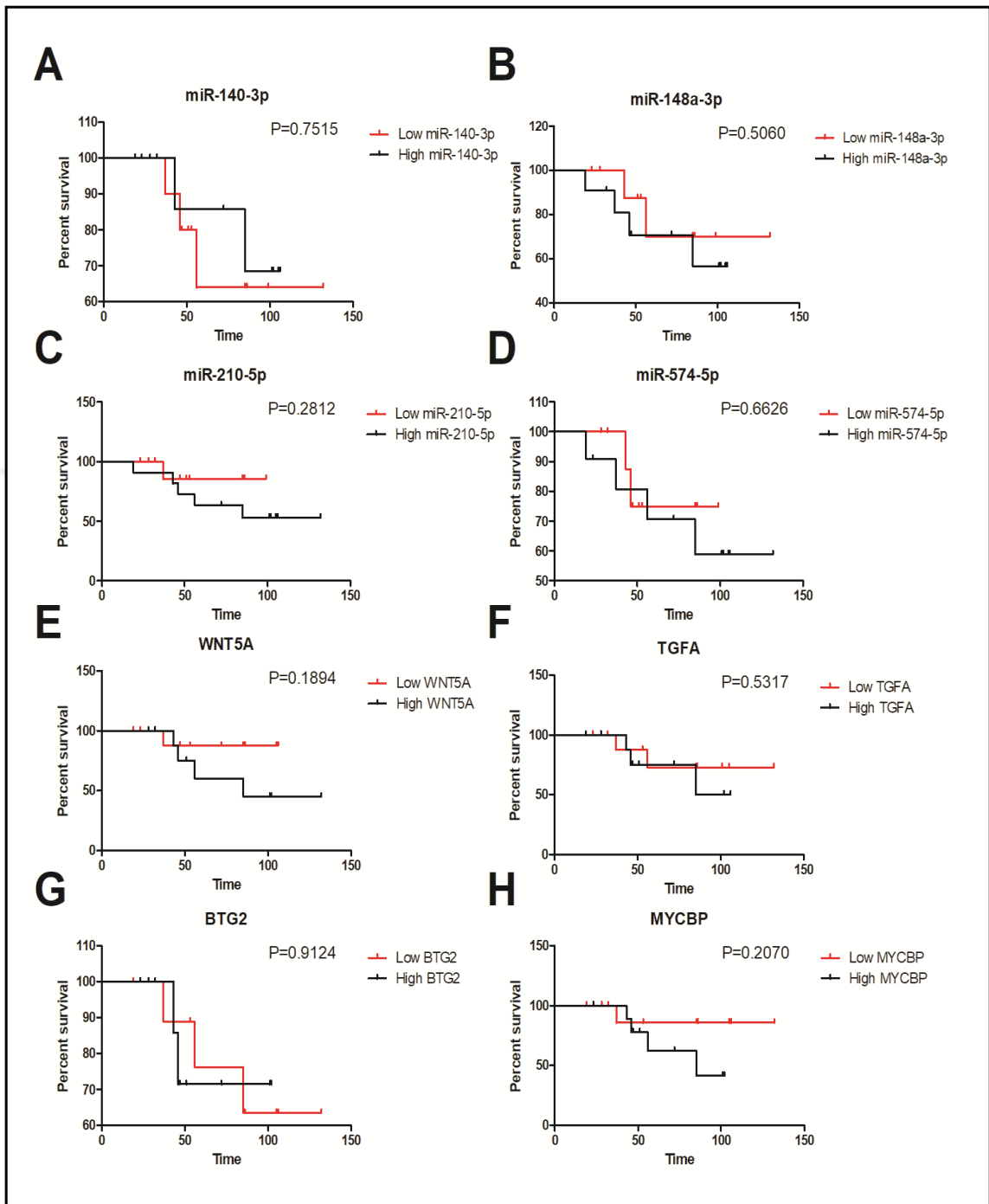


Figure 3.24. Overall survival analysis of A) miR-140-3p, B) miR-148a-3p, C) miR-210-5p, D) miR-574-5p, E) WNT5A, F) TGFA, G) BTG2 and H) MYCBP in patients with chordoma.

## 3.2. IDENTIFICATION OF RECURRENCE MECHANISM IN CHORDOMA

### 3.2.1. Characterization of YU-Chor1 Cell Line

YU-Chor1 cell line was established from 76-years-old male patient diagnosed as recurrent-clivus chordoma (Fig. 3.25). Pathological analysis indicated that Vimentin, EMA, PAN Cytokeratine and S100 were highly expressed in tumor tissue.

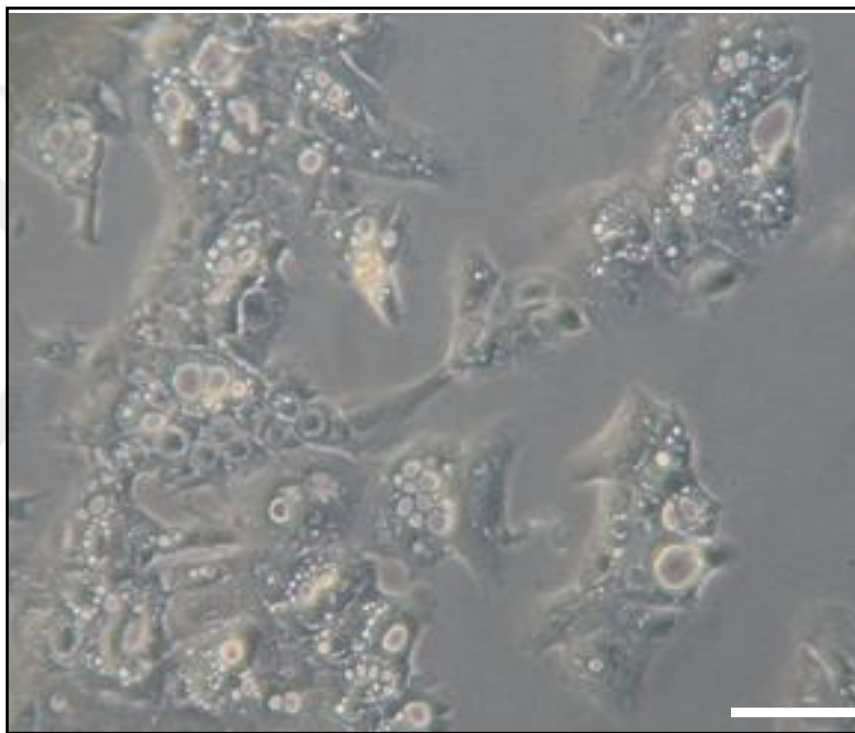


Figure 3.25. Microscopy image of YU-Chor1 cell line at 100X magnification. Scale bar represents 50  $\mu\text{m}$ .

Percentage of CD90, CD44, CD24, CD133 and CD15 in YU-Chor1 cell line was 90.2 percent, 98.4 percent, 98.4 percent, 1.6 percent and 1.0 percent, respectively. U-CH1 and MUG-Chor1 were used as positive controls. Ratio of CD90, CD44, CD24, CD133 and CD15 was 98.8 percent, 98.5percent, 99.5 percent, 2.8 percent and 0.5 percent, respectively. In addition, percentage of these markers in MUG-Chor1 was 69.2 percent, 97.5 percent, 98.7 percent, 1.6 percent and 0.7 percent, separately (Fig. 3.26).

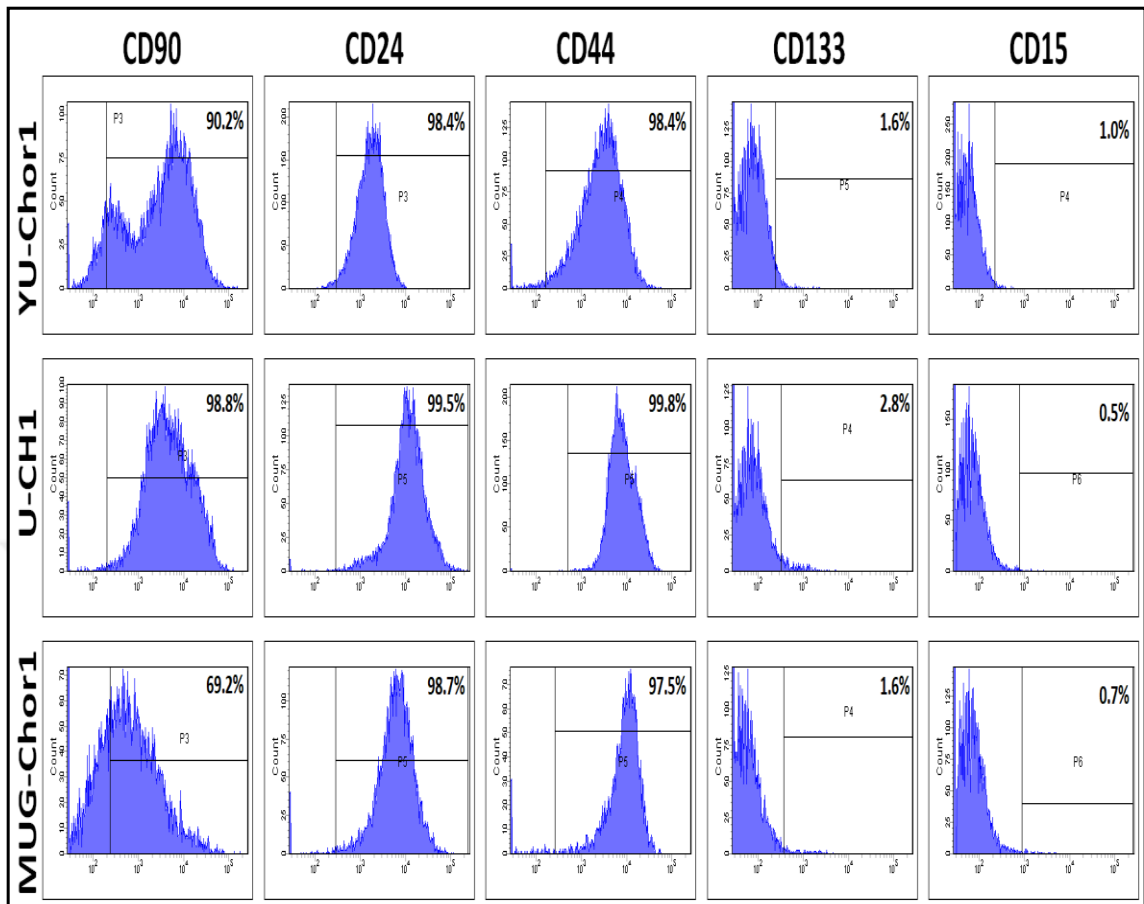


Figure 3.26. Percentage of both chordoma- and CSC- related surface proteins including CD90, CD24, CD44, CD133 and CD15 in chordoma cell lines.

Expression levels of chordoma markers, EMT, and MET markers of these chordoma cell lines were then checked. Gene expression results demonstrated that while expression of *Brachyury* and *Vimentin* was found to be increased approximately 0.45-fold and 0.8-fold in YU-Chor1 compared with U-CH1, respectively, whereas their expression was decreased by 0.65-fold and 0.85-fold compared with MUG-Chor1. Moreover, expression of *EMA* was diminished in YU-Chor1 compared with other cell lines (Fig. 3.27).

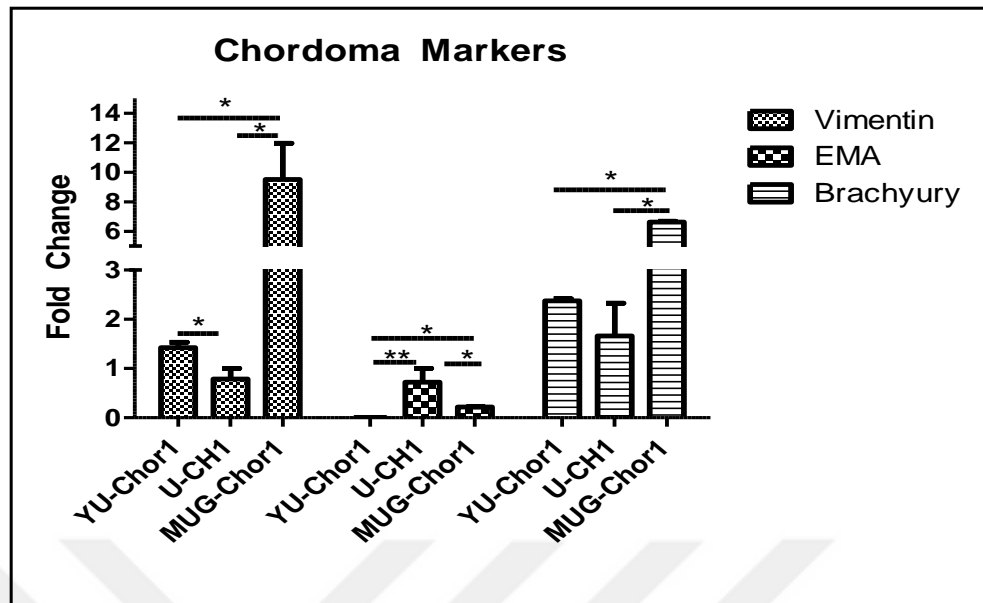


Figure 3.27 Expression of chordoma-associated genes. Cell line which had the lowest expression for each gene among the cell lines were used for normalization. \*:  $p < 0.05$ , \*\*:  $p < 0.01$ .

The expression levels of the both EMT and MET associated genes with the inclusion of *E-CAD*, *KRT19*, *N-CAD*, *TWIST*, *SNAIL*, and *SLUG* were examined and it is found that the expression of *E-CAD*, a MET marker, was upregulated in YU-Chor1 by 2.8-fold and 4.5-fold more in comparison to U-CH1 and MUG-Chor1, respectively. Expression of *KRT19* was not statistically significant among the groups. Moreover, expression of both *SNAIL* and *TWIST* was diminished by in YU-Chor1 among three cell lines. *N-CAD* was also highly expressed in YU-Chor1 by 7-fold compared with U-CH1 whereas it was downregulated by 0.5-fold compared with MUG-Chor1. Expression of *SLUG* was not statistically significant in YU-Chor1 and U-CH1 but its expression in YU-Chor1 was decreased by 0.9 fold compared with MUG-Chor1 (Fig. 3.28 and Fig. 3.29).

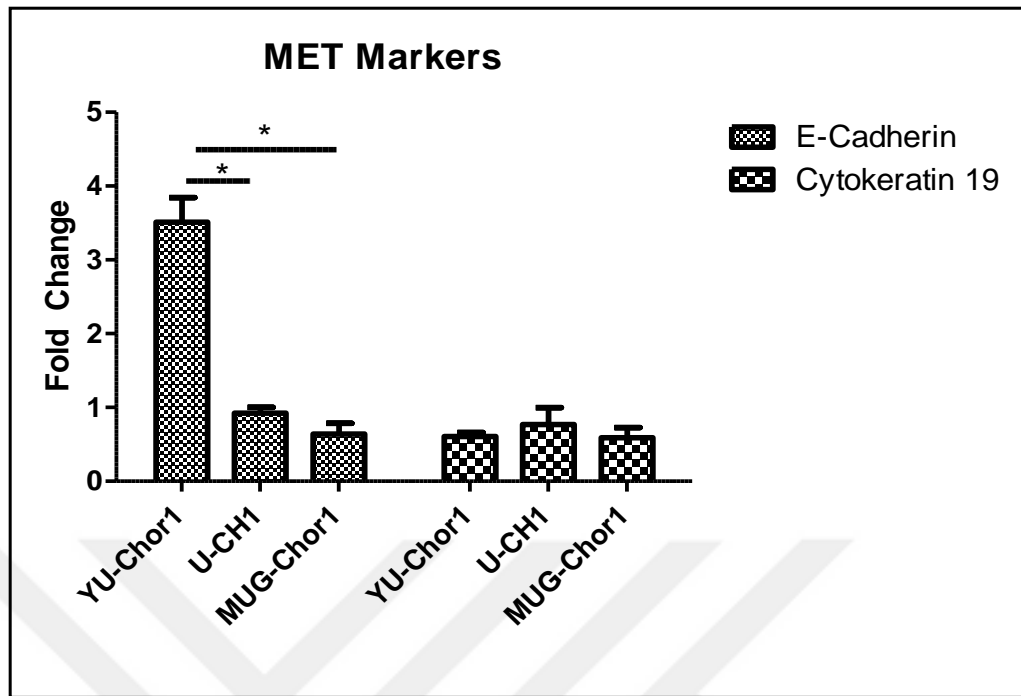


Figure 3.28. Expression level of MET-related genes. Cell line which had the lowest expression for each gene among the cell lines were used for normalization. \*:  $p < 0.05$ .



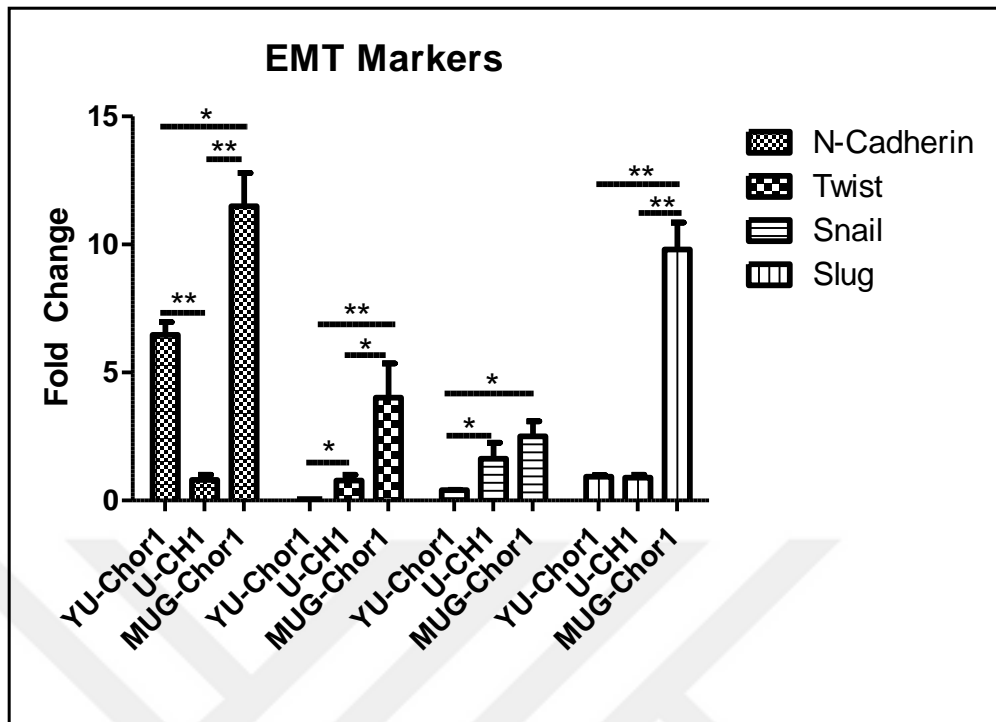


Figure 3.29. Expression level of EMT-related genes. Cell line which had the lowest expression for each gene among the cell lines were used for normalization. \*:  $p < 0.05$ , \*\*:  $p < 0.01$ .

Short Tandem Repeat (STR) analysis, which is widely used in order to authenticate cell lines, revealed that STR analysis of YU-Chor1 matched at a high ratio patient's blood (Table 3.6).

Table 3.6. STR analysis of YU-Chor1 cell line and patient's blood.

Locus Designation	Locus	YU-Chor1		Patient's blood	
D8S1179	8q24.13	12	13	12	13
D21S11	21q21.1	30		29	30
D7S820	7q21.11	10	12	10	12
CSF1PO	5q33.1	10	12	10	12
D3S1358	3p21.31	18		18	
THO1	11p15.5	6		6	9
D13S317	13q31.1	13		11	13
D16S539	16q241.1	12		11	12
VWA	12p13.31	15	16	15	16
TPOX	2p25.3	8		8	
D18S51	18q21.33	12	14	12	14
AMELOGENIN	Xp22.1-22.3, Yp11.12	X		X	Y
D5S818	5q23.2	11	13	11	13
FGA	4q31.3	19	22	19	22

It is known that cancer cells have genomic re-arrangements which are hallmark of cancer in their genome. Thus, array Comparative Genomic Hybridization (CGH) was carried out for YU-Chor1. Array CGH results indicated that YU-Chor1 cell lines have lots of gains and losses in their genome (Fig. 3.30). Briefly, q arm of chromosome 2, and chromosome 5 had big gains (>30000 KBP) whereas q arm of chromosome 11, chromosome 13, chromosome 14 and chromosome 16, chromosome 21 and chromosome and p arm of chromosome 10 had big losses (>30000 KBP) in their genome. Although patient was a male, chromosome Y could not have been detected.

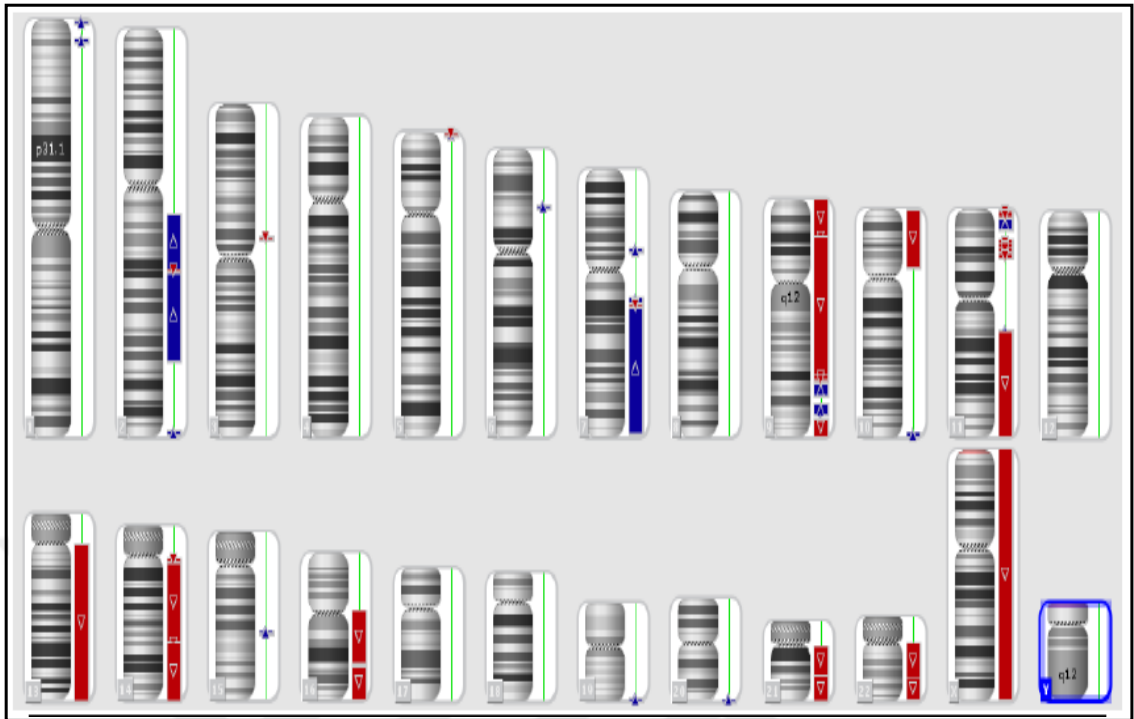


Figure 3.30. Array CGH profile of YU-Chor1 cell line. Red represents losses and blue represents gains.

### 3.2.2. Identification of Dysregulated mRNAs in Recurrent Chordoma Samples

mRNA expression level of chordoma samples were compared using two recurrent clival chordoma (who had the poorest prognosis) and two primary chordoma (who had the best prognosis) from our patient cohort. mRNA microarray analysis revealed that 226 mRNAs were differentially expressed (142 upregulated, 84 downregulated) in recurrent chordoma samples compared with primary chordoma samples (Fig. 3.31).

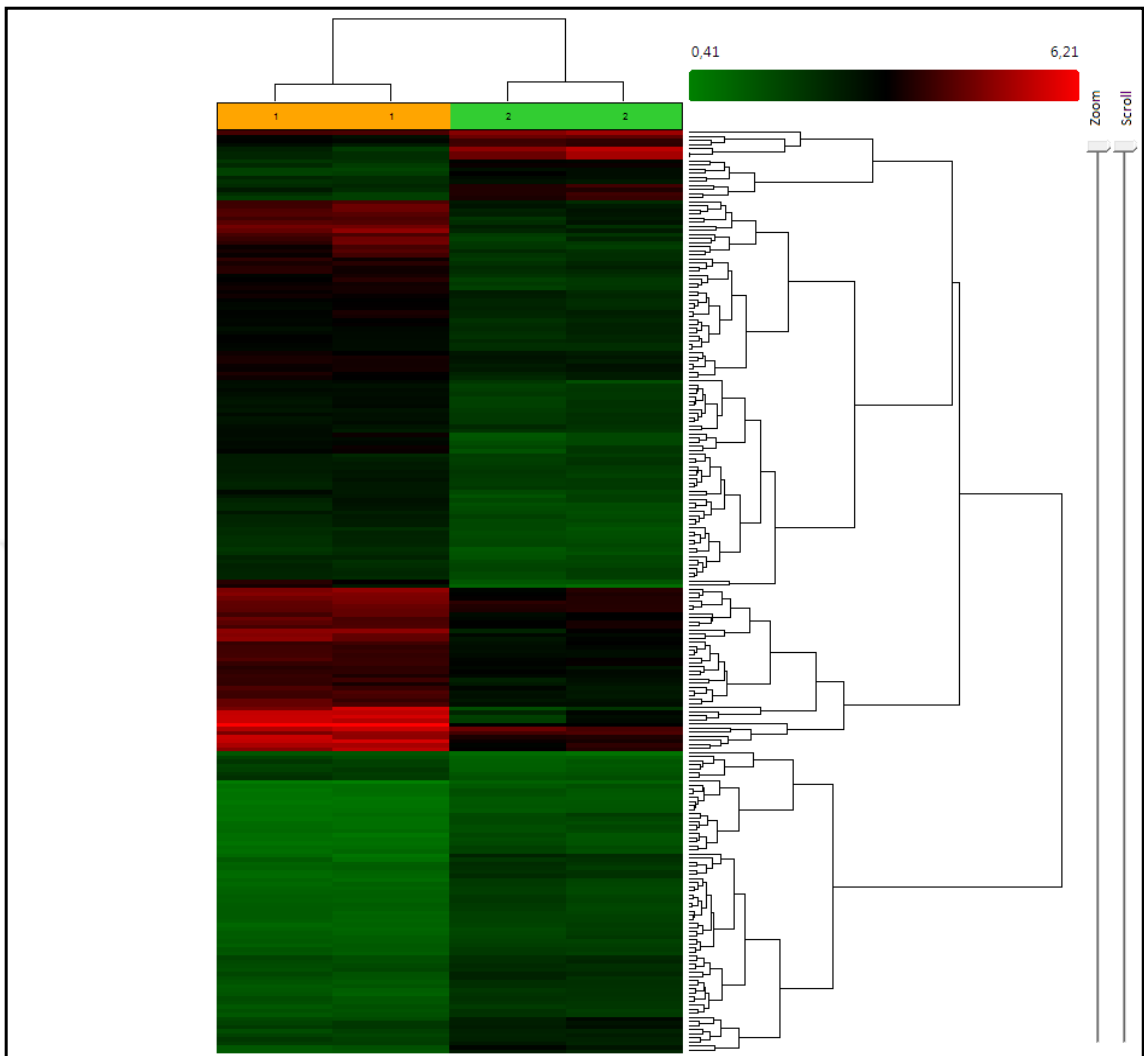


Figure 3.31. mRNA microarray results for two recurrent and two primary chordoma tumor tissues. Number of upregulated and downregulated mRNAs with hierarchical clustering generated by TAC software. Number 1 represents recurrent chordoma samples; number 2 represents primary chordoma samples.

Bioinformatical analysis of mRNA microarray using The Database for Annotation, Visualization and Integrated Discovery (DAVID) indicated that several signaling pathways were dysregulated in recurrent chordoma samples compared with primary chordoma samples (Table 3.7).

Table 3.7. Bioinformatical analysis of mRNA microarray results using DAVID database.

Signaling Pathway	Gene Count	P Value	Benjamini
Fructose and Mannose Metabolism	3	2,1E-2	9,0E-1
AMPK Signaling Pathway	4	5,4E-2	9,5E-1
Insulin Signaling Pathway	4	7,1E-2	9,3E-1
Central Carbon Metabolism in Cancer	3	7,3E-2	8,8E-1
Cytokine-Cytokine Receptor Interaction	5	8,8E-2	8,2E-1

An extensive bioinformatics analysis provided us with 4 different genes that could be highly related to the recurrence in chordoma: *CREB1*, *IGFBP6*, *LGR5*, and *TBX18*. Once determination of the genes that would be responsible in recurrence, expression levels of these genes were detected through qPCR in our patient cohort and clinicopathological analysis were carried out. Firstly, our mRNA microarray results were confirmed through qPCR. qPCR results indicated that expression of *CREB1*, *IGFBP6*, *LGR5*, and *TBX18* were higher by 2.85-fold, 17.85-fold, 124.7-fold, and 20.25-fold in recurrent chordoma samples compared with primary chordoma samples (Fig. 3.32). Clinicopathological analysis demonstrated that increased expression of *IGFBP6* was related with decreased survival time. While increased expression of *LGR5* also related with decreased overall survival time, it was not statistically significant. There was no relationship between the expression of both *CREB1* and *TBX18* and overall survival time (Fig. 3.33).

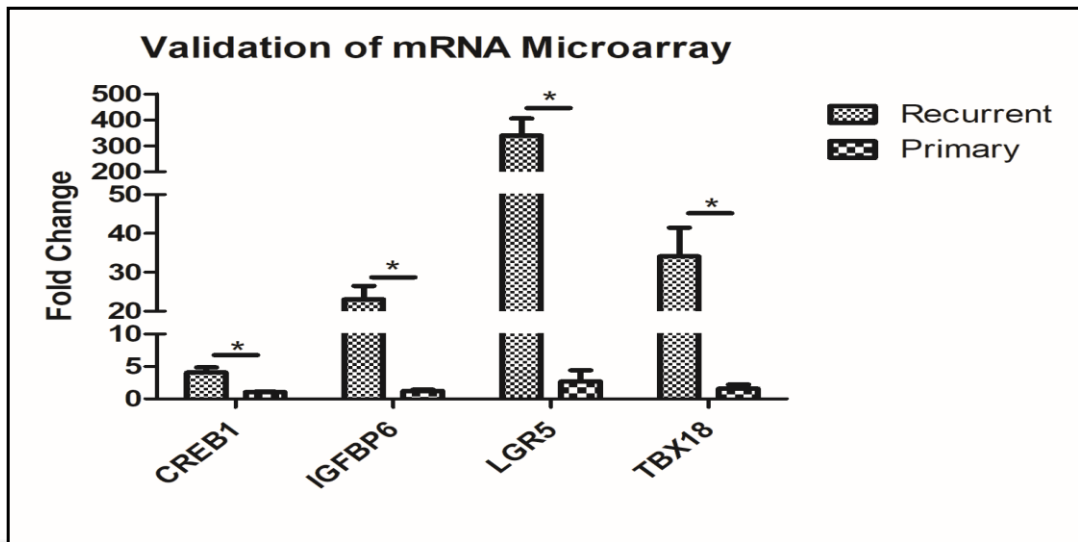


Figure 3.32. Expression level of CREB1, IGFBP6, LGR5 and TBX18. Patient sample which had the lowest expression for each gene among the patient samples were used for normalization. Graph bars indicate average fold change of each group. \*:  $p < 0.05$ .

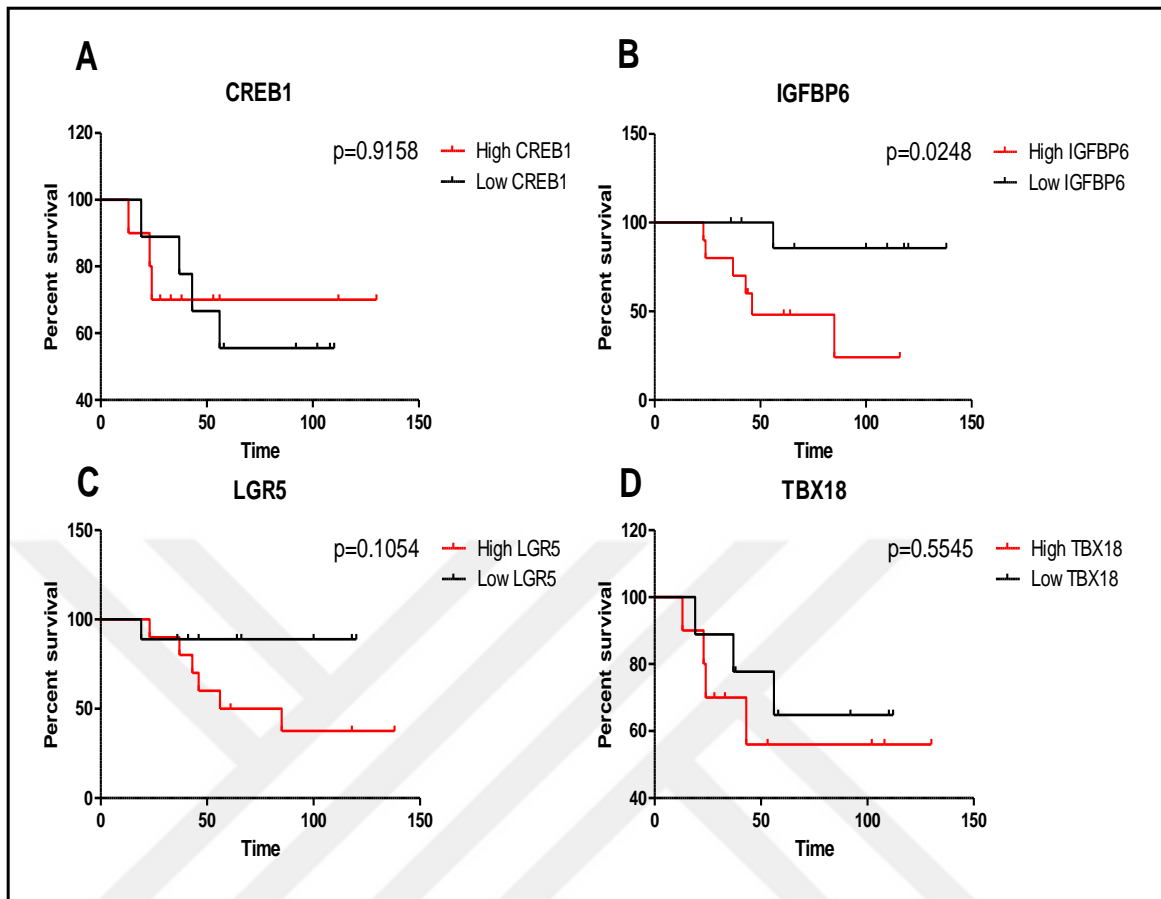


Figure 3.33. Overall survival analysis of chordoma samples using selected genes A) *CREB1*, B) *IGFBP6*, C) *LGR5* and D) *TBX18*.

In addition, increased expression of *IGFBP6* was related with recurrence, metastasis and high expression of P53, but increased expression of *LGR5* was related with decreased Ki67 and Tumor volume in our patient cohort (Table 3.8).

Table 3.8. Correlation of selected genes with clinicopathological features. P-value of significant results was shown in bold.

Clinicopathological Features	Molecule Name	Low	High	Total	<i>p-Value</i>
<b>P53</b>	<b>CREB1</b>				
	< 2%	5	6	11	<b>0.3137</b>
	≥ 2%	2	4	6	
	<b>IGFBP6</b>				

	< 2%	7	4	11	<b>0.0319</b>
	≥ 2%	1	5	6	
	<b>LGR5</b>				
	< 2%	5	6	13	0.3137
	≥ 2%	2	4	5	
	<b>TBX18</b>				
	< 2%	5	6	11	0.3137
	≥ 2%	2	4	6	
<b>Ki67</b>	<b>CREB1</b>				
	< 7%	6	7	13	0.2261
	≥ 7%	1	3	4	
	<b>IGFBP6</b>				
	< 7%	5	8	13	0.1002
	≥ 7%	3	1	4	
	<b>LGR5</b>				
	< 7%	5	8	13	<b>0.0155</b>
	≥ 7%	4	0	4	
	<b>TBX18</b>				
	< 7%	8	5	13	0.1002
	≥ 7%	1	3	4	
<b>Gender</b>	<b>CREB1</b>				
	Female	6	6	12	0.3818
	Male	3	4	7	
	<b>IGFBP6</b>				
	Female	6	6	12	0.3818
	Male	3	4	7	
	<b>LGR5</b>				
	Female	4	8	12	0.0543
	Male	5	2	7	
	<b>TBX18</b>				
	Female	4	8	12	0.0543
	Male	5	2	7	
<b>Age</b>	<b>CREB1</b>				
	< 47	5	3	8	0.1300
	≥ 47	4	7	11	



	<b>IGFBP6</b>				
	< 47	5	3	8	0.1300
	≥ 47	4	7	11	
	<b>LGR5</b>				
	< 47	3	5	8	0.2313
	≥ 47	6	5	11	
	<b>TBX18</b>				
	< 47%	3	5	8	0.2313
	≥ 47%	6	5	11	
<b>Recurrence</b>	<b>CREB1</b>				
	Yes	4	4	8	0.8447
	No	5	6	11	
	<b>IGFBP6</b>				
	Yes	2	6	8	<b>0.0479</b>
	No	7	4	11	
	<b>LGR5</b>				
	Yes	2	6	8	<b>0.0479</b>
	No	7	4	11	
	<b>TBX18</b>				
	Yes	3	5	8	0.4625
	No	6	5	11	
<b>Metastasis</b>	<b>CREB1</b>				
	Yes	2	1	3	0.4657
	No	7	9	16	
	<b>IGFBP6</b>				
	Yes	3	0	3	<b>0.0367</b>
	No	6	10	16	
	<b>LGR5</b>				
	Yes	1	2	3	0.5957
	No	8	8	16	
	<b>TBX18</b>				
	Yes	1	2	3	0.5957
	No	8	8	16	
<b>Tumor Volume</b>	<b>CREB1</b>				
	< 26 mm <sup>3</sup>	6	6	12	

	$\geq 26 \text{ mm}^3$	3	4	7	0.3818
<b>IGFBP6</b>					
	$< 26 \text{ mm}^3$	6	6	12	0.3818
	$\geq 26 \text{ mm}^3$	3	4	7	
<b>LGR5</b>					
	$< 26 \text{ mm}^3$	2	9	12	<b>0.0014</b>
	$\geq 26 \text{ mm}^3$	7	1	7	
<b>TBX18</b>					
	$< 26 \text{ mm}^3$	8	4	12	<b>0.0137</b>
	$\geq 26 \text{ mm}^3$	1	6	7	

## 4. DISCUSSION

To date, many dysregulated miRNAs were reported in chordoma [200,204–207,216–223]. However, the role of miRNAs in chordoma CSCs was firstly investigated in this study. Previous studies revealed that *KLF4*, *OCT3/4*, *C-MYC*, and *NANOG* were highly active genes in CSCs [173,224,225]. Expression of *OCT3/4*, *C-MYC*, and *NANOG* was upregulated in CD133<sup>+</sup> cancer cells [224,225]. CSCs have higher invasion, migration, tumorsphere-forming and colony-forming abilities along with EMT phenotype as opposed to the non-CSCs [173,183,226,227]. Studies suggested that CSCs have the ability to grow in the absence of the attachment known as spheroids [228]. In addition, colony formation assay is used in order to determine the functional capacity of CSCs [168]. Our results demonstrated that CSC- and EMT-related genes were highly expressed in CD133<sup>+</sup>CD15<sup>+</sup> chordoma cells and they had increased invasion, migration, tumorsphere-forming and colony-forming abilities consistent with CSC phenotype.

There are lots of studies regarding the role of miRNAs in CSCs. As an example, reduced expression of miR-20a-5p and let-7i-5p, which are also downregulated in chordoma CSCs, is associated with resistance to chemotherapy and CSC phenotype in osteosarcoma and gastric carcinoma [229,230]. miR-3175 and miR-106-5p were also downregulated in gastric cancer side population and CD133<sup>+</sup> larynx CSCs consistent with our miRNA microarray results [231,232].

In the course of this study, our results revealed that miR-140-3p affected both viability and apoptosis in U-CH1 cells. However, no effect of this miRNA was detected on viability and apoptosis for MUG-Chor1 cells. It was shown that miR-140-3p caused reduced viability of lung cancer cells [233]. Pre-mir-148a-3p showed two-way responses for chordoma cells, for instance, pre-mir-148a reduced viability by 20 percent in U-CH1 and yet increased viability in MUG-Chor1 cells by 10 percent. Our results showed that anti-miR-148a-3p reduced viability and increased apoptosis in both chordoma cell lines. Studies suggested that miR-148a-3p could target *BCL2* and stimulate apoptosis in colorectal and pancreas cancer [234,235]. Conversely, it can induce proliferation by targeting *P27* [236]. It is possible that while miR-148a-3p targets *P27* in U-CH1, *BCL2* can be targeted by miR-148a-3p in MUG-Chor1 cells. Pre- and anti-mimic transfection of miR-210-5p shared the

same pattern for both cell lines. Pre-miR-210-5p decreased viability and increased apoptosis rate in both cell lines. Consistently, transfection of anti-miR-210-5p increased proliferation in MUG-Chor1 and decreased apoptosis in U-CH1. Studies showing that anti-miRNA-210-5p transfection enhanced cell number and inhibited apoptosis was in agreement with our data [237,238]. Pre-miR-574-5p decreased viability and increased apoptosis in U-CH1 cells while it had no effect on both viability and apoptosis in MUG-Chor1 cells. Several studies determined that miR-574-5p overexpression caused a high proliferation rate and inhibited apoptosis in cancer [239,240]. Viability and apoptosis assays showed different patterns (except for miR-210-5p) in both cell lines upon transfection with related miRNAs. This could arise from the differences between basal expression levels in chordoma cell lines and different binding affinity to their target genes. Moreover, miRNAs can regulate hundreds of genes. Although target genes of selected miRNAs were confirmed through qPCR, miRNAs could have targeted different genes and caused different responses to miRNAs for proliferation and apoptosis.

Our results indicated that *WNT5A*, *TGF- $\alpha$* , *BTG2* and *MYCBP* were regulated by miR-140-3p, miR-148a-3p, miR-210-5p and miR-574-5p, respectively. Wnt pathway has crucial role in CSCs [241]. *WNT5A* promotes invasion and migration ability, which led increasing in metastasis and tumorigenesis through increasing CSC phenotype in nasopharyngeal carcinoma [242]. Therewithal, miR-140-3p, a regulator of *WNT5A*, is downregulated in several cancers and considered as a poor prognosis factor. Downregulation of miR-140-3p which is also associated with immune checkpoint receptor PD-L1, is correlated with metastasis in chordoma and can be overexpressed by IFN- $\gamma$  [243–246]. Although miR-140-3p is highly expressed and related with poor prognosis in chordoma [220], its expression diminished in chordoma CSCs. It is previously determined that miR-148a-3p is elevated in chordoma compared with healthy control, nucleus pulposus cells [205,206]. Overexpression of miR-148a-3p reduced proliferation, cell motility and EMT through blocking ERBB3/AKT/C-MYC axis in bladder cancer [247]. Our results revealed that miR-148a-3p is less expressed in CSCs and can regulate *TGF- $\alpha$*  which was found to be upregulated in CSCs [248]. miR-210-5p plays a role in hypoxia, which can enhance the survival of stem cells under low oxygen conditions [249]. *BTG2*, a target of miR-210-5p, inhibited CSC features of hepatocellular carcinoma side population [250]. *BTG2* also can inhibit invasion and migration and stimulate apoptosis [251]. *MYCBP* binds N-terminal

domain of C-MYC and activates it to exalt tumorigenesis [252]. miR-574-5p that targeted *MYCBP* in our study showed decreased expression pattern in gastric CSCs consistent with our study [230]. We observed that while expression of miR-140-3p, miR-148a-3p, and miR-574-5p diminished in chordoma CSCs, miR-210-5p expression level increased. Collective transfection of anti-miR-140-3p, anti-miR-148a-3p, anti-miR-574-5p and pre-mir-210-5p stimulated invasive and migratory phenotype along with high ALDH activity which is widely used to detect stem cell characteristic in various cancers [253], whereas pre-mir-140-3p, pre-mir-148a-3p, pre-mir-574-5p and anti-miR-210-5p inhibited them. Data from experiment of miR-152-3p targeting was not convincing enough since it is expected for a decrease upon transfection of pre-mimic miRNA and an increase of anti-mimic miRNA. Thus, miR-152-3p was excluded from subsequent experiments because of inconsistent data. Moreover, expression level of *TNFAIP2* displayed inconsistent results in different chordoma cell lines (Data not shown). Dysregulation of miRNAs in CSCs could have contributed to CSC phenotype in chordoma. All of these findings support that miR-140-3p, miR-148a-3p, miR-210-5p and miR-574-5p might be important regulators of multiple functions that lead to invasion, migration, immune escape, and stem cell maintenance in chordoma.

It is known that CSCs have decreased proliferation rate integrated with excellent DNA repair mechanism and could escape apoptosis through G2 arrest in cell cycle [254,255]. In addition, CSCs are associated with metastasis, self-renewal, invasion and migration abilities [173,183,226,256]. Dysregulation of miRNA responsible in cell cycle arrest, proliferation, self-renewal capacity, metastasis, apoptosis, migration and invasion capacity could have sustained CSC phenotype in chordoma CSCs.

mRNA microarray results demonstrated that chordoma CSCs exhibited a decrease expression patterns for gene cascades related to cell cycle, DNA replication, and caspase cascade in apoptosis. Proliferation of CSCs is slower and their DNA repair mechanism works well than non-CSCs and they are resistant to apoptosis through G2 arresting in cell cycle [254,255]. Alteration of genes' expression responsible in cell cycle, DNA replication and apoptosis related pathways could have sustained CSC phenotype in chordoma CSCs. Our results collected from Ingenuity pathway analysis put forward that while NUPR1 could be activated in chordoma CSCs, FOXO1 could have been inhibited. Besides, FoxO signaling pathway is also downregulated in chordoma CSCs according to DAVID analysis.

Grasso *et al.* showed that *NUPR1* negatively regulates *FOXO3a* [257]. Song *et al.* revealed that *ALDH<sup>high</sup>* and *CD133<sup>high</sup>* pancreatic ductal adenocarcinoma cells were null for *FoxO1* [258]. Activation of *NUPR1* concurrent with decreased FoxO signaling pathway may have a role in maintenance of CSCs in chordoma.

Dysregulated miRNAs and their targets associated with important clinicopathological properties in our patient group. miR-140-3p and miR-148a-3p positively correlated with Ki67, which had prognostic significance in many cancers [259,260]. Moreover, pre-miR-140-3p and TGF- $\alpha$  level correlated with p53 which was associated with poor prognosis in chordoma [261]. MYCBP was also positively correlated with tumor volume as Leukemia Inhibitory Factor (LIF) increased number of CD133<sup>+</sup> and/or CD15<sup>+</sup> chordoma cells. In a prior study, administration of LIF on chordoma cells also promoted invasion, migration, colony formation and tumorsphere formation, which were related to CSC phenotype [262]. TGF- $\alpha$  which was responsible in osteosarcoma metastasis through activating PI3K and Akt signaling pathway, was also associated with metastasis in our patient cohort [263]. miR-210-5p, upregulated in chordoma CSCs, was also positively correlated with metastasis.

Cancer cell lines are the best *in vitro* model to detect molecular mechanism of different cancer subtypes. To date, a few cancer cell lines have been established due to rarity of chordoma. Moreover, recurrent-clivus chordoma cell line has not been established and defined yet. Here, a new chordoma cell line named YU-Chor1 was firstly established. Our results showed that YU-Chor1 cell line was highly positive for CD90, CD44 and CD24, which are used to characterize chordoma cell lines [264]. Ratio of CD133 and CD15 was also similar as much as other chordoma cell lines. *Brachyury* expression is also used in order to characterize chordoma cell lines as chordoma foundation suggested. In YU-Chor1 cell line, *Brachyury* expression was higher than U-CH1, whereas it was less than MUG-Chor1. All of these results suggested that YU-Chor1 cell line is suitable cancer cell line to explore recurrence mechanism of clivus-originated chordomas.

STR analysis is a DNA-finger printing method based on determining the length of STR regions. Our STR analysis showed that, although STR profile of YU-Chor1 cell line was highly similar with patient's blood there were still some differences. This difference could have been due to genomic rearrangements in the tumor genome. For example, loci of

THO1, D22S1045, D2S41, D13S317, D16S539 and D21S11 partially matched with patient's DNA and locus of these loci had genomic rearrangements (loss) as array CGH results showed. Moreover, locus of D10S1248 loci which partially matched with patient's blood had also a gain in YU-Chor1 cell line.

DAVID analysis revealed that several signaling pathways were dysregulated in recurrent clivus chordoma samples. Fructose and mannose metabolism is highly active during carcinogenesis and accounted for energy requirements for DNA replication and protein synthesis [265]. AMPK signaling pathway which can act as both tumor suppressor and tumor promoter was also highly active in recurrent chordoma samples and MYC requires ARK5 which is a kind of AMPK associated kinase [266]. Insulin signaling pathway can also be regulated by NANOG, a CSC marker. Cytokines which are secreted by cells (especially immune cells) found in tumor microenvironment are important trimmer of immune system and they may promote aggressiveness of tumor through activating several signaling cascades [267]. To summarize, dysregulation of these signaling pathways might be a target in recurrent chordoma.

LGR5, is a master regulator of canonical Wnt signaling pathway and is used as a stem cell marker for intestinal epithelium and hair follicle. LGR5 is also highly expressed in U-CH1 [187] and CSC marker in colorectal cancer (CRC) [268]. Our clinicopathological analysis demonstrated that chordoma patients concurrent with increased *LGR5* activation had poor prognosis. In brief, *LGR5* expression was related with recurrence, metastasis, decreased P53 and lesser overall survival time after the surgery. Consequently, targeting LGR5 through monoclonal antibodies before and/or after the surgical resection of tumor could be useful to cure the patients with chordoma.

IGFBP6 is a IGF-binding protein that regulates insulin signaling pathway. Insulin signaling pathway has two different receptors IGF1R and IGFR2, which are type of RTK. IGF-1 and IGF-2 specifically bind to these receptors and activate several pathways including PI3K signaling pathway and RAS/RAF/MEK/ERK axis [269]. IGF-binding proteins (IGFBP) have an affinity to bind IGFs and regulate IGF signaling pathway. There are 6 different IGFBPs were identified. IGFBP6 targets IGF2 rather than IGF1. Studies revealed that HIF1 $\alpha$  can activate IGFBP6 [270]. IGFBP6 can then increase both proliferation and cell migration [271,272]. In addition, stem cell properties of MSCs could

be maintained by IGFBP6 and sonic hedgehog (SHH) signaling pathway could increase expression of IGFBP6 [273,274]. Both HIF1 $\alpha$  and SHH signaling pathway contribute CSC phenotype which is responsible in recurrence in patients with cancer. That's why specific therapies for IGFBP6 might increase life quality of patients with chordoma.





## 5. CONCLUSION

This is the first exhaustive study about identification and characterization of chordoma CSCs. This study displayed molecular mechanisms of chordoma CSCs and relationship between clinicopathological features and CSC-related molecules. Taken together, this study showed that CD133<sup>+</sup>CD15<sup>+</sup> chordoma cells represented CSC population in chordoma. Role of miRNAs in chordoma CSCs was firstly identified in this study. Briefly, our results showed that *WNT5A*, *TGF- $\alpha$* , *BTG2*, and *MYCBP* were regulated by miR-140-3p, miR-148a-3p, miR-210-5p and miR-574-5p, respectively. Moreover, these miRNAs increased invasion and migration ability and stem cell phenotype in chordoma cell lines. *In vivo* studies are needed to validate that CD133<sup>+</sup>CD15<sup>+</sup> chordoma cells are real CSCs in chordoma. These findings are important since it is known that CSCs have a prominent role in recurrence, metastasis, chemo- and radio-resistance. As a result, understanding molecular mechanism of chordoma CSCs could be useful to target them and can be provide novel and unique therapeutic option for patients with chordoma.

Additionally, a new recurrent-clivus chordoma cell line named YU-Chor1 was firstly established by our group. Our study demonstrated that almost all the YU-Chor1 cells were positive for CD90, CD24 and CD44 which are markers used for chordoma characterization. We also determined expression level of chordoma markers (especially *brachyury*), EMT- and MET-related markers and found that YU-Chor1 cells highly express all of these markers (except EMA). After that, mRNA profile of both recurrent chordoma samples and primary chordoma samples was identified and compared in order to explore mechanism of recurrence in chordoma. Finally, clinicopathological analysis indicated that high expression of both IGFBP6 and LGR5 were poor prognostic factors for patients with chordoma. Taken together, these findings suggested that identification of recurrence-related signaling pathways could be useful to prevent recurrence in patients with chordoma.

In the first part of this study, role of miRNAs were studied and their role was identified in maintenance of CSC-phenotype in chordoma. mRNA profile of chordoma CSCs were also determined and data obtained from mRNA microarray were analyzed through bioinformatical tools including IPA and DAVID. However, no functional studies were

carried out using mRNA microarray data. In the future, it is planned that genes that will be selected through bioinformatical analysis of mRNA microarray data will be used in order to identify differentially activated signaling pathways in chordoma CSCs. Briefly, expression of genes whose expression is downregulated in chordoma CSCs will be increased and/or expression of genes whose expression is upregulated in chordoma CSCs will be decreased. Next, functional studies such as invasion, migration, colony-formation, tumorsphere-formation ability of chordoma cells will be assessed and results of functional studies will be validated with *in vivo* studies and clinicopathological analysis. In addition, our results revealed that high expression of both *IGFBP6* and *LGR5* was a poor prognostic marker for chordoma in our patient cohort. Thus, siRNAs specific for *IGFBP6* and *LGR5* will be introduced into chordoma cell lines and the contribution of these biomarkers to chordoma pathogenesis (especially recurrence) will be investigated in addition to *IGFBP6*- and *LGR5*-induced signaling pathways.

This study was supported by TÜBİTAK as a 3501-Career Project (Grant number: 112S485) and Yeditepe University Hospital.

## REFERENCES

1. Kinzler KW, Vogelstein B. Lessons from hereditary colorectal cancer. *Cell*. 1996;87(2):159–70.
2. Hanahan D, Weinberg RA. Hallmarks of cancer: the next generation. *Cell*. 2011;144(5):646–74.
3. Dalerba P, Clarke MF. Cancer stem cells and tumor metastasis: First steps into uncharted territory. *Cell Stem Cell*. 2007;1(3):241–2.
4. Clarke MF, Dick JE, Dirks PB, Eaves CJ, Jamieson CHM, Jones DL, et al. Cancer stem cells-perspectives on current status and future directions: AACR workshop on cancer stem cells. *Cancer Research*. 2006;66(19):9339–44.
5. Zarkowska T, Mitnacht S. Differential phosphorylation of the retinoblastoma protein by G1/S cyclin-dependent kinases. *Journal of Biological Chemistry*. 1997;272(19):12738–46.
6. Murphree AL, Benedict WF. Retinoblastoma: Clues to human oncogenesis. *Science*. 1984;223(4640):1028–33.
7. Parisi T, Bronson RT, Lees JA. Inactivation of the retinoblastoma gene yields a mouse model of malignant colorectal cancer. *Oncogene*. 2015;34(48):5890–9.
8. Egger JV., Lane MV., Antonucci LA, Dedi B, Krucher NA. Dephosphorylation of the Retinoblastoma protein (Rb) inhibits cancer cell EMT via Zeb. *Cancer Biology and Therapy*. 2016;17(11):1197–205.
9. Rivlin N, Brosh R, Oren M, Rotter V. Mutations in the p53 tumor suppressor gene: Important milestones at the various steps of tumorigenesis. *Genes and Cancer*. 2011;2(4):466–74.
10. Muller PAJ, Vousden KH. P53 mutations in cancer. *Nature Cell Biology*. 2013;15(1):2–8.
11. Kandoth C, McLellan MD, Vandin F, Ye K, Niu B, Lu C, et al. Mutational

landscape and significance across 12 major cancer types. *Nature*. 2013;502(7471):333–9.

12. Wang SP, Wang WL, Chang YL, Wu CT, Chao YC, Kao SH, et al. p53 controls cancer cell invasion by inducing the MDM2-mediated degradation of Slug. *Nature Cell Biology*. 2009;11(6):694–704.

13. Aas T, Børresen AL, Geisler S, Smith-Sørensen B, Johnsen H, Varhaug JE, et al. Specific P53 mutations are associated with de novo resistance to doxorubicin in breast cancer patients. *Nature Medicine*. 1996;2(7):811–4.

14. Rusch V, Martini N, Klimstra D, Oliver J, Venkatraman E, Kris M, et al. Aberrant p53 expression predicts clinical resistance to cisplatin-based chemotherapy in locally advanced non-small cell lung cancer. *Cancer Research*. 1995;55(21):5038–42.

15. Starzynska T, Bromley M, Ghosh A, Stern PL. Prognostic significance of p53 overexpression in gastric and colorectal carcinoma. *British Journal of Cancer*. 1992;66(3):558–62.

16. Chu EC, Tarnawski AS. PTEN regulatory functions in tumor suppression and cell biology. *Medical Science Monitor : International Medical Journal of Experimental and Clinical Research*. 2004;10(10):235-41.

17. Cairns P, Evron E, Okami K, Halachmi N, Esteller M, Herman JG, et al. Point mutation and homozygous deletion of PTEN/MMAC1 in primary bladder cancers. *Oncogene*. 1998;16(24):3215–8.

18. Duerr EM, Rollbrocker B, Hayashi Y, Peters N, Meyer-Puttlitz B, Louis DN, et al. PTEN mutations in gliomas and glioneuronal tumors. *Oncogene*. 1998;16(17):2259–64.

19. Shao X, Tandon R, Samara G, Kanki H, Yano H, Close LG, et al. Mutational analysis of the PTEN gene in head and neck squamous cell carcinoma. *International Journal of Cancer*. 1998;77(5):684–8.

20. Hollander MC, Blumenthal GM, Dennis PA. PTEN loss in the continuum of common cancers, rare syndromes and mouse models. *Nature Reviews Cancer*. 2011;11(4):289–301.

21. Yuan XJ, Whang YE. PTEN sensitizes prostate cancer cells to death receptor-mediated and drug-induced apoptosis through a FADD-dependent pathway. *Oncogene*. 2002;21(2):319–27.
22. Bandyopadhyay S, Pai SK, Hirota S, Hosobe S, Takano Y, Saito K, et al. Role of the putative tumor metastasis suppressor gene Drg-1 in breast cancer progression. *Oncogene*. 2004;23(33):5675–81.
23. Lee HS, Lee HK, Kim HS, Yang HK, Kim WH. Tumour suppressor gene expression correlates with gastric cancer prognosis. *Journal of Pathology*. 2003;200(1):39–46.
24. Hu TH, Huang CC, Lin PR, Chang HW, Ger LP, Lin YW, et al. Expression and prognostic role of tumor suppressor gene PTEN/MMAC1/TEP1 in hepatocellular carcinoma. *Cancer*. 2003;97(8):1929–40.
25. Easton DF. How many more breast cancer predisposition genes are there? *Breast Cancer Research*. 1999;1(1):14–7.
26. Campeau PM, Foulkes WD, Tischkowitz MD. Hereditary breast cancer: New genetic developments, new therapeutic avenues. *Human Genetics*. 2008;124(1):31–42.
27. Pal T, Permuth-Wey J, Betts JA, Krischer JP, Fiorica J, Arango H, et al. BRCA1 and BRCA2 mutations account for a large proportion of ovarian carcinoma cases. *Cancer*. 2005;104(12):2807–16.
28. Roy R, Chun J, Powell SN. BRCA1 and BRCA2: Different roles in a common pathway of genome protection. *Nature Reviews Cancer*. 2012;12(1):68–78.
29. Antoniou A, Pharoah PDP, Narod S, Risch HA, Eyfjord JE, Hopper JL, et al. Average risks of breast and ovarian cancer associated with BRCA1 or BRCA2 mutations detected in case series unselected for family history: A combined analysis of 22 studies. *The American Journal of Human Genetics*. 2003;72(5):1117–30.
30. Chen S, Parmigiani G. Meta- Analysis of BRCA1 and BRCA2 penetrance. *Journal of Clinical Oncology*. 2007;25(11):1329–33.

31. Chen GG, Lai PBS. *Apoptosis in carcinogenesis and chemotherapy*. Dordrecht, The Netherlands: Springer; 2009.
32. Matsui T, Heidaran M, Miki T, Popescu N, La Rochelle W, Kraus M, et al. Isolation of a novel receptor cDNA establishes the existence of two PDGF receptor genes. *Science*. 1989;243(4892):800–4.
33. Ebert M, Yokoyama M, Friess H, Kobrin MS, Büchler MW, Korc M. Induction of platelet-derived growth factor A and B chains and over-expression of their receptors in human pancreatic cancer. *International Journal of Cancer*. 1995;62(5):529–35.
34. Suzuki S, Dobashi Y, Hatakeyama Y, Tajiri R, Fujimura T, Heldin CH, et al. Clinicopathological significance of platelet-derived growth factor (PDGF)-B and vascular endothelial growth factor-A expression, PDGF receptor- $\beta$  phosphorylation, and microvessel density in gastric cancer. *BMC Cancer*. 2010;10(1):659.
35. Fleming T, Saxena A, Clark W. Amplification and/or overexpression of platelet-derived growth factor receptors and epidermal growth factor receptor in human glial tumors. *Cancer research*. 1992;(22):4550–3.
36. Bos R, Van Diest PJ, De Jong JS, Van Der Groep P, Van Der Valk P, Van Der Wall E. Hypoxia-inducible factor-1 $\alpha$  is associated with angiogenesis, and expression of bFGF, PDGF-BB, and EGFR in invasive breast cancer. *Histopathology*. 2005;46(1):31–6.
37. Gotzmann J, Fischer ANM, Zojer M, Mikula M, Proell V, Huber H, et al. A crucial function of PDGF in TGF- $\beta$ -mediated cancer progression of hepatocytes. *Oncogene*. 2006;25(22):3170–85.
38. Seymour L, Bezwoda WR. Positive immunostaining for platelet derived growth factor (PDGF) is an adverse prognostic factor in patients with advanced breast cancer. *Breast Cancer Research and Treatment*. 1994;32(2):229–33.
39. Mitin N, Rossman KL, Der CJ. Signaling interplay in ras superfamily function. *Current Biology*. 2005;15(14):563–74.
40. Serrano C, Romagosa C, Hernández-Losa J, Simonetti S, Valverde C, Moliné T, et al. RAS/MAPK pathway hyperactivation determines poor prognosis in undifferentiated

pleomorphic sarcomas. *Cancer*. 2016;122(1):99–107.

41. Wright KL, Adams JR, Liu JC, Loch AJ, Wong RG, Jo CEB, et al. Ras signaling is a key determinant for metastatic dissemination and poor survival of luminal breast cancer patients. *Cancer Research*. 2015;75(22):4960–72.

42. Prabhu A, Sarcar B, Miller CR, Kim SH, Nakano I, Forsyth P, et al. Ras-mediated modulation of pyruvate dehydrogenase activity regulates mitochondrial reserve capacity and contributes to glioblastoma tumorigenesis. *Neuro-Oncology*. 2015;17(9):1220–30.

43. Kannan A, Krishnan A, Ali M, Subramaniam S, Halagowder D, Sivasithamparam ND. Caveolin-1 promotes gastric cancer progression by up-regulating epithelial to mesenchymal transition by crosstalk of signalling mechanisms under hypoxic condition. *European Journal of Cancer*. 2014;50(1):204–15.

44. Nicholson RI, Gee JM, Harper ME. EGFR and cancer prognosis. *European Journal of Cancer*. 2001;37(4):9-15.

45. Ang KK, Berkey BA, Tu X, Zhang HZ, Katz R, Hammond EH, et al. Impact of epidermal growth factor receptor expression on survival and pattern of relapse in patients with advanced head and neck carcinoma. *Cancer Research*. 2002;62(24):7350–6.

46. Trinh XB, Tjalma WAA, Vermeulen PB, Van Den Eynden G, Van Der Auwera I, Van Laere SJ, et al. The VEGF pathway and the AKT/mTOR/p70S6K1 signalling pathway in human epithelial ovarian cancer. *British Journal of Cancer*. 2009;100(6):971–8.

47. Fang J, Xia C, Cao Z, Zheng JZ, Reed E, Jiang B-H. Apigenin inhibits VEGF and HIF-1 expression via PI3K/AKT/p70S6K1 and HDM2/p53 pathways. *The FASEB Journal*. 2005;19(3):342–53.

48. Xu Q, Briggs J, Park S, Niu G, Kortylewski M, Zhang S, et al. Targeting Stat3 blocks both HIF-1 and VEGF expression induced by multiple oncogenic growth signaling pathways. *Oncogene*. 2005;24(36):5552–60.

49. Han H, Silverman JF, Santucci TS, Macherey RS, D'Amato TA, Tung MY, et al. Vascular endothelial growth factor expression in stage I non-small cell lung cancer correlates with neoangiogenesis and a poor prognosis. *Annals of Surgical Oncology*.

2001;8(1):72–9.

50. Campisi J, Gray HE, Pardee AB, Dean M, Sonenshein GE. Cell-cycle control of c-myc but not c-ras expression is lost following chemical transformation. *Cell*. 1984;36(2):241–7.

51. Frost M, Newell J, Lones MA, Tripp SR, Cairo MS, Perkins SL. Comparative immunohistochemical analysis of pediatric burkitt lymphoma and diffuse large B-cell lymphoma. *American Journal of Clinical Pathology*. 2004;121(3):384–92.

52. Nesbit CE, Tersak JM, Prochownik EV. MYC oncogenes and human neoplastic disease. *Oncogene*. 1999;18(19):3004–16.

53. Savage KJ, Johnson NA, Ben-Neriah S, Connors JM, Sehn LH, Farinha P, et al. MYC gene rearrangements are associated with a poor prognosis in diffuse large B-cell lymphoma patients treated with R-CHOP chemotherapy. *Blood*. 2009;114(17):3533–7.

54. Thomas SJ, Snowden JA, Zeidler MP, Danson SJ. The role of JAK/STAT signalling in the pathogenesis, prognosis and treatment of solid tumours. *British Journal of Cancer*. 2015;113(3):365–71.

55. Kan Z, Zheng H, Liu X, Li S, Barber TD, Gong Z, et al. Whole-genome sequencing identifies recurrent mutations in hepatocellular carcinoma. *Genome Research*. 2013;23(9):1422–33.

56. Centers for Disease Control and Prevention (US); National Center for Chronic Disease Prevention and Health Promotion (US); Office on Smoking and Health (US). How Tobacco Smoke Causes Disease: The Biology and Behavioral Basis for Smoking-Attributable Disease: A Report of the Surgeon General. Atlanta (GA): Centers for Disease Control and Prevention (US) 2010 [cited 2019 9 July]. Available from: <https://www.ncbi.nlm.nih.gov/books/NBK53017/>

57. Nimmakayala RK, Seshacharyulu P, Lakshmanan I, Rachagani S, Chugh S, Karmakar S, et al. Cigarette smoke induces stem cell features of pancreatic cancer cells via PAF1. *Gastroenterology*. 2018;155(3):892-908.e6.

58. Mark Elwood J, Jopson J. Melanoma and sun exposure: An overview of published



studies. *International Journal of Cancer*. 1997;73(2):198–203.

59. Sardas S. The role of antioxidants in cancer prevention and treatment. *Indoor and Built Environment*. 2003;12(6):401–4.

60. Bressac B, Puisieux A, Kew M, Volkmann M, Bozcall S, Bella Mura J, et al. P53 mutation in hepatocellular carcinoma after aflatoxin exposure. *The Lancet*. 1991;338(8779):1356–9.

61. Shiratori Y, Yoshida H, Omata M. Management of hepatocellular carcinoma: Advances in diagnosis, treatment and prevention. *Expert Review of Anticancer Therapy*. 2001;1(2):277–90.

62. Cagatay T, Ozturk M. P53 Mutation as a source of aberrant B-Catenin accumulation in cancer cells. *Oncogene*. 2002;21(52):7971–80.

63. Parfenov M, Pedamallu CS, Gehlenborg N, Freeman SS, Danilova L, Bristow CA, et al. Characterization of HPV and host genome interactions in primary head and neck cancers. *Proceedings of the National Academy of Sciences*. 2014;111(43):15544–9.

64. Parrella P, Poeta ML, Gallo AP, Prencipe M, Scintu M, Apicella A, et al. Nonrandom distribution of aberrant promoter methylation of cancer-related genes in sporadic breast tumors. *Clinical Cancer Research*. 2004;10(16):5349–54.

65. Pulukuri SM, Patibandla S, Patel J, Estes N, Rao JS. Epigenetic inactivation of the tissue inhibitor of metalloproteinase-2 (TIMP-2) gene in human prostate tumors. *Oncogene*. 2007;26(36):5229–37.

66. Calin GA, Dumitru CD, Shimizu M, Bichi R, Zupo S, Noch E, et al. Frequent deletions and down-regulation of micro- RNA genes miR15 and miR16 at 13q14 in chronic lymphocytic leukemia. *Proceedings of the National Academy of Sciences* 2002;99(24):13–8.

67. Bottoni A, Piccin D, Tagliati F, Luchin A, Zatelli MC, Uberti ECD. miR-15a and miR-16-1 down-regulation in pituitary adenomas. *Journal of Cellular Physiology*. 2005;204(1):280–5.

68. Cimmino A, Calin GA, Fabbri M, Iorio MV., Ferracin M, Shimizu M, et al. miR-15 and miR-16 induce apoptosis by targeting BCL2. *Proceedings of the National Academy of Sciences*. 2005;102(39):13944–9.
69. Trotman LC, Wang X, Alimonti A, Chen Z, Teruya-Feldstein J, Yang H, et al. Ubiquitination regulates PTEN nuclear import and tumor suppression of PTEN that target post-translational modification and demonstrate how a discrete molecular mechanism dictates tumor-progression by differentiating between degradation and protection of P. *Cell January*. 2007;12(1281):141–56.
70. Dolcet X, Llobet D, Pallares J, Matias-Guiu X. NF- $\kappa$ B in development and progression of human cancer. *Virchows Archiv*. 2005;446(5):475–82.
71. Robbins DJ, Zhen E, Owaki H, Vanderbilt CA, Ebert D, Geppert TD, et al. Regulation and properties of extracellular signal-regulated protein kinases 1 and 2 in vitro. *Journal of Biological Chemistry*. 1993;268(7):5097–106.
72. Lindahl T, Barnes DE. Repair of endogenous DNA damage. *Cold Spring Harbor Symposia on Quantitative Biology*. 2000;65(0):127–34.
73. Alexandrov LB, Nik-Zainal S, Wedge DC, Aparicio SAJR, Behjati S, Biankin AV., et al. Signatures of mutational processes in human cancer. *Nature*. 2013;500(7463):415–21.
74. Roberts SA, Lawrence MS, Klimczak LJ, Grimm SA, Fargo D, Stojanov P, et al. An APOBEC cytidine deaminase mutagenesis pattern is widespread in human cancers. *Nature Genetics*. 2013;45(9):970–6.
75. Bernstein C, Prasad AR, Nfonam V, Bernstei H. DNA damage, DNA repair and cancer. *New Research Directions in DNA Repair*. 2013:413-65.
76. Cavalieri EL, Rogan EG. Depurinating estrogen-DNA adducts, generators of cancer initiation: Their minimization leads to cancer prevention. *Clinical and Translational Medicine*. 2016;5(1):12.
77. Bernstein C. Epigenetic reduction of DNA repair in progression to gastrointestinal cancer. *World Journal of Gastrointestinal Oncology*. 2015;7(5):30.

78. Reuter S, Gupta SC, Chaturvedi MM, Aggarwal BB. Oxidative stress, inflammation, and cancer: How are they linked? *Free Radical Biology and Medicine*. 2010;49(11):1603–16.
79. Oberley TD. Oxidative damage and cancer. *American Journal of Pathology*. 2002;160(2):403–8.
80. Torgovnick A, Schumacher B. DNA repair mechanisms in cancer development and therapy. *Frontiers in Genetics*. 2015;6:157.
81. McCabe N, Turner NC, Lord CJ, Kluzek K, Białkowska A, Swift S, et al. Deficiency in the repair of DNA damage by homologous recombination and sensitivity to poly(ADP-ribose) polymerase inhibition. *Cancer Research*. 2006;66(16):8109–15.
82. Nikolaev A, Yang ES. The impact of DNA repair pathways in cancer biology and therapy. *Cancers*. 2017;9(9):126.
83. Rosenzweig KE, Youmell MB, Palayoor ST, Price BD. Radiosensitization of human tumor cells by the phosphatidylinositol 3- kinase inhibitors wortmannin and LY294002 correlates with inhibition of DNA- dependent protein kinase and prolonged G2-M delay. *Clinical Cancer Research*. 1997;3(7):1149–56.
84. Gavande NS, Vandervere-Carozza PS, Hinshaw HD, Jalal SI, Sears CR, Pawelczak KS, et al. DNA repair targeted therapy: The past or future of cancer treatment? *Pharmacology and Therapeutics*. 2016;100(160):65–83.
85. Patel KJ, Yu VPCC, Lee H, Corcoran A, Thistlethwaite FC, Evans MJ, et al. Involvement of BRCA2 in DNA repair. *Molecular Cell*. 1998;1(3):347–57.
86. Moynahan ME, Jasin M. Mitotic homologous recombination maintains genomic stability and suppresses tumorigenesis. *Nature Reviews Molecular Cell Biology*. 2010;11(3):196–207.
87. Malumbres M, Barbacid M. To cycle or not to cycle: a critical decision in cancer. *Nature Reviews Cancer*. 2001;1(3):222–31.
88. Sherr CJ, Beach D, Shapiro GI. Targeting CDK4 and CDK6: From discovery to

therapy. *Cancer Discovery*. 2016;6(4):353–67.

89. Otto T, Sicinski P. Cell cycle proteins as promising targets in cancer therapy. *Nature Reviews Cancer*. 2017;17(2):93–115.

90. Chohan TA, Qian H, Pan Y, Chen JZ. Cyclin-dependent kinase-2 as a target for cancer therapy: progress in the development of CDK2 inhibitors as anti-cancer agents. *Current Medicinal Chemistry*. 2015;22(2):237–63.

91. Franchi A. Epidemiology and classification of bone tumors. *Clinical Cases in Mineral and Bone Metabolism*. 2012:92–5.

92. Hauben EI, Arends J, Vandenbroucke JP, van Asperen CJ, Van Marck E, Hogendoorn PCW. Multiple primary malignancies in osteosarcoma patients. Incidence and predictive value of osteosarcoma subtype for cancer syndromes related with osteosarcoma. *European Journal of Human Genetics*. 2003;11(8):611–8.

93. Hameetman L, Bovée JV, Taminiau AH, Kroon HM, Hogendoorn PC. Multiple osteochondromas: Clinicopathological and genetic spectrum and suggestions for clinical management. *Hereditary Cancer in Clinical Practice*. 2010;2(4):161.

94. Kindblom LG. Bone tumors: Epidemiology, classification, pathology. *Imaging of Bone Tumors and Tumor-Like Lesions*. 2009:1–15.

95. Pawel BR, Sansgiri RK. Malignant bone tumors. *Pediatric Malignancies: Pathology and Imaging*. 2015:69–101.

96. Meyers PA, Schwartz CL, Krailo M, Kleinerman ES, Betcher D, Bernstein ML, et al. Osteosarcoma: A randomized, prospective trial of the addition of ifosfamide and/or muramyl tripeptide to cisplatin, doxorubicin, and high-dose methotrexate. *Journal of Clinical Oncology*. 2005;23(9):2004–11.

97. Baumhoer D, Amary F, Flanagan AM. An update of molecular pathology of bone tumors. Lessons learned from investigating samples by next generation sequencing. *Genes Chromosomes and Cancer*. 2019;58(2):88–99.

98. Miller CW, Aslo A, Won A, Tan M, Lampkin B, Koeffler HP. Alterations of the

p53, Rb and MDM2 genes in osteosarcoma. *Journal of Cancer Research and Clinical Oncology*. 1996;122(9):559–65.

99. Feugeas O, Guriec N, Babin-Boilletot A, Marcellin L, Simon P, Babin S, et al. Loss of heterozygosity of the RB gene is a poor prognostic factor in patients with osteosarcoma. *Journal of Clinical Oncology*. 1996;14(2):467–72.

100. Kovac M, Blattmann C, Ribl S, Smida J, Mueller NS, Engert F, et al. Exome sequencing of osteosarcoma reveals mutation signatures reminiscent of BRCA deficiency. *Nature Communications*. 2015;6:8940.

101. Fernanda Amary M, Ye H, Berisha F, Khatri B, Forbes G, Lehovsky K, et al. Fibroblastic growth factor receptor 1 amplification in osteosarcoma is associated with poor response to neo-adjuvant chemotherapy. *Cancer Medicine*. 2014;3(4):980–7.

102. Shin KH, Rougraff BT, Simon MA. Oncologic Outcomes of Primary Bone Sarcomas of the Pelvis. *Clinical Orthopaedics and Related Research*. 1994;(304):207–17.

103. Fiorenza F, Abudu A, Grimer RJ, Carter SR, Tillman RM, Ayoub K, et al. Risk factors for survival and local control in chondrosarcoma of bone. *The Journal of Bone and Joint Surgery-British Volume*. 2002;84(1):93–9.

104. Wyman JJ, Hornstein AM, Meitner PA, Mak S, Verdier P, Block JA, et al. Multidrug resistance-1 and P-glycoprotein in human chondrosarcoma cell lines: Expression correlates with decreased intracellular doxorubicin and in vitro chemoresistance. *The Journal of Bone and Joint Surgery-American Volume*. 2000;82(4):22.

105. Terek RM, Healey JH, Garin-Chesa P, Mak S, Huvos A, Albino AP. P53 mutations in chondrosarcoma. *Diagnostic Molecular Pathology*. 1998;7(1):51–6.

106. Amary MF, Ye H, Forbes G, Damato S, Maggiani F, Pollock R, et al. Isocitrate dehydrogenase 1 mutations (IDH1) and p16/CDKN2A copy number change in conventional chondrosarcomas. *Virchows Archiv*. 2015;466(2):217–22.

107. Tarpey PS, Behjati S, Cooke SL, Van Loo P, Wedge DC, Pillay N, et al. Frequent mutation of the major cartilage collagen gene COL2A1 in chondrosarcoma. *Nature*

*Genetics*. 2013;45(8):923–6.

108. Riggi N, Suvà ML, Suvà D, Cironi L, Provero P, Tercier S, et al. EWS-FLI-1 expression triggers a ewing's sarcoma initiation program in primary human mesenchymal stem cells. *Cancer Research*. 2008;68(7):2176–85.

109. Rocchi A, Manara MC, Sciandra M, Zambelli D, Nardi F, Nicoletti G, et al. CD99 inhibits neural differentiation of human Ewing sarcoma cells and thereby contributes to oncogenesis. *Journal of Clinical Investigation*. 2010;120(3):668–80.

110. Ventura S, Aryee DNT, Felicetti F, De Feo A, Mancarella C, Manara MC, et al. CD99 regulates neural differentiation of Ewing sarcoma cells through MIR-34a-Notch-mediated control of NF- $\kappa$ B signaling. *Oncogene*. 2016;35(30):3944–54.

111. Casali PG, Stacchiotti S, Sangalli C, Olmi P, Gronchi A. Chordoma. *Current Opinion in Oncology*. 2007;19(4):367–70

112. McMaster ML, Goldstein AM, Bromley CM, Ishibe N, Parry DM. Chordoma: Incidence and survival patterns in the United States, 1973-1995. *Cancer Causes and Control*. 2001;12(1):1–11.

113. Bergh P, Kindblom LG, Gunterberg B, Remotti F, Ryd W, Meis-Kindblom JM. Prognostic factors in chordoma of the sacrum and mobile spine: A study of 39 patients. *Cancer*. 2000;88(9):2122–34.

114. Gay E, Sekhar LN, Rubinstein E, Wright DC, Sen C, Janecka IP, et al. Chordomas and chondrosarcomas of the cranial base: Results and follow-up of 60 patients. *Neurosurgery*. 1995;36(5):887–97.

115. Carrabba G, Dehdashti AR, Gentili F. Surgery for clival lesions: open resection versus the expanded endoscopic endonasal approach. *Neurosurgical Focus*. 2008;25(6):E7.

116. Park L, DeLaney TF, Liebsch NJ, Hornicek FJ, Goldberg S, Mankin H, et al. Sacral chordomas: Impact of high-dose proton/photon-beam radiation therapy combined with or without surgery for primary versus recurrent tumor. *International Journal of Radiation Oncology Biology Physics*. 2006;65(5):1514–21.

117. Yang XR, Ng D, Alcorta DA, Liebsch NJ, Sheridan E, Li S, et al. T (brachyury) gene duplication confers major susceptibility to familial chordoma. *Nature Genetics*. 2009;41(11):1176–8.
118. Barresi V, Ieni A, Branca G, Tuccari G. Brachyury: A diagnostic marker for the differential diagnosis of chordoma and hemangioblastoma versus neoplastic histological mimickers. *Disease Markers*. 2014;2014:1–7.
119. Stewart MJ, Burrow JLEF. E chordosis physaliphora sphenoccipitalis. *Journal of Neurology, Neurosurgery and Psychiatry*. 1923;1-4(15):218–20.
120. Persons DL, Bridge JA, Neff JR. Cytogenetic analysis of two sacral chordomas. *Cancer Genetics and Cytogenetics*. 1991;56(2):197–201.
121. Bayrakli F, Guney I, Kilic T, Ozek M, Pamir MN. New candidate chromosomal regions for chordoma development. *Surgical Neurology*. 2007;68(4):425–30.
122. Hallor KH, Staaf J, Jönsson G, Heidenblad M, Vult Von Steyern F, Bauer HCF, Ijszenga M, et al. Frequent deletion of the CDKN2A locus in chordoma: Analysis of chromosomal imbalances using array comparative genomic hybridisation. *British Journal of Cancer*. 2008;98(2):434–42.
123. Scheil S, Brüderlein S, Liehr T, Starke H, Herms J, Schulte M, et al. Genome-wide analysis of sixteen chordomas by comparative genomic hybridization and cytogenetics of the first human chordoma cell line, U-CHI. *Genes Chromosomes and Cancer*. 2001;32(3):203–11.
124. Huang M, Anand S, Murphy EA, Desgrosellier JS, Stupack DG, Shattil SJ, et al. EGFR-dependent pancreatic carcinoma cell metastasis through Rap1 activation. *Oncogene*. 2012;31(22):2783–93.
125. Itakura Y, Sasano H, Shiga C, Furukawa Y, Shiga K, Mori S, et al. Epidermal growth factor receptor overexpression in esophageal carcinoma. An immunohistochemical study correlated with clinicopathologic findings and DNA amplification. *Cancer*. 1994;74(3):795–804.
126. Bonaccorsi L, Carloni V, Muratori M, Formigli L, Zecchi S, Forti G, et al. EGF

receptor (EGFR) signaling promoting invasion is disrupted in androgen-sensitive prostate cancer cells by an interaction between EGFR and androgen receptor (AR). *International Journal of Cancer*. 2004;112(1):78–86.

127. De Castro Msc CV, Guimaraes G, Aguiar S, Lopes A, Baiocchi G, Da Cunha IW, et al. Tyrosine kinase receptor expression in chordomas: Phosphorylated AKT correlates inversely with outcome. *Human Pathology*. 2013;44(9):1747–55.

128. Ptaszyński K, Szumera-Ciećkiewicz A, Owczarek J, Mrozkowiak A, Pekul M, Barańska J, et al. Epidermal growth factor receptor (EGFR) status in chordoma. *Polish Journal of Pathology*. 2009;60(2):81–7.

129. Tamborini E, Viridis E, Negri T, Orsenigo M, Brich S, Conca E, et al. Analysis of receptor tyrosine kinases (RTKs) and downstream pathways in chordomas. *Neuro-Oncology*. 2010;12(8):776–89.

130. Schwab JH, Boland PJ, Agaram NP, Socci ND, Guo T, O'Toole GC, et al. Chordoma and chondrosarcoma gene profile: Implications for immunotherapy. *Cancer Immunology, Immunotherapy*. 2009;58(3):339–49.

131. Weinberger PM, Yu Z, Kowalski D, Joe J, Manger P, Psyrrri A, et al. Differential expression of epidermal growth factor receptor, c-Met, and HER2/neu in chordoma compared with 17 other malignancies. *Archives of Otolaryngology - Head and Neck Surgery*. 2005;131(8):707–11.

132. Akhavan-Sigari R, Gaab MR, Rohde V, Abili M, Ostertag H. Expression of PDGFR- $\alpha$ , EGFR and c-MET in spinal chordoma: A series of 52 patients. *Anticancer Research*. 2014;34(2):623–30.

133. Williams LT. Signal transduction by the platelet-derived growth factor receptor. *Science*. 1989;243(4898):1564–70.

134. Jechlinger M, Sommer A, Moriggl R, Seither P, Kraut N, et al. Autocrine PDGFR signaling promotes mammary cancer metastasis. *Journal of Clinical Investigation*. 2006;116(6):1561-70

135. Taeger J, Moser C, Hellerbrand C, Mycielska ME, Glockzin G, Schlitt HJ, et al.



Targeting FGFR/PDGFR/VEGFR impairs tumor growth, angiogenesis, and metastasis by effects on tumor cells, endothelial cells, and pericytes in pancreatic cancer. *Molecular Cancer Therapeutics*. 2011;10(11):2157–67.

136. Tamborini E, Miselli F, Negri T, Lagonigro MS, Staurenco S, et al. Molecular and biochemical analyses of platelet-derived growth factor receptor (PDGFR) B, PDGFRA, and KIT receptors in chordomas. *Clinical Cancer Research*. 2006;12(23):6920–8.

137. Morgensztern D, McLeod HL. PI3K/Akt/mTOR pathway as a target for cancer therapy. *Anti-cancer drugs*. 2005;16(8):797–803.

138. Presneau, Shalaby A, Idowu B, Gikas P, Cannon SR, Gout I, Diss T, et al. Potential therapeutic targets for chordoma: PI3K/AKT/TSC1/TSC2/mTOR pathway. *British Journal of Cancer*. 2009;100(9):1406–14.

139. Schwab J, Antonescu C, Boland P, Healey J, Rosenberg A, Nielsen P, et al. Combination of PI3K/mTOR inhibition demonstrates efficacy in human chordoma. *Anticancer Research*. 2009;29(6):1867–71.

140. Chappell WH, Steelman LS, Long JM, Kempf RC, Abrams SL, Franklin RA, et al. Ras/Raf/MEK/ERK and PI3K/PTEN/Akt/mTOR inhibitors: Rationale and importance to inhibiting these pathways in human health. *Oncotarget*. 2011;2(3):135.

141. Cseh B, Doma E, Baccarini M. “RAF” neighborhood: Protein-protein interaction in the Raf/Mek/Erk pathway. *FEBS Letters*. 2014;588(15):2398–406.

142. Knight T, Irving JAE. Ras/Raf/MEK/ERK pathway activation in childhood acute lymphoblastic leukemia and its therapeutic targeting. *Frontiers in Oncology*. 2014;4:160.

143. Ott PA, Bhardwaj N. Impact of MAPK pathway activation in BRAFV600 melanoma on T cell and dendritic cell function. *Frontiers in Immunology*. 2013;4:346.

144. Zhang K, Chen H, Zhang B, Sun J, Lu J, Chen K, et al. Overexpression of Raf-1 and ERK1/2 in sacral chordoma and association with tumor recurrence. *International Journal of Clinical and Experimental Pathology*. 2015;8(1):608–14.

145. Beddington RS, Rashbass P, Wilson V. Brachyury--a gene affecting mouse

gastrulation and early organogenesis. *Development* 1992;116(Supplement):157-65

146. Kilic N, Feldhaus S, Kilic E, Tennstedt P, Wicklein D, Von Wasielewski R, et al. Brachyury expression predicts poor prognosis at early stages of colorectal cancer. *European Journal of Cancer*. 2011;47(7):1080–5.

147. Zhang L, Guo S, Schwab JH, Nielsen GP, Choy E, Ye S, et al. Tissue microarray immunohistochemical detection of brachyury is not a prognostic indicator in chordoma. *PLoS ONE*. 2013;8(9):75851.

148. Naka T, Iwamoto Y, Shinohara N, Ushijima M, Chuman H, Tsuneyoshi M. Expression of c-met proto-oncogene product (c-MET) in benign and malignant bone tumors. *Modern Pathology: An Official Journal of the United States and Canadian Academy of Pathology, Inc*. 1997;10(8):832.

149. Naka T, Kuester D, Boltze C, Scheil-Bertram S, Samii A, Herold C, et al. Expression of hepatocyte growth factor and c-MET in skull base chordoma. *Cancer*. 2008;112(1):104–10.

150. Chen C, Yang HL, Chen KW, Wang GL, Lu J, Yuan Q, et al. High expression of survivin in sacral chordoma. *Medical Oncology*. 2013;30(2):1-5.

151. Froehlich EV, Rinner B, Deutsch AJA, Meditz K, Knausz H, Troppan K, et al. Examination of survivin expression in 50 chordoma specimens - A histological and in vitro study. *Journal of Orthopaedic Research*. 2015;33(5):771–8.

152. Tamaki N, Nagashima T, Ehara K, Motooka Y, Barua KK. Surgical approaches and strategies for skull base chordomas. *Neurosurgical Focus*. 2008;10(3):1–7.

153. Rich TA, Schiller A, Suit HD, Mankin HJ. Clinical and pathologic review of 48 cases of chordoma. *Cancer*. 1985;56(1):182–7.

154. Kaiser TE, Pritchard DJ, Unni KK. Clinicopathologic study of sacrococcygeal chordoma. *Cancer*. 1984;53(11):2574–8.

155. Boriani S, Bandiera S, Biagini R, Bacchini P, Boriani L, Cappuccio M, et al. Chordoma of the mobile spine: Fifty years of experience. *Spine*. 2006;31(4):493–503.

156. Vergara G, Belinchón B, Valcárcel F, Veiras M, Zapata I, De La Torre A. Metastatic disease from chordoma. *Clinical and Translational Oncology*. 2008;10(8):517–21.
157. Koutourousiou M, Snyderman CH, Fernandez-Miranda J, Gardner PA. Skull base chordomas. *Otolaryngologic Clinics of North America*. 2011;44(5):1155–71.
158. Otto BA, Jacob A, Klein MJ, Welling DB. Chondromyxoid fibroma of the temporal bone: Case report and review of the literature. *Annals of Otology, Rhinology and Laryngology*. 2007;116(12):922–7.
159. Magrini SM, Papi MG, Marletta F, Tomaselli S, Cellai E, Mungai V, et al. Chordoma-natural history, treatment and prognosis the Florence radiotherapy department experience (1956-1990) and a critical review of the literature. *Acta Oncologica*. 1992;31(8):847–51.
160. Amichetti M, Cianchetti M, Amelio D, Enrici RM, Minniti G. Proton therapy in chordoma of the base of the skull: A systematic review. *Neurosurgical Review*. 2009;32(4):403–16.
161. Takahashi S, Kawase T, Yoshida K, Hasegawa A, Mizoe JE. Skull base chordomas: Efficacy of surgery followed by carbon ion radiotherapy. *Acta Neurochirurgica*. 2009;151(7):759–69.
162. Casali PG, Messina A, Stacchiotti S, Tamborini E, Crippa F, Gronchi A, et al. Imatinib mesylate in chordoma. *Cancer*. 2004;101(9):2086–97.
163. Orzan F, Terreni MR, Longoni M, Boari N, Mortini P, Doglioni C, et al. Expression study of the target receptor tyrosine kinase of Imatinib mesylate in skull base chordomas. *Oncology Reports*. 2007;18(1):249–52.
164. Cao X, Lu Y, Liu Y, Zhou Y, Song H, Zhang W, et al. Combination of PARP inhibitor and temozolomide to suppress chordoma progression. *Journal of Molecular Medicine*. 2019;97(8):1183-93.
165. Yang Y, Li Y, Liu W, Xu H, Niu X. The clinical outcome of recurrent sacral chordoma with further surgical treatment. *Medicine*. 2018;97(52):e13730.

166. Rosenberg AE, Nielsen GP, Keel SB, Renard LG, Fitzek MM, Munzenrider JE, et al. Chondrosarcoma of the base of the skull: A clinicopathologic study of 200 cases with emphasis on its distinction from chordoma. *American Journal of Surgical Pathology*. 1999;23(11):1370–8.
167. Dick JE. Stem cell concepts renew cancer research. *Blood*. 2008;112(13):4793–807.
168. Reya T, Morrison SJ, Clarke MF, Weissman IL. Stem cells, cancer, and cancer stem cells. *Nature*. 2001;414(6859):105–11.
169. Dalerba P, Cho RW, Clarke MF. Cancer stem cells: models and concepts. *Annual Review of Medicine*. 2007;58(1):267–84.
170. O’Flaherty JD, Barr M, Fennell D, Richard D, Reynolds J, O’Leary J, et al. The cancer stem-cell hypothesis: Its emerging role in lung cancer biology and its relevance for future therapy. *Journal of Thoracic Oncology*. 2012;7(12):1880–90.
171. Dean M, Fojo T, Bates S. Tumour stem cells and drug resistance. *Nature Reviews Cancer*. 2005;5(4):275–84.
172. Nandy SB, Lakshmanaswamy R. Cancer stem cells and metastasis. *Progress in Molecular Biology and Translational Science*. 2017:137–76.
173. Yu F, Li J, Chen H, Fu J, Ray S, Huang S, et al. Kruppel-like factor 4 (KLF4) is required for maintenance of breast cancer stem cells and for cell migration and invasion. *Oncogene*. 2011;30(18):2161–72.
174. Lapidot T, Sirard C, Vormoor J, Murdoch B, Hoang T, Caceres-Cortes J, et al. A cell initiating human acute myeloid leukaemia after transplantation into SCID mice. *Nature*. 1994;367(6464):645–8.
175. Singh SK, Hawkins C, Clarke ID, Squire JA, Bayani J, Hide T, et al. Identification of human brain tumour initiating cells. *Nature*. 2004;432(7015):396–401.
176. Bao S, Wu Q, Sathornsumetee S, Hao Y, Li Z, Hjelmeland AB, et al. Stem cell-like glioma cells promote tumor angiogenesis through vascular endothelial growth factor.

*Cancer Research*. 2006;66(16):7843–8.

177. Beier D, Hau P, Proescholdt M, Lohmeier A, Wischhusen J, Oefner PJ, et al. CD133+ and CD133- glioblastoma-derived cancer stem cells show differential growth characteristics and molecular profiles. *Cancer Research*. 2007;67(9):4010–5.

178. Singec I, Knoth R, Meyer RP, Maciaczyk J, Volk B, Nikkhah G, et al. Defining the actual sensitivity and specificity of the neurosphere assay in stem cell biology. *Nature Methods*. 2006;3(10):801–6.

179. Mao X, Zhang X, Xue X, Guo G, Wang P, Zhang W, et al. Brain tumor stem-like cells identified by neural stem cell marker CD15. *Translational Oncology*. 2014;2(4):247–57.

180. Al-Hajj M, Wicha MS, Benito-Hernandez A, Morrison SJ, Clarke MF. Prospective identification of tumorigenic breast cancer cells. *Proceedings of the National Academy of Sciences of the United States of America*. 2003;100(7):3983–8.

181. Li X, Lewis MT, Huang J, Gutierrez C, Osborne CK, Wu MF, et al. Intrinsic resistance of tumorigenic breast cancer cells to chemotherapy. *Journal of the National Cancer Institute*. 2008;100(9):672–9.

182. Charafe-Jauffret E, Ginestier C, Iovino F, Wicinski J, Cervera N, Finetti P, et al. Breast cancer cell lines contain functional cancer stem cells with metastatic capacity and a distinct molecular signature. *Cancer Research*. 2009;69(4):1302–13.

183. Croker AK, Goodale D, Chu J, Postenka C, Hedley BD, Hess DA, et al. High aldehyde dehydrogenase and expression of cancer stem cell markers selects for breast cancer cells with enhanced malignant and metastatic ability. *Journal of Cellular and Molecular Medicine*. 2009;13(8):2236–52.

184. Parry P V., Engh JA. CD90 is identified as a marker for cancer stem cells in high-grade gliomas using tissue microarrays. *Neurosurgery*. 2012;70(4):23–4.

185. Friedmann-Morvinski D, Verma IM. Dedifferentiation and reprogramming: Origins of cancer stem cells. *EMBO Reports*. 2014;15(3):244–53.

186. Medema JP. Cancer stem cells: The challenges ahead. *Nature Cell Biology*. 2013;15(4):338–44.
187. Aydemir E, Bayrak OF, Sahin F, Atalay B, Kose GT, Ozen M, et al. Characterization of cancer stem-like cells in chordoma. *Journal of Neurosurgery*. 2012;116(4):810–20.
188. Bayrak OF, Aydemir E, Gulluoglu S, Sahin F, Sevli S, Yalvac ME, et al. The effects of chemotherapeutic agents on differentiated chordoma cells. *Journal of Neurosurgery: Spine*. 2011;15(6):620–4.
189. Lohberger B, Rinner B, Stuenkel N, Absenger M, Liegl-Atzwanger B, Walzer SM, et al. Aldehyde dehydrogenase 1, a potential marker for cancer stem cells in human Sarcoma. *PLoS ONE*. 2012;7(8):43664.
190. Hsu W, Mohyeldin A, Shah SR, Gokaslan ZL, Quinones-Hinojosa A. Role of cancer stem cells in spine tumors: Review of current literature. *Neurosurgery*. 2012;71(1):117–25.
191. Bartel DP. MicroRNAs: genomics, biogenesis, mechanism, and function. *Cell*. 2004;116(2):281–97.
192. Lagos-Quintana M, Rauhut R, Lendeckel W, Tuschl T. Identification of novel genes coding for small expressed RNAs. *Science*. 2001;294(5543):853–8.
193. Winter J, Jung S, Keller S, Gregory RI, Diederichs S. Many roads to maturity: microRNA biogenesis pathways and their regulation. *Nature Cell Biology*. 2009;11(3):228–34.
194. Wang T, Wang G, Hao D, Liu X, Wang D, Ning N, et al. Aberrant regulation of the LIN28A/LIN28B and let-7 loop in human malignant tumors and its effects on the hallmarks of cancer. *Molecular Cancer*. 2015;14(1):125.
195. Mizuno R, Kawada K, Sakai Y. The molecular basis and therapeutic potential of let-7 microRNAs against colorectal cancer. *Canadian Journal of Gastroenterology and Hepatology*. 2018;2018:1–7.

196. Zhang L, Liao Y, Tang L. MicroRNA-34 family: A potential tumor suppressor and therapeutic candidate in cancer. *Journal of Experimental and Clinical Cancer Research*. 2019;38(1):53.
197. Hayashita Y, Osada H, Tatematsu Y, Yamada H, Yanagisawa K, Tomida S, et al. A polycistronic MicroRNA cluster, miR-17-92, is overexpressed in human lung cancers and enhances cell proliferation. *Cancer Research*. 2005;65(21):9628–32.
198. He L, Thomson JM, Hemann MT, Hernando-Monge E, Mu D, Goodson S, et al. A microRNA polycistron as a potential human oncogene. *Nature*. 2005;435(7043):828–33.
199. Voorhoeve PM, Sage C Le, Schrier M, Gillis AJM, Stoop H, Nagel R, et al. A genetic screen implicates miRNA-372 and miRNA-373 as oncogenes in testicular germ cell tumors. *Advances in Experimental Medicine and Biology*. 2007;604:17–46.
200. Duan Z, Choy E, Petur Nielsen G, Rosenberg A, Iafrate J, Yang C, et al. Differential expression of microRNA (miRNA) in chordoma reveals a role for miRNA-1 in met expression. *Journal of Orthopaedic Research*. 2010;28(6):746–52.
201. Duan Z, Shen J, Yang X, Yang P, Osaka E, Choy E, et al. Prognostic significance of miRNA-1 (miR-1) expression in patients with chordoma. *Journal of Orthopaedic Research*. 2014;32(5):695–701.
202. Osaka E, Yang X, Shen JK, Yang P, Feng Y, Mankin HJ, et al. MicroRNA-1 (miR-1) inhibits chordoma cell migration and invasion by targeting slug. *Journal of Orthopaedic Research*. 2014;32(8):1075–82.
203. Osaka E, Kelly AD, Spentzos D, Choy E, Yang X, Shen JK, et al. MicroRNA-155 expression is independently predictive of outcome in chordoma. *Oncotarget*. 2015;6(11):9125.
204. Zhang Y, Schiff D, Park D, Abounader R. MicroRNA-608 and microRNA-34a regulate chordoma malignancy by targeting EGFR, Bcl-xL and MET. *PLoS ONE*. 2014;9(3):91546.
205. Bayrak OF, Gulluoglu S, Aydemir E, Ture U, Acar H, Atalay B, et al. MicroRNA expression profiling reveals the potential function of microRNA-31 in chordomas. *Journal*

*of Neuro-Oncology*. 2013;115(2):143–51.

206. Gulluoglu S, Tuysuz EC, Kuskucu A, Ture U, Atalay B, Sahin F, et al. The potential function of microRNA in chordomas. *Gene*. 2016;585(1):76–83.

207. Long C, Jiang L, Wei F, Ma C, Zhou H, Yang S, et al. Integrated miRNA-mRNA analysis revealing the potential roles of miRNAs in chordomas. *PLoS ONE*. 2013;8(6):66676.

208. Gustincich S, Manfioletti G, Del Sal G, Schneider C, Carninci P. A fast method for high-quality genomic DNA extraction from whole human blood. *BioTechniques*. 1991;11(3):298-300.

209. Krämer A, Green J, Pollard J, Tugendreich S. Causal analysis approaches in ingenuity pathway analysis. *Bioinformatics*. 2014;30(4):523–30.

210. Tuysuz EC, Gulluoglu S, Yaltirik CK, Ozbey U, Kuskucu A, Çoban EA, et al. Distinctive role of dysregulated miRNAs in chordoma cancer stem-like cell maintenance. *Experimental Cell Research*. 2019;380(1):9–19.

211. Wong N, Wang X. miRDB: An online resource for microRNA target prediction and functional annotations. *Nucleic Acids Research*. 2015;43(D1):D146–52.

212. John B, Enright AJ, Aravin A, Tuschl T, Sander C, Marks DS. Human microRNA targets. *PLoS Biology*. 2004;2(11):363.

213. Krek A, Grün D, Poy MN, Wolf R, Rosenberg L, Epstein EJ, et al. Combinatorial microRNA target predictions. *Nature Genetics*. 2005;37(5):495–500.

214. Kiriakidou M, Nelson PT, Kouranov A, Fitziev P, Bouyioukos C, Mourelatos Z, et al. A combined computational-experimental approach predicts human microRNA targets. *Genes and Development*. 2004;18(10):1165–78.

215. Lewis BP, Shih I, Jones-Rhoades MW, Bartel DP, Burge CB. Prediction of mammalian microRNA targets. *Cell*. 2003;115(7):787–98.

216. Malgulwar PB, Pathak P, Singh M, Kale SS, Suri V, Sarkar C, et al. Downregulation of SMARCB1/INI1 expression in pediatric chordomas correlates with



upregulation of miR-671-5p and miR-193a-5p expressions. *Brain Tumor Pathology*. 2017;34(4):155–9.

217. Wang W, Tang L, Li Q, Tan J, Yao H, Duan Z, et al. Overexpression of miR-31-5p inhibits human chordoma cells proliferation and invasion by targeting the oncogene c-Met through suppression of AKT/PI3K signaling pathway. *International Journal of Clinical and Experimental Pathology*. 2017;10(7):8000–9.

218. Wang Y, Chen K, Chen H, Zhang K, Lu J, Mao H, et al. Low expression of miRNA-1290 associated with local invasion and recurrence in sacral chordoma. *International Journal of Clinical and Experimental Pathology*. 2017;10(11):10934–40.

219. Zou MX, Huang W, Wang XB, Li J, Lv GH, Wang B, et al. Reduced expression of miRNA-1237-3p associated with poor survival of spinal chordoma patients. *European Spine Journal*. 2015;24(8):1738–46.

220. Zou MX, Huang W, Wang XB, Lv GH, Li J, Deng YW. Identification of miR-140-3p as a marker associated with poor prognosis in spinal chordoma. *International Journal of Clinical and Experimental Pathology*. 2014;7(8):4877–85.

221. Zou MX, Guo KM, Lv GH, Huang W, Li J, Wang XB, et al. Clinicopathologic implications of CD8 + /Foxp3 + ratio and miR-574-3p/PD-L1 axis in spinal chordoma patients. *Cancer Immunology, Immunotherapy*. 2018;67(2):209–24.

222. Wei W, Zhang Q, Wang Z, Yan B, Feng Y, Li P. MiR-219-5p inhibits proliferation and clonogenicity in chordoma cells and is associated with tumor recurrence. *Oncology Letters*. 2016;12(6):4568–76.

223. Kuang L, Lv G, Wang B, Li L, Dai Y, Li Y. Overexpression of adenosine deaminase acting on RNA 1 in chordoma tissues is associated with chordoma pathogenesis by reducing miR-125a and miR-10a expression. *Molecular Medicine Reports*. 2015;12(1):93–8.

224. Bertolini G, Roz L, Perego P, Tortoreto M, Fontanella E, Gatti L, et al. Highly tumorigenic lung cancer CD133+ cells display stem-like features and are spared by cisplatin treatment. *Proceedings of the National Academy of Sciences*.

2009;106(38):16281–6.

225. Wang J, Wang H, Li Z, Wu Q, Lathia JD, McLendon RE, et al. c-Myc is required for maintenance of glioma cancer stem cells. *PLoS ONE*. 2008;3(11):3769.

226. Liu S, Cong Y, Wang D, Sun Y, Deng L, Liu Y, et al. Breast cancer stem cells transition between epithelial and mesenchymal states reflective of their normal counterparts. *Stem Cell Reports*. 2014;2(1):78–91.

227. Scheel C, Weinberg RA. Cancer stem cells and epithelial-mesenchymal transition: Concepts and molecular links. *Seminars in Cancer Biology*. 2012;22(5-6):396–403.

228. Wright MH, Calcagno AM, Salcido CD, Carlson MD, Ambudkar SV, Varticovski L. Brca1 breast tumors contain distinct CD44+/CD24- and CD133+ cells with cancer stem cell characteristics. *Breast Cancer Research*. 2008;10(1):10.

229. Pu Y, Yi Q, Zhao F, Wang H, Cai W, Cai S. MiR-20a-5p represses multi-drug resistance in osteosarcoma by targeting the KIF26B gene. *Cancer Cell International*. 2016;16(1):64.

230. Liu J, Ma L, Wang Z, Wang L, Liu C, Chen R, et al. MicroRNA expression profile of gastric cancer stem cells in the MKN-45 cancer cell line. *Acta Biochimica et Biophysica Sinica*. 2014;46(2):92–9.

231. Karatas OF, Suer I, Yuceturk B, Yilmaz M, Oz B, Guven G, et al. Identification of microRNA profile specific to cancer stem-like cells directly isolated from human larynx cancer specimens. *BMC Cancer*. 2016;16(1):853.

232. Zhang HH, Gu GL, Zhang XY, Li FZ, Ding L, Fan Q, et al. Primary analysis and screening of microRNAs in gastric cancer side population cells. *World Journal of Gastroenterology*. 2015;21(12):3519–26.

233. Kong XM, Zhang GH, Huo YK, Zhao XH, Cao DW, Guo SF, et al. MicroRNA-140-3p inhibits proliferation, migration and invasion of lung cancer cells by targeting ATP6AP2. *International Journal of Clinical and Experimental Pathology*. 2015;8(10):12845–52.

234. Zhang H, Li Y, Huang Q, Ren X, Hu H, Sheng H, et al. MiR-148a promotes apoptosis by targeting Bcl-2 in colorectal cancer. *Cell Death and Differentiation*. 2011;18(11):1702–10.
235. Zhang R, Li M, Zang W, Chen X, Wang Y, Li P, et al. MiR-148a regulates the growth and apoptosis in pancreatic cancer by targeting CCKBR and Bcl-2. *Tumor Biology*. 2014;35(1):837–44.
236. Guo SL, Peng Z, Yang X, Fan KJ, Ye H, Li ZH, et al. Mir-148a Promoted Cell Proliferation By Targeting P27 in Gastric Cancer Cells. *International Journal of Biological Sciences*. 2011;7(5):567–74.
237. Deppe J, Steinritz D, Santovito D, Egea V, Schmidt A, Weber C, et al. Upregulation of miR-203 and miR-210 affect growth and differentiation of keratinocytes after exposure to sulfur mustard in normoxia and hypoxia. *Toxicology Letters*. 2016;244:81–7.
238. Li Y, Yang C, Zhang L, Yang P. MicroRNA-210 induces endothelial cell apoptosis by directly targeting PDK1 in the setting of atherosclerosis. *Cellular and Molecular Biology Letters*. 2017;22(1):3.
239. Lai Z, Lin P, Weng X, Su J, Chen Y, He Y, et al. MicroRNA-574-5p promotes cell growth of vascular smooth muscle cells in the progression of coronary artery disease. *Biomedicine and Pharmacotherapy*. 2018;97:162–7.
240. Li Q, Li X, Guo Z, Xu F, Xia J, Liu Z, et al. MicroRNA-574-5p was pivotal for TLR9 signaling enhanced tumor progression via down-regulating checkpoint suppressor 1 in human lung cancer. *PLoS ONE*. 2012;7(11):48278.
241. Cui J, Li P, Liu X, Hu H, Wei W. Abnormal expression of the notch and Wnt/ $\beta$ -catenin signaling pathways in stem-like ALDHhiCD44+ cells correlates highly with Ki-67 expression in breast cancer. *Oncology Letters*. 2015;9(4):1600–6.
242. Qin L, Yin YT, Zheng FJ, Peng LX, Yang CF, Bao YN, Liang YY, et al. WNT5A promotes stemness characteristics in nasopharyngeal carcinoma cells leading to metastasis and tumorigenesis. *Oncotarget*. 2015;6(12):10239.

243. Fujii R, Friedman ER, Richards J, Tsang KY, Heery CR, Schlom J, et al. Enhanced killing of chordoma cells by antibody-dependent cell-mediated cytotoxicity employing the novel anti-PD-L1 antibody avelumab. *Oncotarget*. 2016;7(23):33498.
244. Kapodistrias N, Bobori C, Theocharopoulou G. Mir-140-3p downregulation in association with pdl-1 overexpression in many cancers: a review from the literature using predictive bioinformatics tools. *Advances in Experimental Medicine and Biology*. 2017;988:225–33.
245. Li Q, Yao Y, Eades G, Liu Z, Zhang Y, Zhou Q. Downregulation of miR-140 promotes cancer stem cell formation in basal-like early stage breast cancer. *Oncogene*. 2014;33(20):2589–600.
246. Feng Y, Shen J, Gao Y, Liao Y, Cote G, Choy E, et al. Expression of programmed cell death ligand 1 (PD-L1) and prevalence of tumor-infiltrating lymphocytes (TILs) in chordoma. *Oncotarget*. 2015;6(13):11139.
247. Wang X, Liang Z, Xu X, Li J, Zhu Y, Meng S, et al. MIR-148a-3p represses proliferation and EMT by establishing regulatory circuits between ERBB3/AKT2/c-myc and DNMT1 in bladder cancer. *Cell Death and Disease*. 2016;7(12):2503.
248. Schober M, Fuchs E. Tumor-initiating stem cells of squamous cell carcinomas and their control by TGF- and integrin/focal adhesion kinase (FAK) signaling. *Proceedings of the National Academy of Sciences*. 2011;108(26):10544–9.
249. Kim HW, Haider HK, Jiang S, Ashraf M. Ischemic preconditioning augments survival of stem cells via miR-210 expression by targeting caspase-8-associated protein 2. *Journal of Biological Chemistry*. 2009;284(48):33161–8.
250. Huang CS, Zhai JM, Zhu XX, Cai JP, Chen W, Li JH, et al. BTG2 is down-regulated and inhibits cancer stem cell-like features of side population cells in hepatocellular carcinoma. *Digestive Diseases and Sciences*. 2017;62(12):3501–10.
251. Zhang L, Huang H, Wu K, Wang M, Wu B. Impact of BTG2 expression on proliferation and invasion of gastric cancer cells in vitro. *Molecular Biology Reports*. 2010;37(6):2579–86.

252. Xiong J, Du Q, Liang Z. Tumor-suppressive microRNA-22 inhibits the transcription of E-box-containing c-Myc target genes by silencing c-Myc binding protein. *Oncogene*. 2010;29(35):4980–8.
253. Liu P, Brown S, Goktug T, Channathodiyil P, Kannappan V, Hugnot JP, et al. Cytotoxic effect of disulfiram/copper on human glioblastoma cell lines and ALDH-positive cancer-stem-like cells. *British Journal of Cancer*. 2012;107(9):1488–97.
254. Enderling H. Cancer stem cells: Small subpopulation or evolving fraction? *Integrative Biology*. 2015;7(1):14-23.
255. Chappell J, Dalton S. Altered cell cycle regulation helps stem-like carcinoma cells resist apoptosis. *BMC Biology*. 2010;8(1):63.
256. Shiozawa Y, Nie B, Pienta KJ, Morgan TM, Taichman RS. Cancer stem cells and their role in metastasis. *Pharmacology and Therapeutics*. 2013;138(2):285-93.
257. Grasso D, Garcia MN, Hamidi T, Cano C, Calvo E, Lomber G, et al. Genetic inactivation of the pancreatitis-inducible gene *Nupr1* impairs PanIN formation by modulating *Kras*<sup>G12D</sup>-induced senescence. *Cell Death and Differentiation*. 2014;21(10):1633–41.
258. Song W, Li Q, Wang L, Huang W, Wang L. FoxO1-negative cells are cancer stem-like cells in pancreatic ductal adenocarcinoma. *Scientific Reports*. 2015;5:10081.
259. Gallardo A, Garcia-Valdecasas B, Murata P, Teran R, Lopez L, Barnadas A, et al. Inverse relationship between Ki67 and survival in early luminal breast cancer: confirmation in a multivariate analysis. *Breast Cancer Research and Treatment*. 2018;167(1):31–7.
260. Luo G, Hu Y, Zhang Z, Wang P, Luo Z, Lin J, et al. Clinicopathologic significance and prognostic value of Ki-67 expression in patients with gastric cancer: a meta-analysis. *Oncotarget*. 2017;8(30):50273.
261. Pallini R, Maira G, Pierconti F, Falchetti ML, Alvino E, Cimino-Reale G, et al. Chordoma of the skull base: predictors of tumor recurrence. *Journal of Neurosurgery*. 2009;98(4):812–22.

262. Gulluoglu S, Sahin M, Tuysuz EC, Yaltirik CK, Kuskucu A, Ozkan F, et al. Leukemia inhibitory factor promotes aggressiveness of chordoma. *Oncology Research Featuring Preclinical and Clinical Cancer Therapeutics*. 2017;25(7):1177–88.
263. Hou CH, Lin FL, Tong KB, Hou SM, Liu JF. Transforming growth factor alpha promotes osteosarcoma metastasis by ICAM-1 and PI3K/Akt signaling pathway. *Biochemical Pharmacology*. 2014;89(4):453–63.
264. Kim JY, Lee J, Koh JS, Park MJ, Chang UK. Establishment and characterization of a chordoma cell line from the tissue of a patient with dedifferentiated-type chordoma. *Journal of Neurosurgery: Spine*. 2016;25(5):626–35.
265. Schramm G, Surmann EM, Wiesberg S, Oswald M, Reinelt G, Eils R, et al. Analyzing the regulation of metabolic pathways in human breast cancer. *BMC Medical Genomics*. 2010;3(1):39.
266. Zadra G, Batista JL, Loda M. Dissecting the dual role of AMPK in cancer: From experimental to human studies. *Molecular Cancer Research*. 2015;13(7):1059–72.
267. Galdiero MR, Marone G, Mantovani A. Cancer inflammation and cytokines. *Cold Spring Harbor Perspectives in Biology*. 2018;10(8):028662.
268. Shimokawa M, Ohta Y, Nishikori S, Matano M, Takano A, Fujii M, et al. Visualization and targeting of LGR5 + human colon cancer stem cells. *Nature*. 2017;545(7653):187–92.
269. Denduluri SK, Idowu O, Wang Z, Liao Z, Yan Z, Mohammed MK, et al. Insulin-like growth factor (IGF) signaling intumorigenesis and the development of cancer drug resistance. *Genes and Diseases*. 2015;2(1):13–25.
270. Bach LA, Fu P, Yang Z. Insulin-like growth factor-binding protein-6 and cancer. *Clinical Science*. 2012;124(4):215–29.
271. Romero D, O'Neill C, Terzic A, Contois L, Young K, Conley BA, et al. Endoglin regulates cancer-stromal cell interactions in prostate tumors. *Cancer Research*. 2011;71(10):3482–93.

272. Fu P, Yang Z, Bach LA. Prohibitin-2 binding modulates insulin-like growth factor-binding protein-6 (IGFBP-6)-induced rhabdomyosarcoma cell migration. *Journal of Biological Chemistry*. 2013;288(41):29890–900.
273. Aboalola D, Han VKM. Insulin-Like growth factor binding protein-6 alters skeletal muscle differentiation of human mesenchymal stem cells. *Stem Cells International*. 2017;2017:1–17.
274. Lipinski RJ, Cook CH, Barnett DH, Gipp JJ, Peterson RE, Bushman W. Sonic Hedgehog signaling regulates the expression of insulin-like growth factor binding protein-6 during fetal prostate development. *Developmental Dynamics*. 2005;233(3):829–36.

**APPENDIX A: ETHICAL APPROVAL FORM**







## YEDİTEPE ÜNİVERSİTESİ TIP FAKÜLTESİ KLİNİK ARAŞTIRMALAR DEĞERLENDİRME KOMİTESİ KARAR FORMU

<b>KURUL ADI</b>	<b>YEDİTEPE ÜNİVERSİTESİ TIP FAKÜLTESİ KLİNİK ARAŞTIRMALAR DEĞERLENDİRME KOMİTESİ</b>
<b>AÇIK ADRES</b>	YEDİTEPE ÜNİVERSİTESİ HASTANESİ Devlet Yolu Ankara Cad. No: 102-104, 34752 Kozyatağı, İstanbul
<b>TELEFON</b>	0216 578 47 97
<b>E-POSTA</b>	gulin.demir@yeditepe.edu.tr

<b>BAŞVURU BİLGİLERİ</b>	ARAŞTIRMANIN AÇIK ADI	Kordoma Hücre Kültürleri ve Ksenograft Modellerinden Kanser Kök Hücre İzolasyonu ve Karakterizasyonu: Kök Hücrelerde miRNA Profili ve Kemoterapötik Ajanlara Yanıtların İncelenmesi.		
	ARAŞTIRMA PROTOKOLÜNÜN KODU			
	EUDRACT NUMARASI			
	SORUMLU ARAŞTIRMACI ÜNVANI/ADI/SOYADI	Yrd.Doç.Dr.Ömer Faruk Bayrak		
	SORUMLU ARAŞTIRMACININ UZMANLIK ALANI	Tıbbi Genetik		
	KOORDİNATÖRÜN ÜNVANI/ADI/SOYADI	Yrd.Doç.Dr.Ömer Faruk Bayrak		
	KOORDİNATÖRÜN UZMANLIK ALANI	Tıbbi Genetik		
	ARAŞTIRMA MERKEZİ	YEDİTEPE ÜNİVERSİTESİ TIP FAKÜLTESİ TIBBİ GENETİK ANABİLİM DALI VE GENETİK VE BIYOMÜHENDİSLİK BÖLÜMÜ		
	ARAŞTIRMA MERKEZİNİN AÇIK ADRESİ	YEDİTEPE ÜNİVERSİTESİ TIP FAKÜLTESİ TIBBİ GENETİK ANABİLİM DALI VE GENETİK VE BIYOMÜHENDİSLİK BÖLÜMÜ		
	DESTEKLEYİCİ VE AÇIK ADRESİ DESTEKLEYİCİNİN YASAL TEMSİLCİSİ VE ADRESİ UZMANLIK TEZİ/AKADEMİK AMAÇLI	UZMANLIK TEZİ <input type="checkbox"/> AKADEMİK AMAÇLI <input checked="" type="checkbox"/>		
ARAŞTIRMANIN FAZI VE TÜRÜ	FAZ 1	<input type="checkbox"/>		
	FAZ 2	<input type="checkbox"/>		
	FAZ 3	<input type="checkbox"/>		
	FAZ 4	<input type="checkbox"/>		
	BE/BY	<input type="checkbox"/>		
DİĞER	<input type="checkbox"/>		Diğer ise belirtiniz:	
İLAC ARAŞTIRMA	DIŞI <input type="checkbox"/>		Belirtiniz:	
ARAŞTIRMAYA KATILAN MERKEZLER	TEK MERKEZ <input type="checkbox"/>	ÇOK MERKEZLİ <input checked="" type="checkbox"/>	ULUSAL <input checked="" type="checkbox"/>	ULUSLARARASI <input type="checkbox"/>

<b>DEĞERLENDİRİLEN BELGELER</b>	Belge Adı	Tarihi	Versiyon Numarası	Dili
	ARAŞTIRMA PROTOKOLÜ	09.02.2012		Türkçe <input checked="" type="checkbox"/> İngilizce <input type="checkbox"/> Diğer <input type="checkbox"/>
	ARAŞTIRMA BROŞÜRÜ			Türkçe <input type="checkbox"/> İngilizce <input type="checkbox"/> Diğer <input type="checkbox"/>
	BİLGİLENDİRİLMİŞ GÖNÜLLÜ OLUR FORMU			Türkçe <input checked="" type="checkbox"/> İngilizce <input type="checkbox"/> Diğer <input type="checkbox"/>
	OLGU RAPOR FORMU			Türkçe <input checked="" type="checkbox"/> İngilizce <input type="checkbox"/> Diğer <input type="checkbox"/>

<b>DEĞERLENDİRİLEN DİĞER BELGELER</b>	Belge Adı		Açıklama
	ARAŞTIRMA BÜTÇESİ	<input type="checkbox"/>	
SİGORTA	<input type="checkbox"/>		



## YEDİTEPE ÜNİVERSİTESİ TIP FAKÜLTESİ KLİNİK ARAŞTIRMALAR DEĞERLENDİRME KOMİTESİ KARAR FORMU

HASTA KARTI/GÜNLÜKLERİ	<input type="checkbox"/>	
İLAN	<input type="checkbox"/>	
YILLIK BİLDİRİM	<input type="checkbox"/>	
SONUÇ RAPORU	<input type="checkbox"/>	
GÜVENLİLİK BİLDİRİMLERİ	<input type="checkbox"/>	
DİĞER	<input type="checkbox"/>	

<b>KARAR BİLGİLERİ</b>	<b>Karar No:</b> 166	<b>Tarih:</b> 14/02/2012
	Yrd.Doç.Dr.Ömer Faruk Bayrak sorumluluğunda yapılması tasarlanan ve yukarıda başvuru bilgileri verilen klinik araştırma başvuru dosyası ve ilgili belgeler araştırmanın gerekçe, amaç, yaklaşım ve yöntemleri dikkate alınarak incelenmiş, gerçekleştirilmesinde etik bir sakınca bulunmadığına toplantıya katılan değerlendirme kurulu üyelerinin oy çokluğu ile karar verilmiştir.	

### DEĞERLENDİRME KOMİTESİ BİLGİLERİ

<b>ÇALIŞMA ESASI</b>	Klinik Araştırmalar Hakkında Yönetmelik, İyi Klinik Uygulamaları Kılavuzu, Yeditepe Üniversitesi Tıp Fakültesi, Klinik Araştırmalar Değerlendirme Komitesi Kuruluş ve Çalışma Esasları.
----------------------	---

<b>DEĞERLENDİRME KURUL BAŞKANI UNVANI/ADI/SOYADI:</b> Prof. Dr. R. Serdar ALPAN
<b>DEĞERLENDİRME KOMİTESİ ÜYELERİ</b>

Unvanı/Adı/Soyadı	Uzmanlık Alanı	Kurumu	Cinsiyet		İlişki *		Katılım **		İmza
Prof. Dr. R. Serdar Alpan	Farmakoloji	YÜTF	E <input checked="" type="checkbox"/>	K <input type="checkbox"/>	E <input type="checkbox"/>	H <input checked="" type="checkbox"/>	E <input checked="" type="checkbox"/>	H <input type="checkbox"/>	
Prof. Dr. M. Reha Cengizlier	Pediyatri	YÜTF	E <input checked="" type="checkbox"/>	K <input type="checkbox"/>	E <input type="checkbox"/>	H <input checked="" type="checkbox"/>	E <input checked="" type="checkbox"/>	H <input type="checkbox"/>	
Prof. Dr. S. Sami Kartı	Hematoloji	YÜTF	E <input checked="" type="checkbox"/>	K <input type="checkbox"/>	E <input type="checkbox"/>	H <input checked="" type="checkbox"/>	E <input checked="" type="checkbox"/>	H <input type="checkbox"/>	
Prof. Dr. Serdar Öztezcan	Biyokimya	YÜTF	E <input checked="" type="checkbox"/>	K <input type="checkbox"/>	E <input type="checkbox"/>	H <input type="checkbox"/>	E <input type="checkbox"/>	H <input type="checkbox"/>	
Yrd. Doç. Dr. Baki Ekçi	Genel Cerrahi	YÜTF	E <input checked="" type="checkbox"/>	K <input type="checkbox"/>	E <input type="checkbox"/>	H <input checked="" type="checkbox"/>	E <input checked="" type="checkbox"/>	H <input type="checkbox"/>	
Doç Dr. Ferda Özkan	Patoloji	YÜTF	E <input type="checkbox"/>	K <input checked="" type="checkbox"/>	E <input type="checkbox"/>	H <input type="checkbox"/>	E <input type="checkbox"/>	H <input type="checkbox"/>	
Prof.Dr. Nural Bekiroğlu	Biyoistatistik	MÜTF	E <input type="checkbox"/>	K <input checked="" type="checkbox"/>	E <input type="checkbox"/>	H <input checked="" type="checkbox"/>	E <input checked="" type="checkbox"/>	H <input type="checkbox"/>	
Doç. Dr. Esra Can Say	Diş Has. Ted.	YÜDF	E <input type="checkbox"/>	K <input checked="" type="checkbox"/>	E <input type="checkbox"/>	H <input checked="" type="checkbox"/>	E <input checked="" type="checkbox"/>	H <input type="checkbox"/>	
Doç. Dr. Meriç Köksal	Eczacılık	YÜEF	E <input type="checkbox"/>	K <input checked="" type="checkbox"/>	E <input type="checkbox"/>	H <input checked="" type="checkbox"/>	E <input checked="" type="checkbox"/>	H <input type="checkbox"/>	
Prof. Dr. Ali Rıza Okur	Hukuk	YÜHF	E <input checked="" type="checkbox"/>	K <input type="checkbox"/>	E <input type="checkbox"/>	H <input type="checkbox"/>	E <input checked="" type="checkbox"/>	H <input type="checkbox"/>	
Doç. Dr. Başar Atalay	Beyin Cerrahi	YÜTF	E <input checked="" type="checkbox"/>	K <input type="checkbox"/>	E <input type="checkbox"/>	H <input type="checkbox"/>	E <input type="checkbox"/>	H <input type="checkbox"/>	
Yrd.Doç.Dr.Esin Öztürk Işık	Biyomedikal Müh.	YÜMF	E <input type="checkbox"/>	K <input checked="" type="checkbox"/>	E <input type="checkbox"/>	H <input checked="" type="checkbox"/>	E <input checked="" type="checkbox"/>	H <input type="checkbox"/>	
Doç.Dr.Nesrin Sarıman	Göğüs Hastalıkları	MÜTF	E <input type="checkbox"/>	K <input checked="" type="checkbox"/>	E <input type="checkbox"/>	H <input checked="" type="checkbox"/>	E <input checked="" type="checkbox"/>	H <input type="checkbox"/>	
Bilge Firuzbay	Sivil Üye		E <input type="checkbox"/>	K <input checked="" type="checkbox"/>	E <input type="checkbox"/>	H <input type="checkbox"/>	E <input type="checkbox"/>	H <input type="checkbox"/>	

\* : Araştırma ile İlişki

\*\* : Toplantıda Bulunma

**Önemli Not:** Çalışmanın Klinik Araştırmalar Değerlendirme Komitesi tarafından onaylanan protokole göre yürütülmesi ve çalışma protokolündeki değişikliklerin kurulumuza bildirilmesi gerekmektedir.

2 / 2  
Değerlendirme Formu 21 Nisan 2010 No:3

BAŞH.P.06-F.05 Rev 1, 15.09.2010